Age-Associated Arrhythmogenic Substrate and Trigger in a Rabbit Model of Cardiac Aging

By

Leroy Leon Cooper

BS, Clemson University, 2005

AM, Brown University, 2011

Submitted in Partial Fulfillment of the Requirements for the Degree of Doctor of Philosophy in the Division of Biology and Medicine at Brown University

Providence, Rhode Island

May 2013

This dissertation by Leroy Leon Cooper is accepted in its present form by the Division of Biology and Medicine as satisfying the dissertation requirement for the degree of Doctor of Philosophy.

Date _____ _____

Gideon Koren, MD, Advisor

Recommended to the Graduate Council

Date _____ _____

Ulrike Mende, MD, Reader

Date _____ _____

Elizabeth Harrington, PhD, Reader

Date _____ _____

John Sedivy, PhD, Reader

Date _____ _____

Edward Lakatta, MD, External Reader
National Institute on Aging

Approved by the Graduate Council

Date _____ _____

Peter Weber, PhD
Dean of the Graduate School

LEROY LEON COOPER
Curriculum Vitae

May 2013

CONTACT INFORMATION

Personal Address:	555 Roosevelt Avenue, Unit 208 Central Falls, RI 02863
Laboratory Address:	Cardiovascular Research Center (CVRC) Rhode Island Hospital W. Alpert Medical School of Brown University Coro West Center, Room 5100 1 Hoppin Street, Providence, RI 02903-4141
Phone:	(864) 650-3826, personal (401) 444-9857, laboratory
Email:	leroy_cooper@brown.edu

EDUCATION

2007 – Present	**Brown University**, Providence, Rhode Island *Expected graduation: May 2013* **PhD** in Biology and Medicine: Molecular Pharmacology and Physiology Advisor: Gideon Koren, MD Dissertation Title: "Age-associated Arrhythmogenic Substrate and Trigger in a Rabbit Model of Cardiac Aging" **AM** in Biology and Medicine
2001 – 2005	**Clemson University**, Clemson, South Carolina **BS** in Biochemistry with Honors **BS** in Sociology with Honors Advisors: Kerry Smith, PhD and Cheryl Ingram-Smith, PhD Research Project Title: "Characterization of a novel archaeal acyl-CoA synthetase from *M. acetivorans*"

PROFESSIONAL EXPERIENCE

2006 – 2007 **Martek Biosciences Corporation**, Kingstree, SC
Research Associate for Technical Support

- Developed, executed, monitored, and troubleshot fermentation and recovery processes
- Planned, organized and performed pilot plant trials and scaled up to plant-level operations

TECHNIQUES AND INSTRUMENTATION

In vivo Species	Rabbit and *E. coli*
In vivo Techniques	Cardiac electrophysiology, cardiac hemodynamics, calcium imaging, echocardiography, organ and tissue extraction, injection, IV infusion, blood draw, and large animal care
Molecular Biology	Reverse-transcriptase PCR, qPCR, ELISA, DNA, RNA and protein extraction and purification, Western blot analysis
Protein Production	Protein expression in *E. coli*, protein extraction, purification, and stabilization
Cell Culture	Primary cell culture, mammalian cell culture and transfection
Immunostaining	Immunohistochemistry, immunocytochemistry, fluorescent *in situ* hybridization (immunoFISH)
Microscopy	Phase contrast, epi-fluorescence, and confocal microscopy

PEER-REVIEWED PUBLICATIONS

Research Articles:

Cooper, L. L., Li, W., Lu, Y. C., Centracchio, J., Terentyeva, R. Koren, G., Terentyev, D. (2013). Redox modification of ryanodine receptors by mitochondria-derived reactive oxygen species contributes to aberrant Ca^{2+} handling in ageing rabbit hearts. *The Journal of Physiology (under review).*

Kim, T. Y., Jeng, P., Hwang, J., Patel, B., Pfeiffer, Z., Patel, D., **Cooper, L. L.** Kossidas, K., Centracchio, J., Peng, X., Koren, G., Qu, Z., and Choi, B. (2013). Short-Long Heart Rate Variation Increases Action Potential Dispersion in Transgenic Rabbit Model of Long QT Type 2. *Heart Rhythm (under review).*

Cooper, L. L.*, Odening, K. E.*, Hwang, M., Chaves, L., Schofield, L., Taylor, C. A., Gemignani, A. S., Mitchell, G. F., Forder, J. R., Choi, B., and Koren, G. (2012). Electromechanical and structural alterations in the aging rabbit heart and aorta. *American Journal of Physiology – Heart Circulatory Physiology.* 302(8). H1625 – H1635. (*shared authorship)

Meng, Y., Ingram-Smith, C., **Cooper, L. L**., and Smith, K. S. (2010). Characterization of an archaeal medium-chain acyl-CoA synthetase from *Methanosarcina acetivorans. Journal of Bacteriology*. 192(22). 5982 – 5990.

Shah, M. B., Ingram-Smith, C., **Cooper, L. L.**, Ou, J., Meng, Y., Smith, K. S., Gulick, A. M. (2009). The 2.1Å crystal structure of an acyl-CoA synthetase from *Methanosarcina acetivorans* reveals an alternate acyl binding pocket for small branched acyl substrates. *Proteins*. 77(3). 685 – 698.

Presented Abstracts:

Cooper, L. L., Li, W., Lu, Y. C., Centracchio, J., Terentyeva, R., Koren, G., Terentyev, D. Redox modification of ryanodine receptors underlies abnormal calcium handling in aging rabbit hearts. *Biophysical Society*. February 6, 2013. Philadelphia, DC. Poster presentation.

Cooper, L. L., Odening, K. E., Ziv, O., Chaves, L., Schofield, Gemigani, A., Mitchell, G. F., and Koren, G. Parallel stiffening and remodeling of the aging heart and aorta *FASEB J* March 17, 2011 25:644.12. Washington, DC. Poster presentation.

Cooper, L. L., Odening, K. E., Ziv, O., Chaves, L., Schofield, L., Choi, B., Mitchell, G., and Koren, G. The aging rabbit heart as a model for cardiac aging. *FASEB J* April 6, 2010 24:595.6. Anaheim, CA. Poster presentation.

Odening, K. E., Ziv, O., Choi, B., **Cooper, L. L.**, Chaves, L., Schofield, L., and Koren, G. Aging Slows Conduction in Rabbit His-Purkinje-System and Ventricles and Increases Arrhythmogeneity. "30th Annual Scientific Sessions of the Heart Rhythm Society", *Heart Rhythm* 6 (5S): S236. Boston, MA. Poster presentation.

ORAL PRESENTATIONS

2012 Providence Area Aging Research Forum (PAARF). W. Alpert Medical School of Brown University, Providence, RI. “Age-associated alterations of the pro-arrhythmic substrate and trigger in a rabbit model of cardiac aging." October 2.

2010 Molecular Pharmacology, Physiology, and Biotechnology Seminar Series. Brown University. Providence, RI. “The aging rabbit heart as a model for cardiac senescence.” May 28.

HONORS AND AWARDS

2013 Travel Award from the Biophysical Society to present an abstract at the annual meeting of the Biophysical Society in Philadelphia, PA

2011 Travel Award from the American Physiological Society to present an abstract at the annual Experimental Biology Meeting in Washington, DC

2010 – 2013 Ruth L. Kirschstein National Research Service Awards for Individual Pre-doctoral Fellows (F31), National Heart, Lung and Blood Institute/National Institutes of Health

2010 Porter Physiology Fellowship**/**Eleanor Ison Franklin Fellow, American Physiological Society *(Awarded but declined)*

2010 Travel Award from the American Physiological Society to present an abstract at the annual Experimental Biology Meeting in Anaheim, CA

2010 Founders Affiliate Pre-doctoral Fellowship, American Heart Association *(Awarded but declined*)

2009 – 2010 Porter Physiology Fellowship, American Physiological Society

2007 – 2008 Helen Fitzgerald Cserr Pre-doctoral Fellowship, Brown University

2001 – 2005 Cum Laude, Calhoun Honors College Graduate, Clemson University

2005 Coca-Cola Scholar, Clemson University

TEACHING EXPERIENCE

2009 Graduate Assistant for Introductory Biochemistry, Brown University Providence, RI 02912

2005 Substitute Teacher, Florence County School District Five Johnsonville, SC 29555

SOCIETY MEMBERSHIPS

2012 – present Biophysical Society

2009 – present American Physiological Society

Dedication

This dissertation is dedicated to the memory of Jessie Mae Gordon Cooper.

Acknowledgements

I would like to express my gratitude to my advisor, Dr. Gideon Koren, who accepted and welcomed me into his lab. I thank him for his patience, support, mentorship, and wisdom that helped me overcome challenges and inspired me to press forward. Also, I greatly appreciate my dissertation committee. Thank you to Drs. Ulrike Mende, Elizabeth Harrington, John Sedivy, and Edward Lakatta for their advice and continued support, which cultivated and will continue to nurture me in my scientific journey.

During this project, I have engaged with Dr. Koren's collaborators, and I am particularly thankful for the mentorship of Dr. Dmitry Terentyev. Thank you to Dr. Terentyev for welcoming me into his laboratory space and training me in the cardiac calcium field and on the confocal microscope. I would also like to thank Drs. Bum-Rak Choi and Gary Mitchell for their training and support.

I have been truly fortunate to have trained alongside awesome and diverse individuals at the Cardiovascular Research Center (CVRC). I am especially thankful for Dr. Cindy Park-Windhol who provided day-to-day intellectual and emotional support, empathy, and unqualified friendship throughout this process and beyond. I thank Dr. Karim Roder, Dr. Hitesh Jindal, Dr. Katja Odening, Dr. Louise Organ-Darling, Lorraine Schofield, Dr. Laura Gravelin, Dr. Konstantinos Kossidas, Dr. Weiyan Li, Yi Chun Lu, Dr. Karni Moshal, Jason Centracchio, Leonard Chaves, Mary-Ann Machado, and other members of the CVRC for making it a warm, intellectually stimulating, and imaginative work environment. I am also particularly thankful for my undergraduate mentee Ezinne Ihenachor for her hard work and dedication.

I am thankful to have grown to know my fellow Brunonians, colleagues, and now friends. I am particularly grateful for Courtney Frederick, Dr. Nadine Wicks, Dr. Nicholas Everage, Chloe Poston, Christopher Peete, and Rui (Hillary) Yang who were all there along the way and post-graduation and provided true friendship. I also appreciate the rest of my cohort – Dana Francis and Dr. Amalia Avila Figueroa – for their camaraderie as well as their intellectual and emotional support and empathy as we proceeded through graduate school.

While at Brown, I have met and come to know some great people who have made my time in Rhode Island most pleasant. I am extremely thankful to have found the unqualified friendship, support, and companionship of Drs. Ryan LaBrozzi and Jessie Jeyapalan. They have provided limitless inspiration, encouragement, and support. I also thank Trae White, Ricky White, Richard Gennette, Dr. Ravi Perry, T'Sey-Haye Preaster, Dr. Marcus Allen, and Dr. Shawn Christian for their friendship, support, and company.

Before Brown, I was very grateful to have had these wonderful Clemson professors – Drs. James Witte, Kerry Smith, Cheryl Ingram-Smith, and Bess Rothenberg. They inspired me to pursue this degree, and I am grateful for their continued support and friendship. Moreover, I am particularly thankful for my Clemson friends, especially, Eric Stukes, Aleksandrs Aperans, Maurice Smith, Janéa Jenkins, and Katie Burns. Even though they are not near, I carry them all in my heart.

I am most thankful for my family, especially my parents Leroy Cooper Jr. and Edna Barr Cooper, without whom I could not have completed this endeavor. I appreciate their endless love. I also appreciate the love and encouragement of my sisters Michelline,

Kimberley, and Laronda, my brother-in-law Michael, and aunts, uncles, and cousins (especially Aunt Sally and fellow Brunonian and Cousin Laura).

This dissertation is based upon work supported by pre-doctoral fellowships from the American Physiological Society and National Heart, Lung and Blood Institute.

Thank you all!

Table of Contents

List of Figures and Tables

Chapter 1: Introduction and Specific Aims

1.1 Cardiac Structure and Function

1.1A Cardiac Structure and Function Overview

The heart is a vital muscular organ that generates pressures to supply blood as a medium for oxygen and nutrients throughout an organism's body [1, 2]. The mammalian heart functions as a two-sided pump and consists of four chambers (two atria and two ventricles) and four valves that maintain unidirectional flow [1, 2]. Under relatively low pressure, the right heart receives deoxygenated blood via the vena cavae from the systemic circulation and directs blood to the lungs via the pulmonary artery where it becomes oxygenated [1, 2]. Oxygenated blood is returned to the left atrium via the pulmonary vein and crosses the mitral valve into the left ventricle (LV) [1, 2]. Here, the LV contracts and generates relatively higher pressure (compared to the right ventricle) in order to eject the blood across the aortic valve into the aorta and sustain arterial pressures and blood flow adequate to perfuse the entire body [1, 2]. To this end, the heart has both electrical and mechanical properties that must be coordinated into a rhythmic pattern [1, 2].

1.1B Cardiac Electrical and Mechanical Function

To convey synchronization between the ventricles and atria, the heart maintains an electrical cycle known as normal sinus rhythm [3]. The heart generates electrical impulses automatically and independently of the autonomic nervous system. The heart's electrical activity originates in the sinoatrial node (SA node), which is within the

right atrium, and is propagated to the left atrium and down the interatrial septum to the atrioventricular node (AV node), which also has intrinsic automaticity and serves as a secondary pacemaker to the SA node [1, 2]. After a brief pause, the electrical impulse is carried through the His bundle before rapidly branching off into the right and left bundle-branches and Purkinje fibers and eventually to the ventricles [1, 2]. A summation of this electrical activity can be recorded via a noninvasive, surface electrocardiogram (ECG) [3]. However, to assess the electrical function of the heart, electrophysiology (EP) studies have been employed as a minimally invasive tool to examine the electrical conduction system and assess the surface and intracardiac electrical activity and the conduction pathway [4].

The mechanical function of the heart during normal sinus rhythm can be described by the cardiac cycle in the ventricle [1, 5]. These events consist of changes in pressure and volume of the ventricular leading to the contraction of the ventricle and movement of blood [1, 5]. Upon complete filling of the LV, the heart becomes electrically activated and the systolic process begins: LV pressure rises and contraction begins isovolumically [1, 5]. Eventually, LV pressure exceeds the aortic pressure opening the aortic valve, and the blood is ejected into the aorta, thus deceasing LV volume [1, 5]. Once the heart reaches maximal contraction, ejection slows, then the aortic valve closes, and the LV enters diastole or relaxation [1, 5]. With both the aortic and mitral valves closed, the LV relaxes isovolumically as the pressure decreases [1, 5]. Once the LV pressure is lower than the left atrium pressure, the mitral valve opens and the LV fills with blood increasing the volume [1, 5]. Upon complete filling, the cycle repeats [1, 5]. Although the events in LV have only been described here, the right ventricle cardiac

cycle is similar, albeit under lower pressure and different timing [1]. Both non-invasive and minimally invasive techniques are available to assess cardiac mechanical function, including (but not limited to) echocardiography and hemodynamic studies via real time pressure-volume (PV) loops [6, 7], which were employed in this dissertation. Echocardiography is a non-invasive sonogram of the heart, which provides an assessment of ventricular morphology, such as wall thickness and chamber dimension, and provides data in order to calculate function, (e.g., ejection fraction and fractional shortening) [6]. Additionally, real-time PV loops provide valuable information in order to develop indices of systolic and diastolic elastance, such as end systolic pressure-volume relation (ESPVR) and end diastolic pressure-volume relation (EDPVR) [7].

1.2 Cardiac Cellular Function

1.2A Cardiac Cellular Composition

The heart is composed of several cell types including cardiomyocytes, cardiofibroblasts, endothelial cells, and vascular smooth muscle cells [8]. Also, a very small portion of cells are progenitor cells or stem cells that have the ability to differentiate into the above mentioned cell types. Although cardiomyocytes mostly contribute to the cardiac mass (~75%), they only contribute to approximately 30 – 40% of the total cellular composition in terms of cell numbers; whereas, up to two-thirds of the cells in the adult heart are cardiofibroblasts [8-10]. Yet, both cardiomyocytes and cardiofibroblasts are integral in myocardial structure and electromechanical function in a healthy heart.

1.2B Cardiomyocyte Function and Excitation-Contraction (EC) Coupling

Cardiomyocytes are the fundamental excitable and contractile cell of the heart (reviewed in [11, 12]). The sarcolemma of the cardiomyocyte contains ion channels and pumps that control the influx and efflux of ions responsible for action potentials (AP) [1]. The cardiac action potential has five phases and represents the summation of the effect of various currents on the membrane potential of the cardiomyocyte (described below as outlined in [1, 2, 11]). At the resting membrane potential (Phase 4), the membrane is only permeable to K^+. The beginning of an AP occurs at Phase 0 as a rapid upstroke of membrane potential once voltage-gated Na^+ channels are activated causing a positive inward current and myocyte depolarization. At Phase 1, Na^+ channels become inactivated (about +40 mv), and transient voltage-gated potassium channels open causing a slight repolarization via I_{to} in order to optimize the function of L-type Ca^{2+} channels. Phase 2 follows this transient repolarization and is characterized by a prolonged stable membrane potential (or plateau) caused by opposing inward and outward currents from the opening of voltage-gated, L-type Ca^{2+} and repolarizing K^+ channels (I_{Kr}, I_{Ks}, and I_{K1}), respectively. Finally in Phase 3, the L-type Ca^{2+} channels inactivate. SR Ca^{2+}-ATPase and Na^+/Ca^{2+} exchanger remove Ca^{2+}, along with continued efflux from K^+ channels, continue to repolarize the cell to its resting potential. The resting membrane potential (Phase 4) is maintained by I_{K1} (inward rectifier).

Excitation–contraction coupling is the process that incorporates the electrical and contractile properties of the cardiomyocyte and integrally involves calcium (Ca^{2+}) as a second messenger as a direct activator of the myofilaments leading to contraction

(reviewed by [11, 13]). During Phase 2 of the cardiac action potential, Ca^{2+} enters the myocyte through voltage-gated L-type Ca^{2+} channels as the inward I_{Ca}; this sustains the plateau phase of the action and initiates Ca^{2+} release from the sarcoplasmic reticulum (SR) via ryanodine receptors. This increased level of free intracellular Ca^{2+} allows Ca^{2+} to bind to troponin C – a myofilament protein. Binding of Ca^{2+} to troponin C initiates cardiomyocyte contraction. Ca^{2+} exits the cytosolic space via primarily SR Ca^{2+}-ATPase and Na^{+}/Ca^{2+} exchanger and, by a lesser extent, Ca^{2+}-ATPase or mitochondrial Ca^{2+} uniport, and once intracellular [Ca^{2+}] decreases, Ca^{2+} dissociates from troponin and relaxation occurs. Aberrant handling of Ca^{2+} is an important cause of electrical and contractile dysfunction that can lead to arrhythmias in pathophysiological conditions [14], which is the focus of ***Chapter 4*** of this dissertation.

1.2C Cardiofibroblast Function

Cardiofibroblasts are everywhere throughout the cardiac tissue surrounding myocardial fibers and individual cardiomyocytes, and they contribute to structural, biochemical, mechanical and electrical properties of the heart [15-18]. Structurally, cardiofibroblasts sustain tissue structure of the myocardium by regulating extracellular matrix homeostasis and the production of elements that maintain components of connective tissue [15, 17]. Cardiofibroblasts are dynamic cells and play an integral role in the cardiac remodeling process, especially during hypertrophy and fibrosis (discussed below). In the heart, fibroblasts couple with other fibroblasts via gap junction proteins [19]; however, the concept of electrical coupling between cardiomyocytes and cardiofibroblasts remains controversial [20]. Both *in vitro* [21, 22] and *in vivo* [17, 23]

studies have shown that cardiofibroblasts and cardiomyocytes can be electrically coupled via gap junctions, which may allow cardiofibroblasts to act as electrical sinks, contributing to alterations in conduction [24].

1.3 Cardiac Arrhythmia and Sudden Cardiac Death

Although the heart is a robust and vital organ, under particular conditions, the normal electrical and mechanical rhythm becomes irregular and manifests as a cardiac arrhythmia. Many types of arrhythmia exist, but all are characterized by aberrant electrical activation in the myocardium and compromised mechanical activity of the ventricles, with some leading to circulatory deficiency, syncope, and/or sudden cardiac death (SCD) (as reviewed in [25]). Sudden cardiac death is defined as an abrupt and unexpected death in less than an hour from the onset of symptoms from a naturally occurring cardiac event [26]. As a leading cause of morbidity and death, arrhythmias are responsible for about 250,000 – 350,000 incidents of sudden death in the United States and an estimated 4 – 5 million sudden deaths worldwide annually [27-31]. Arrhythmia can sometimes be classified based on the relative frequencies of either a slower or faster than normal rhythm – bradycardia and tachycardia, respectively. Yet, both can be malignant leading to a loss of blood pressure and brain perfusion, syncope, and death [27]. The most life-threatening forms of tachycardia affect ventricular mechanical function: ventricular tachycardia (especially, *torsades de pointes* or polymorphic ventricular tachycardia) and ventricular fibrillation, which is an uncoordinated electrical

activity and contraction characterized by little to no blood ejection and extremely low blood pressure ultimately leading to sudden death [27, 32].

Arrhythmias have been categorized as *triggered* and *reentrant*, and understanding the molecular mechanisms leading to malignant ventricular arrhythmias is clearly important: yet, underlying all arrhythmias are two basic components: substrate (property of the heart that sustains arrhythmia) and trigger (initiator of the arrhythmia) [25, 33, 34]. Thus, arrhythmias may also be thought of as occurring following application of some sort of trigger to a susceptible, pro-arrhythmic substrate [33]. Weiss *et al*. describe normal cardiac action potential propagation as a wave that depolarizes the heart tissue completely followed by a period refractoriness [35]. *Triggered* arrhythmias are thought to arise from extrasystoles (or afterdepolarizations, discussed later), causing abnormally initiated action potential; whereas, *reentrant* arrhythmias occur from re-excitation of tissue that is no longer refractory tissue (but previously excited) after which an action potential wave fails to extinguish completely [36, 37].

Pro-arrhythmic triggers can be anatomical (e.g., fibrosis or infarction) or be physiologic (e.g., extrasystole or the refractoriness caused by an extrasystole) [25]. Extrasystoles can result from dual pacemakers (both AV nodal and Perkinje cells have automaticity properties) [37] and stress from irregular wave reflection on the heart [38]; however, most are early- and delayed-afterdepolarizations (EADs and DADs, respectively). EADs occur before complete repolarization of the action potential during Phases 2 or 3, and DADs occur during diastole and after the myocardium tissue has repolarized (Phase 4) [39]. These afterdepolarizations cause functional barriers by producing areas of

refractoriness [40, 41] that arise *in vivo* because of secondary membrane depolarization at the single cell level [42-44]. When a substrate is present, these functional obstacles provide a point about which the propagating waves are able to rotate [25, 34, 45]. Such substrate could be areas of heterogeneity or slowed conduction velocity (caused by fibrosis, infract, ion channel and gap junction distribution, etc.) where the wave fails to dissipate, and the tissue recovers before the wave returns [25, 46]. This dissertation examines both aspects of substrate and trigger and how they may interact and are enhanced in the aging heart to contribute to a higher incidence of age-associated ventricular arrhythmias.

1.4 Aging and Cellular Senescence

1.4A Overview of Aging and Senescence

Aging is a degenerative process marked by the gradual reduction or loss of function that occurs at the organismal, tissue, cellular, and molecular levels and is marked by a significant increased risk for disease. Although the study of aging is very complex and filled with controversial and sometimes conflicting theories, animal models of aging are ideal as they allow for animals to be studied mainly in protected environments, thus controlling for non-degenerative causes of death and disease found in their natural environments [47]. In most species, ranging from single-celled organisms to large animals, the aging process is apparent via a decline in features at the organ and organismal level. Less apparent is what occurs at the cellular and molecular level. Some have suggested that deleterious cellular and molecular changes occur over time,

and others believe that aging is associated with an intrinsic genetic program that leads to a distinct aging phenotype (as reviewed in [48]). Increasing evidence suggests that cellular senescence is linked to multiple age-related degenerative pathologies.

When first observed in human fibroblasts in the 1960s, cellular senescence was thought to act as a “mitotic clock” to protect against unwonted cellular proliferation [49, 50]. Since then, it has been found that senescent cells remain biologically active but are distinguished not only by irreversible growth arrest but also by changes in nuclear and physical structure, gene expression, protein processing, and metabolism; moreover, these cells have the ability to modify their extracellular environment [51].

1.4B Cell Signaling of Cellular Senescence

The term *cellular senescence* encompasses a phenotype that includes both a great range of stress-induced arrests, as well as senescence states that are characterized by various signaling imbalances (reviewed in [52-54]). Furthermore, no universal biomarker for cellular senescence exists, and many factors are implicated in causing cellular senescence. Yet, the senescent phenotype of cells can be attributed to genotoxic stress mediated via the $p16^{INK4a}$ and p53 pathways [53, 55, 56].

Cellular senescence via a stress stimuli leading to DNA damage response (DDR) is mediated via the p53 pathway [57]. DNA damage causes the activation of DDR proteins, such as checkpoint kinase 2 (CHK2), ataxia telangiectasia mutated (ATM) kinase), p53 binding protein 1 (53BP1), and γH2AX, and leads to the accumulation of

p53 in the cell [58, 59]. p53 is a transcription factor and tumor suppressor protein that induces senescence as it aggregates in the cell upon stress leading to the transcriptional transactivation of p21 (a cyclin-dependent kinase inhibitor, CDKI) and ultimately to cell cycle arrest, and this sustained signaling leads to the senescent phenotype [60]. In humans, p53 pathway is highly regulated by the E3 ubiquitin ligase human double minute 2 homolog (HDM2) and the alternate-reading-frame protein (ARF (p19)), which targets p53 for proteasome-mediated degradation and negatively regulates HDM2, respectively [61]. In addition to cell cycle arrest described above, activation of p53 can lead to DNA repair or apoptosis [62]. p53 activity is also regulated posttranslationally via oxidation, phosphorylation, and acetylation (as reviewed by [63]). Sakaguchi *et al.* showed *in vivo* evidence that p53 is acetylated at Lys382 in humans, which enhances its binding to DNA [64]; however, oxidation of p53 has been shown to decrease DNA binding [65]. Damage of DNA causes the phosphorylation of p53 at Ser15 and Ser20 [66]. p53 phosphorylation at Ser46 controls its ability to induce apoptosis [67]. Ullrich *et al.* also showed in humans that p53 phosphorylation (at Ser392) is increased tumors [68], which is important in regulating p53's growth suppressor and transcriptional activities [69, 70].

Additionally, the cellular senescence phenotype can be mediated by the p16 pathway. p16 is also a CDKI and maintains the transcriptional regulator retinoblastoma protein (pRB) in an active, hypophosphorylated form, which prevents the transcription factor E2F from transcribing genes required for proliferation [61]. Although the mechanism of p16 upregulation is less clear than for p53, it has been shown that activated Ras oncogene activates E26 transformation-specific (ETS) transcription factors [71] or leads

to constitutive mitogen-activated protein kinase (MAPK) signaling [72], which induced p16. DDR can also indirectly lead to senescence via the p16 pathway through p53 signaling through p21 activation of pRb [73, 74].

Along with the upregulation of the p53 and p16 pathways and irreversible growth arrest, both in vitro and in vivo studies have shown that senescent cells express senescence associated (SA)-β-galactosidase, secrete cytokines, growth factors, and numerous other proteins and proteases [75-79]. Senescent cells undergo DNA damage response (DDR) (as presented as DDR foci) and show heterochromatin reorganization [55, 75, 80-82].

1.4C Studies of Cellular Senescence in the Heart

Previous studies of the role of cellular senescence in the heart have been performed in mice [83-85]. Krishnamurthy showed an age-related increase of senescence markers in the heart (and other organs) that was attenuated with calorie restriction [84]. Torella *et al.* used wild-type (WT) mice and examined markers of cellular senescence, cell death, telomerase activity, and telomere integrity to determine whether cellular aging leads to a cardiomyopathy and heart failure [83]. This study showed that expression of senescence markers (p27, p53, p16, and p19) and DNA damage increased with age and that telomerase activity decreased leading to uncapping of telomeres with age in myocytes [83]. Torella *et al.* also showed an age-related increase in markers of cellular senescence and cell death increased in cardiac stem cells (CSCs) [83]. Taken together, this study concluded that myocyte apoptosis and necrosis exceeded renewal by CSCs

in old WT mice leading to fewer myocytes and likely contributed to heart failure (as assessed by myocyte contractility and calcium transients) [83]. Recently, Inuzuka *et al*. also showed that declined cardiac mechanical function, accumulation of ubiquitinated proteins and lipofuscin, and markers of cellular senescence (p16, p19, and senescence-associated β-galactosidase) were correlated in old mice [85]. However, suppression of phosphoinositide-3-kinase – an important effector in insulin/IGF-1 signaling – prevented age-associated cellular senescence, fibrosis, and cardiac dysfunction [85].

Although previous studies have attempted to address the link between senescence and myocardial aging, these studies have not thoroughly addressed cardiac arrhythmia. Later, ***Chapter 3*** will address the role of cellular senescence with regard to arrhythmogenesis in the aging heart.

1.5 Aging and Cardiac Dysfunction

Aging is associated with an 8-fold increase in the incidence of sudden cardiac death between early adulthood and age 65 [86]. Cardiac aging is a biological phenomenon that is complex and diverse and is associated with many changes to structure and function. Of note, several age-related cardiovascular pathologies are associated with co-morbidities and not primarily due to aging alone but are secondary effects; moreover, this dysfunction may affect different areas of the heart and vasculature in different ways and at different times [87]. However, comprehending how aging alters cardiovascular function and structure in regard to increased risk of ventricular arrhythmias is imperative

to the development of therapies for the aging population and to the prevention of sudden cardiac death.

1.5A Age-Associated Structural Changes

Aging is associated with structural remodeling of the myocardium including changes to the anatomy, increase in fibrosis, and physiological hypertrophy (discussed below). Changes in the anatomy include an increased aortic diameter [88], a shift to the right in the ascending aorta and to the left in the descending aorta and an altered interventricular septum [89]. MeLean *et al.* describe a narrowing of the descending aorta and a partial degeneration of sympathetic nerve supply [90]. Also, it has been well documented that the aging heart hypertrophies as evidenced by increased LV mass, which has been attributed to increased cardiomyocyte size and an increase of the extracellular matrix deposition (fibrosis) [91-93]; both hypertrophy and fibrosis have been linked to increased arrhythmogenicity. Fibrosis creates a heterogeneous tissue environment that includes both electrically passive and excitable areas leading to asynchronous propagation making fibrosis an obvious arrhythmogenic substrate [94]. Exhibiting greater arrhythmogenic potential, myocardium that is hypertrophied has been shown to behave similarly to infracted hearts with scarring [86]. Additionally, although the substrate is under debate, the extent of hypertrophy and the occurrence of sudden cardiac death are positively correlated in patients with hypertrophic cardiomyopathy [95].

1.5B Aging and Mechanical Dysfunction

Over the years, studies have shown the major cardiac mechanical dysfunction with age to be arterial stiffness and diastolic dysfunction [96-98]. For example, at rest, systolic function, as measured by ejection fraction, stroke volume and cardiac output, are maintained with age; whereas, diastolic function is reduced as presented as an age-related reduction in early diastolic filling [99, 100]. Moreover, the aging heart shows signs of relaxation dysfunction as evidenced by delayed relaxation time as a consequence of enhanced duration of contraction and prolonged action potential duration [87, 101]. Ferrari *et al.* also suggest that these age-related changes in diastolic function may be a functional substrate for the development of diastolic heart failure, which affects many elderly individuals [87]. Interestingly, a more recent study using men and women >45 years, Redfield *et al.* also found that aging is associated with increased vascular and ventricular stiffness during systole and diastole in the absence of any cardiovascular disease [102]. Increased ventricular and vascular stiffening increases hemodynamic stress on the heart and, because of the ill-timed reflected wave, may incur coronary damage and likely contributes to the increased incidence of SCD via initiation of extrasystoles as both triggers and substrates of arrhythmia.

In addition to the heart's lusitropic function, aging blunts the response to both endogenous and exogenous *β*-adrenergic stimulation: catecholamine- and exercise-induced heart rate and contractility parameters were attenuated with increasing age [103]. However, despite insufficient heart rate and contractile reserves, an aged

individual can increase cardiac output to sustain metabolic needs albeit not to the same extent as a younger individual (reduction of cardiac output is about 25%) [87, 103].

In studies using mostly rodents, age-related mechanical dysfunction at the whole heart level is reflected by changes in the myocytes. Aging cardiomyocytes show prolonged contraction, reduced contractility and diminished *β*-adrenergic contractile response [104-107]. Also, at the molecular level, aging is associated with a downregulation of genes important for contractility, such as sarcomeric, cytoskeletal, and calcium handling proteins (reviewed in [108].

Additionally, rodents show a gradual switch from *α*-myosin heavy chain (MHC) to *β*-MHC as the primary isoform of MHC present in the aging heart, which suggests that similar mechanisms involved in pathological hypertrophy is also involved in age-associated hypertrophy [109, 110]. However, in human ventricles with pathological hypotrophy leading to heart failure, the MHC isoform expression remained unchanged from non-failing controls [111]. Because of potential species differences, questions and controversy remain to how well small animal species represent human pathologies.

1.5C Aging and Electrical Dysfunction

Aging is associated with alterations in conduction properties of the heart that exert a pro-arrhythmic effect. Cardiomyocytes from old rodents and sheep have shown a prolongation of the action potential [112-116], consistent prolongation of the repolarization phase, which have been attributed to an age-related decreasing density

of the transient outward potassium current, I_{to}, and a prolongation of the L-type calcium current [93, 117-119]. Variation in the distribution of connexins (Cx), such as Cx40, Cx43 and Cx45 in the heart are important contributors in order to generate reentrant arrhythmias [120]. Located predominately in the intercalated disks in the normal heart, gap junctions remodel from the end of cardiomyocytes, and the connexins in the ventricle, Purkinje-ventricular myocardium junction, and SA node are downregulated with age [121-124]. Groups have also shown that aging cardiomyocytes have decreased cardiac sodium channel Nav1.5 expression [125, 126]. Since these key determinants of conduction velocity (Cx43, the predominate gap junction protein electrically connecting cardiomyocytes, and Nav1.5, the major voltage-gated Na^+ channel isoform in cardiomyocytes) are remodeled and have reduced expression during aging, cellular coupling in the cardiac muscle and the specialized conduction system propagation is impaired. This, along with increased fibrosis, can explain attenuated conduction within the ventricular tissue and between the Purkinje system and the ventricular muscle.

1.5D Mitochondrial Function and Autophagy and Calcium Cycling in Cardiac Aging

The heart must sustain mechanical and electrical performance with a continuous supply of energy via a large amount of adenosine triphosphate (ATP) produced primarily by mitochondrial oxidative phosphorylation [127] and (reviewed by [128]). To ensure efficient and localized transport of ATP to support cell activities and homeostasis, mitochondria occupy a large part of the cell and are located below the sarcolemma

between the myofibrils [129]. Mitochondria also mediate programed cell death by the opening of the mitochondrial permeability transition pore (mPTP), dissipating the mitochondrial membrane potential and leading to mitochondrial swelling and ultimately apoptosis or necrosis [130, 131]. As a major source or reactive oxygen species (ROS), mitochondria covert 0.2 – 2 % of oxygen to superoxide via the electron transfer activity (mainly by Complex I and III) [128, 132-134]. However, the heart – particularly the mitochondria – has an endogenous antioxidant system, such as manganese superoxide dismutase (MnSOD), catalase, and glutathione peroxidase (GPx), to balance ROS production [128, 135, 136]. Mitochondrial gene expression, enzymatic activity, and function have been shown to be significantly reduced in aging hearts (reviewed by [137] and [104]). Mitochondria have been shown to change in function in numerous models with age. In a mouse model of aging, mitochondria are swollen and have decreased cristae [138]. In old rats, mitochondria have lower production of ATP [139], and in various species, higher production of reactive oxygen species (ROS) is observed in cardiac mitochondria with age [140-145]. In aging cardiomyocytes, which are post-mitotic cells with high utilization of ATP, it has been suggested that the age-related increase in ROS creates a detrimental cycle leading to more mitochondrial damage and cell death [104].

In addition, autophagy is essential to remove and recycle damaged mitochondria (along with damaged organelle, proteins, and macromolecules) via a lysosomal process to ensure cell survival and function (reviewed in [146] and [147]). However, with age, autophagy also declines leading to the accumulation of dysfunctional mitochondria feeding into the deleterious cycle [148, 149]. Although three main forms of autophagy

exist (macroautophagy, microautophagy, and chaperon-mediated autophagy), macroautophagy is most prevalent [150]. Autophagy is regulated by autophagy-related genes (ATGs) [150]. As cytosolic components are sequestered in autophagosomes, the soluble form of microtubule-associated protein 1 light chain 3 (LC3) (LC3-I) is converted to the autophagic vesicle-associated form (LC3-II), which is a classic marker of autophagy [150]. Next, autophagosomes fuse with lysosomes to form autolysosomes, which also degrade luminal LC3II [151]. Sequestosome 1 (SQSTM1 or p62) binds LC3 on the autophagosome [152] and is degraded as autophagy proceeds and can be used as a measure of autophagic flux [153].

Aging has also been shown to be associated with changes in calcium handling in various model species. In the ovine model, Dibb *et al.* observed an increase in APD_{90} and Ca^{2+} transient amplitude but a maintenance of SR Ca^{2+} load with age, which they attributed to greater inward L-type Ca^{2+} current that provides an increased trigger for Ca^{2+}-induced Ca^{2+} release from the sarcoplasmic reticulum [112]. Additionally, calcium transient amplitudes and decay times have been shown to be reduced with age in murine models at pacing frequencies greater than 2 Hz [154-156]. The reduction of calcium amplitudes and decays in old cardiomyocytes at higher frequencies in murine models are likely due to the reduced role of I_{ca} current in mice and rats as well as an age-associated decrease in CaM kinase phosphorylation of RyR2 and SERCA at high pacing frequencies [157]. Howlett *et al*. found that the frequency of spontaneous Ca^{2+} sparks was increased in myocytes from old mice hearts whilst aging did not alter the spark amplitude and SR Ca^{2+} load [156], and in rat, Zhu *et al.* showed that the aging effects are an increase in spark frequency and a decrease in spark amplitude and SR

Ca^{2+} load as well as an increase in RyR2 open probability [158]. Differences in calcium parameters across aging models further reinforce that many age-related differences at the cellular level exist among species; yet, these models all suggest that major changes with age occur at the level of the SR and implicate age-related changes in calcium handling as a potential substrate or trigger for arrhythmia.

1.6 The Rabbit Model for Cardiac Aging

The rabbit heart is very similar to the human myocardium. Electrically, the cardiac action potentials of the rabbit and human have very similar shapes. Rodents, however, have very short action potential durations and lack the plateau phase [11]. Limiting their generalizability to human patients, rodents also have different channels to produce repolarizing currents [159]. On the other hand, rabbits have the same repolarizing K^+ currents (i.e., I_{Kr} and I_{Ks}) and represent a more physiologically relevant model system with regard to electrical activity [160]. Like humans, the primary adult form of myosin heavy-chain is the β isoform [161, 162]. With regard to Ca^{2+} dynamics, rabbit cardiomyocytes (like humans) derive about 70% of cytosolic Ca^{2+} from the sarcoplasmic reticulum; whereas, rodents rely more heavily on SR Ca^{2+} (~90%) due to the lack of L-type Ca^{2+} channels [161, 162]. Also, rabbits and humans rely on the Na^+/Ca^{2+}-exchanger for about 30% of calcium efflux [161, 162].

New Zealand White (NZW) rabbits, which have a lifespan of 5 – 7 years [163], was the model used in the studies for this dissertation. In previous cardiac electrophysiological

and histological aging studies using New NZW rabbits, Gottwald *et al.* defined “old” rabbits to be 1.5 – 2 years of age, which is similar to rodent aging models [164]. However, Von Holst *et al*. and other groups have documented nearly fifty-percent mortality when housing rabbits from 1 to 4 years of age [165-167]. Since the term *old* is defined as the age at which a population reaches fifty percent mortality, we defined our old population similarly. Thus, in the work in the following chapters, we used young (aged 5 – 9 months) and old (aged 3.5 – 6 years) female, NZW rabbits, which is comparable to adolescent and late-middle aged humans.

1.7 Hypotheses and Specific Aims

1.7A Rationale and Overall Hypothesis

As mentioned above, aging is associated with a drastic increase in the incidence of sudden cardiac death. The aging heart is characterized by an increase in fibrosis in the conduction system associated with slowing of the conduction velocity (CV) and increased incidence of conduction block [168-171]. It is likely that these morphologic changes exert a pro-arrhythmic effect by decreasing the threshold for ventricular fibrillation (VF) and by providing a substrate for deadly arrhythmias [123, 126]. Yet, much remains unknown about the mechanisms that underlie the age-related, pro-arrhythmic changes in the mammalian heart at the cellular and molecular level and how they are related to increased incidence of sudden cardiac death. This putative link connecting organismal aging, cellular aging, and heart disease remains ambiguous and controversial. However, in various species, calcium dynamics – a known trigger of

arrhythmia – has been shown to be altered with age [154-158]. Also, *in vivo* data have demonstrated that senescent cells accumulate with advancing cardiac and organismal age [83, 172]. In their attempt to connect age-associated cellular changes and cardiac aging, these studies have primarily relied on correlative evidence and have not thoroughly provided mechanistic insight to address the age-associated increase in arrhythmia and alterations that occur at the molecular level. Here, we provide evidence supporting the hypothesis that cellular aging leads to *in vivo* dysfunction and is an important component that provides both substrate and trigger for arrhythmias in the aging heart. To that end, ***Chapters 2 – 4*** will address the aims of this dissertation as follows:

1.7B Specific Aim 1

Specific Aim 1: To characterize the age-associated changes in left ventricular and aortic function, excitation, and contractility via a series of *in vivo* hemodynamic and electrophysiological studies in young and old rabbits.

Proper myocardium structure and function is dependent upon absolutely normal tissue architecture that maintains normal action potential propagation via cardiomyocytes, which are easily excitable and properly coupled. ***Chapter 2*** tests the hypothesis that aging alters electromechanical and structural properties of the heart and provides an adequate substrate for arrhythmias. We also characterized the young and old female rabbit hearts in order to prove that their function recapitulates the aging human heart. As part of a larger collaborative project, ***Chapter 2*** also presents published data that

includes my contribution towards elucidating the age-associated, pro-arrhythmic substrate in the rabbit heart via *in vivo* cardiac hemodynamics, aortic compliance studies, echocardiography, and histology.

1.7C Specific Aim 2

Specific Aim 2: To identify, quantify, and compare cellular senescence and hypertrophy in heart tissue and cells from young and old rabbits using known biomarkers of cellular senescence and pathological hypertrophy.

The accumulation of senescent cells with increased age may have deleterious effects on cardiac function. Senescent cells can be identified and quantified at the tissue and cellular level. Senescent (or senescent-like) cardiomyocytes, with altered gene expression, could exhibit abnormal excitability and reduced contractility, as well as be more resistant to apoptosis. This could also partially explain the slowing of conduction velocities and deteriorating ventricular function with regard to age (***Chapter 2***). Also, senescent cardiofibroblasts could have increased levels of extracellular matrix proteins, and an increase in interstitial collagen production between cardiomyocytes may contribute to the age-associated increase in fibrosis as reported in the literature, and confirmed in our preliminary data as well. Thus, ***Chapter 3*** summarizes unpublished data and tests the hypothesis that cellular senescence increases with organismal and cardiac age, which alters gene and protein expression, including pathological hypertrophy markers, and leads to increased trigger for cardiac arrhythmia.

1.7D Specific Aim 3

Specific Aim 3: (a) To characterize the age-related changes in calcium (Ca^{2+}) dynamics, action potential durations (APDs), and depolarizing and repolarizing currents in myocytes derived from young and old rabbits and (**b**) to describe an underlying mechanism for these changes.

Abnormal calcium (Ca^{2+}) cycling is an important contributor to the electrical and contractile dysfunction associated with aging. Yet, the specific molecular mechanisms underlying abnormal Ca^{2+} handling in the aging heart remain poorly understood. Furthermore, age-associated alterations in cardiomyocyte may directly affect ion-channels' functions, and therefore, their corresponding depolarizing and repolarizing currents, as well as calcium handling. These alterations could form the molecular trigger that would initiate arrhythmias in the aging myocardium. Thus, ***Chapter 4*** tests the hypotheses (1) that aging at the cellular level alters Ca^{2+} homeostasis and APD and (2) that changes in Ca^{2+} homeostasis are caused by post-translational modification of ryanodine receptors (RyR) by mitochondria-derived reactive oxygen species (ROS) generated in the aging heart. As part of a collaborative project between the Koren and Terentyev labs, this chapter summarizes data to be submitted as an original research manuscript and includes my contribution toward elucidating the calcium-dependent, pro-arrhythmic trigger in the aging rabbit heart via confocal calcium imaging, imaging of mitochondrial membrane potential and reactive oxygen species, and biochemistry.

1.8 References

1. Mohrman DE, Heller LJ: **Cardiovascular Physiology**, Sixth edn. New York: Lange Medical Books/McGraw-Hill; 2006.
2. Iyer V, Edelman ER, Lilly LS: **Basic Cardiac Structure and Function**. In: *Pathophysiology of Heart Disease.* Fourth edn. Edited by Lilly LS. Philadelphia, Baltimore: Lippincott Williams and Wilkins; 2007: 1 -- 28.
3. Garibyan L, Lilly LS: **The Electrogram**. In: *Pathophysiology of Heart Failure.* Edited by Lilly LS. Philadelphia, Baltimore: Lippincott Williams and Wilkins; 2007: 80 -- 117.
4. Thomas KE, Zimetbaum PJ: **Electrophysiology Study: Indications and Interpretations**. In: *Management of Cardiac Arrhythmias. Volume* New York, Dordrecht, Heidelberg, London, Second edn. Edited by Yan G-X, Kowey PR: Humana Press and Springer; 2011: 123 -- 138.
5. Martin N, Lilly LS: **The Cardiac Cycle: Mechanisms of Heart Sounds and Murmurs**. In: *Pathophysiology of Heart Disease.* Fourth edn. Edited by Lilly LS. Philadelphia, Baltimore: Lippincott Williams and Wilkins; 2007: 29 -- 45.
6. Martin N, Come PC: **Diagnostic Imaging and Cardiac Catheterization**. In: *Pathophysiology of Heart Disease.* Fourth edn. Edited by Lilly LS. Philadelphia, Baltimore: Lippincotte Williams and Wilkins; 2007: 46 -- 79.
7. Shah RV, Fifer MA: **Heart Failue**. In: *Pathophysiology of Heart Disease.* Edited by Lilly LS, Fourth edn. Phiadelphia, Baltimore: Lippincott Williams and Wilkins; 2007: 225 -- 252.

8. Banerjee I, Fuseler JW, Price RL, Borg TK, Baudino TA: **Determination of Cell Types and Numbers During Cardiac Development in the Neonatal and Adult Rat and Mouse**. *Am J Physiol -- Heart C* 2007, **293**(3):H1883 -- 1891.

9. Nag AC: **Study of Non-Muscle Cells of the Adult Mammalian Heart: A Fine Structural Analysis and Distribution**. *Cytobios* 1980, **28**(109):41 -- 61.

10. Vliegen HW, van der Laarse A, Cornelisse CJ, Eulderink F: **Myocardial Changes in Pressure Overload-Induced Left Ventricular Hypertrophy. A Study on Tissue Composition, Polyploidization and Multinucleation**. *Eur Heart J* 1991, **12**(4):488 -- 494.

11. Bers DM: **Excitation-Contraction Coupling and Cardiac Contractile Force**, Second edn. Dordrecht, The Netherlands: Kluwer Academic Publishers; 2001.

12. Pinnell J, Turner S, Howell S: **Cardiac Muscle Physiology**. *CEACCP* 2007, **7**(3):85 -- 88.

13. Bers DM: **Cardiac Excitation-Contraction Coupling**. *Nature* 2002, **415**(6868):198 -- 205.

14. Pogwizd SM, Schlotthauer K, Li L, Yuan W, Bers DM: **Arrhythmogenesis and Contractile Dysfunction in Heart Failure: Roles of Sodium-Calcium Exchange, Inward Rectifier Potassium Current, and Residual Beta-Adrenergic Responsiveness**. *Circ Res* 2001, **88**(11):1159 -- 1167.

15. MacKenna D, Summerour SR, Villarreal FJ: **Role of Mechanical Factors in Modulating Cardiac Fibroblast Function and Extracellular Matrix Synthesis**. *Cardiovasc Res* 2000, **46**(2):257 -- 263.

16. Camelliti P, Green CR, LeGrice I, Kohl P: **Fibroblast Network in Rabbit Sinoatrial Node: Structural and Functional Identification of Homogeneous and Heterogeneous Cell Coupling**. *Circ Res* 2004, **94**(6):828 -- 835.

17. Camelliti P, Borg TK, Kohl P: **Structural and Functional Characterisation of Cardiac Fibroblasts**. *Cardiovas Res* 2005, **65**(1):40 -- 51.

18. Sun Y, Weber KT: **Infarct Scar: A Dynamic Tissue**. *Cardiovasc Res* 2000, **46**(2):250 -- 256.

19. Gaudesius G, Miragoli M, Thomas SP, Rohr S: **Coupling of Cardiac Electrical Activity Over Extended Distances by Fibroblasts of Cardiac Origin**. *Circ Res* 2003, **93**(5):421 -- 428.

20. Baum J, Duffy HS: **Fibroblasts and Myofibroblasts: What Are We Talking About?** *J Cardiovasc Pharm* 2011, **57**(4):376 -- 379.

21. Rook MB, Vanginneken ACG, Dejonge B, Elaoumari A, Gros D, Jongsma HJ: **Differences in Gap Junction Channels Between Cardiac Myocytes, Fibroblasts, and Heterologous Pairs**. *Am J Physiol* 1992, **263**(5):C959 -- C977.

22. Goshima K: **Formation of Nexuses and Electrotonic Transmission Between Myocardial and Fl Cells in Monolayer Culture**. *Exp Cell Res* 1970, **63**(1):124 -- 130.

23. Kohl P, Kamkin AG, Kiseleva IS, Noble D: **Mechanosensitive Fibroblasts in the Sino-Atrial Node Region of Rat Heart: Interaction with Cardiomyocytes and Possible Role**. *Exp Physiol* 1994, **79**(6):943 -- 956.

24. Kohl P, Camelliti P, Burton FL, Smith GL: **Electrical Coupling of Fibroblasts and Myocytes: Relevance for Cardiac Propagation**. *J Electrocardiol* 2005, **38**(4 Suppl):45 -- 50.

25. Kalin A, Usher-Smith J, Jones VJ, Huang CL, Sabir IN: **Cardiac Arrhythmia: A Simple Conceptual Framework**. *Trends Cardiovas Med* 2010, **20**(3):103 -- 107.

26. Engelstein ED, Zipes DP: **Sudden Cardiac Death**. In: *The Heart, Arteries and Veins.* edn. Edited by R.W. A, Schlant RC, Fuster V. New York, NY: McGraw-Hill; 1998.

27. Keating MT, Sanguinetti MC: **Molecular and Cellular Mechanisms of Cardiac Arrhythmias**. *Cell* 2001, **104**(4):569 -- 580.

28. Kannel WB, Doyle JT, Shephard RJ, Stamler J, Vokonas PS: **Prevention Of Cardiovascular-Disease in the Elderly**. *J Am Coll Cardiol* 1987, **10**(2):A25 -- A28.

29. Willich SN, Levy D, Rocco MB, Tofler GH, Stone PH, Muller JE: **Circadian Variation in the Incidence of Sudden Cardiac Death in the Framingham Heart-Study Population**. *Am J Cardiol* 1987, **60**(10):801 -- 806.

30. Chugh SS, Reinier K, Teodorescu C, Evanado A, Kehr E, Al Samara M, Mariani R, Gunson K, Jui J: **Epidemiology of Sudden Cardiac Death: Clinical and Research Implications**. *Prog Cardiovasc Dis* 2008, **51**(3):213 -- 228.

31. Myerburg RJ, Castellanos A: **Sudden Cardiac Death**. In: *Cardiac Electrophysiology: from Cell to Bedside.* Fifth edn. Edited by Zipes DP, Jalife J. Philadelphia, PA: Saunders and Elsevier; 2009: 797 -- 808.

32. Lazzara R: **Twisting of the Points**. *J Am Coll Cardiol* 1997, **29**(4):843 -- 845.

33. Antzelevitch C, Yan GX, Shimizu W: **Transmural Dispersion of Repolarization and Arrhythmogenicity: The Brugada Syndrome Versus the Long QT Syndrome**. *J Electrocardiol* 1999, **32 Suppl**:158 -- 165.

34. Garrey WE: **Auricular Fibrillation**. *Physiol Rev* 1924, **4**(2):215 -- 250.

35. Weiss JN, Chen PS, Qu ZL, Karagueuzian HS, Garfinkel A: **Ventricular Fibrillation - How Do We Stop the Waves from Breaking?** *Circ Res* 2000, **87**(12):1103 -- 1107.

36. Antzelevitch C: **Basic Mechanisms of Reentrant Arrhythmias**. *Curr Opin Cardio* 2001, **16**(1):1 -- 7.

37. Antzelevitch C, Burashnikov A, Di Diego JM: **Cellular and Ionic Mechanisms Underlying Arrhythmogenesis**. In: *Cardiac Repolarization : Bridging Basic and Clinical Science.* edn. Edited by Gussak I, Antzelevitch C. Totowa, N.J.: Humana Press; 2003.

38. Antzelevitch C, Jalife J, Moe GK: **Characteristics of Reflection as a Mechanism of Reentrant Arrhythmias and Its Relationship to Parasystole**. *Circulation* 1980, **61**(1):182 -- 191.

39. Anderson ME, Hodgson-Zingman DM: **Ventricular Tachycardia in Patients with Heart Failure**. In: *Cardiac Electrophysiology: From Cell to Bedside.* Fifth edn. Edited by Zipes DP, Jalife J. Philadelphia, PA: Saunders and Elsevier; 2009.

40. Sabir IN, Killeen MJ, Grace AA, Huang CLH: **Ventricular Arrhythmogenesis: Insights from Murine Models**. *Prog Biophys Mol Bio* 2008, **98**(2-3):208 -- 218.

41. Weiss JN, Karma A, Shiferaw Y, Chen PS, Garfinkel A, Qu Z: **From Pulsus to Pulseless: the Saga of Cardiac Alternans**. *Circ Res* 2006, **98**(10):1244 -- 1253.

42. January CT, Riddle JM: **Early Afterdepolarizations: Mechanism of Induction and Block: A Role for L-type Ca^{2+} Current**. *Circ Res* 1989, **64**(5):977 -- 990.

43. Priori SG, Corr PB: **Mechanisms Underlying Early and Delayed Afterdepolarizations Induced by Catecholamines**. *Am J Physiol* 1990, **258**(6 Pt 2):H1796 -- 1805.

44. Zygmunt AC, Goodrow RJ, Weigel CM: **I_{Na-Ca} and $I_{Cl(Ca)}$ Contribute to Isoproterenol-Induced Delayed After Depolarizations in Midmyocardial Cells**. *Am J Physiol* 1998, **275**(6 Pt 2):H1979 -- 1992.

45. Muñoz V, Noujaim SF, Jalife J: **Dynamics and Molecular Mechanisms of Ventricular Tachycardia and Fibrillation in Normal Hearts**. In: *Cardiac Electrophysiology: From Cell to Bedside.* Fifth edn. Edited by Zipes DP, Jalife J. Philadelphia, PA: Saunders and Elsevier; 2009: 473 -- 482.

46. Kleber AG, Rudy Y: **Basic Mechanisms of Cardiac Impulse Propagation and Associated Arrhythmias**. *Physiol Rev* 2004, **84**(2):431 -- 488.

47. Lapointe J, Hekimi S: **When A Theory of Aging Ages Badly**. *Cell Mol Life Sci* 2010, **67**(1):1 -- 8.

48. Shringarpure R, Davies KJA: **Protein Turnover by the Proteasome in Aging and Disease**. *Free Radical Bio Med* 2002, **32**(11):1084 --1089.

49. Hayflick L, Moorhead PS: **The Serial Cultivation of Human Diploid Cell Strains**. *Exp Cell Res* 1961, **25**:585 -- 621.

50. Campisi J: **Replicative Senescence: An Old Lives' Tale?** *Cell* 1996, **84**(4):497 -- 500.

51. Ben-Porath I, Weinberg RA: **When Cells Get Stressed: an Integrative View of Cellular Senescence**. *J Clin Invest* 2004, **113**(1):8 -- 13.

52. Collado M, Blasco MA, Serrano M: **Cellular Senescence in Cancer and Aging**. *Cell* 2007, **130**(2):223 -- 233.

53. Jeyapalan JC, Sedivy JM: **Cellular Senescence and Organismal Aging**. *Mechanisms of Ageing and Development* 2008, **129**(7-8):467 -- 474.

54. Rodier F, Campisi J: **Four Faces of Cellular Senescence**. *J Cell Biol* 2011, **192**(4):547 -- 556.

55. d'Adda di Fagagna F, Reaper PM, Clay-Farrace L, Fiegler H, Carr P, Von Zglinicki T, Saretzki G, Carter NP, Jackson SP: **A DNA Damage Checkpoint Response in Telomere-Initiated Senescence**. *Nature* 2003, **426**(6963):194 -- 198.

56. Herbig U, Jobling WA, Chen BPC, Chen DJ, Sedivy JM: **Telomere Shortening Triggers Senescence of Human Cells Through a Pathway Involving ATM, p53, And p21^{Cip1}, but Not p16^{INK4a}**. *Mol Cell* 2004, **14**(4):501 -- 513.

57. Campisi J, d'Adda di Fagagna F: **Cellular Senescence: When Bad Things Happen to Good Cells**. *Nat Rev Mol Cell Bio* 2007, **8**(9):729 -- 740.

58. Bartkova J, Horejsi Z, Koed K, Kramer A, Tort F, Zieger K, Guldberg P, Sehested M, Nesland JM, Lukas C *et al*: **DNA Damage Response as a Candidate Anti-Cancer Barrier in Early Human Tumorigenesis**. *Nature* 2005, **434**(7035):864 -- 870.

59. Gorgoulis VG, Vassiliou LV, Karakaidos P, Zacharatos P, Kotsinas A, Liloglou T, Venere M, Ditullio RA, Jr., Kastrinakis NG, Levy B *et al*: **Activation of the DNA Damage Checkpoint and Genomic Instability in Human Precancerous Lesions**. *Nature* 2005, **434**(7035):907 -- 913.

60. Farnebo M, Bykov VJ, Wiman KG: **The p53 Tumor Suppressor: A Master Regulator of Diverse Cellular Processes and Therapeutic Target in Cancer**. *Biochem Biophys Res Commun* 2010, **396**(1):85 -- 89.

61. Sherr CJ, McCormick F: **The RB and p53 Pathways in Cancer**. *Cancer Cell* 2002, **2**(2):103 -- 112.

62. Levine AJ: **p53, The Cellular Gatekeeper for Growth and Division**. *Cell* 1997, **88**(3):323 -- 331.

63. Vousden KH, Prives C: **Blinded by the Light: The Growing Complexity of p53**. *Cell* 2009, **137**(3):413 -- 431.

64. Sakaguchi K, Herrera JE, Saito S, Miki T, Bustin M, Vassilev A, Anderson CW, Appella E: **DNA Damage Activates p53 Through a Phosphorylation-Acetylation Cascade**. *Genes Dev* 1998, **12**(18):2831 -- 2841.

65. Sun XZ, Vinci C, Makmura L, Han S, Tran D, Nguyen J, Hamann M, Grazziani S, Sheppard S, Gutova M *et al*: **Formation of Disulfide Bond in p53 Correlates with Inhibition of DNA Binding and Tetramerization**. *Antioxid Redox Signal* 2003, **5**(5):655 -- 665.

66. Shieh SY, Ikeda M, Taya Y, Prives C: **DNA Damage-Induced Phosphorylation of p53 Alleviates Inhibition by MDM2**. *Cell* 1997, **91**(3):325 -- 334.

67. Oda K, Arakawa H, Tanaka T, Matsuda K, Tanikawa C, Mori T, Nishimori H, Tamai K, Tokino T, Nakamura Y *et al*: **p53AIP1, A Potential Mediator of p53-Dependent Apoptosis, and Its Regulation by Ser-46-phosphorylated p53**. *Cell* 2000, **102**(6):849 -- 862.

68. Ullrich SJ, Sakaguchi K, Lees-Miller SP, Fiscella M, Mercer WE, Anderson CW, Appella E: **Phosphorylation at Ser-15 and Ser-392 in Mutant p53 Molecules from Human Tumors Is Altered Compared To Wild-Type p53**. *Proc Natl Acad Sci USA* 1993, **90**(13):5954 -- 5958.

69. Hao M, Lowy AM, Kapoor M, Deffie A, Liu G, Lozano G: **Mutation of Phosphoserine 389 Affects p53 Function *In Vivo***. *J Biol Chem* 1996, **271**(46):29380 -- 29385.

70. Lohrum M, Scheidtmann KH: **Differential Effects of Phosphorylation of Rat p53 on Transactivation of Promoters Derived from Different p53 Responsive Genes**. *Oncogene* 1996, **13**(12):2527 -- 2539.

71. Ohtani N, Zebedee Z, Huot TJ, Stinson JA, Sugimoto M, Ohashi Y, Sharrocks AD, Peters G, Hara E: **Opposing Effects of Ets and Id Proteins on p16^{INK4a} Expression During Cellular Senescence**. *Nature* 2001, **409**(6823):1067 -- 1070.

72. Lin AW, Barradas M, Stone JC, van Aelst L, Serrano M, Lowe SW: **Premature Senescence Involving p53 and p16 Is Activated in Response to Constitutive MEK/MAPK Mitogenic Signaling**. *Genes Dev* 1998, **12**(19):3008 -- 3019.

73. Xue LX, Wu JF, Zheng WJ, Wang PC, Li J, Zhang ZY, Tong TJ: **Sp1 is involved in the Transcriptional Activation of p16^{INK4} by p21^{Waf1} in HeLa Cells**. *FEBS Lett* 2004, **564**(1-2):199 -- 204.

74. Mitra J, Dai CY, Somasundaram K, El-Deiry WS, Satyamoorthy K, Herlyn M, Enders GH: **Induction of p21$^{WAF1/CIP1}$ and Inhibition of Cdk2 Mediated by the Tumor Suppressor p16^{INK4a}**. *Mol Cell Biol* 1999, **19**(5):3916 -- 3928.

75. Rodier F, Coppe JP, Patil CK, Hoeijmakers WAM, Munoz DP, Raza SR, Freund A, Campeau E, Davalos AR, Campisi J: **Persistent DNA Damage Signalling Triggers Senescence-Associated Inflammatory Cytokine Secretion**. *Nat Cell Biol* 2009, **11**(8):973 -- 979.

76. Dimri GP, Lee X, Basile G, Acosta M, Scott G, Roskelley C, Medrano EE, Linskens M, Rubelj I, Pereira-Smith O *et al*: **A Biomarker That Identifies Senescent Human Cells in Culture and in Aging Skin *In Vivo***. *Proc Natl Acad Sci USA* 1995, **92**(20):9363 -- 9367.

77. Acosta JC, O'Loghlen A, Banito A, Guijarro MV, Augert A, Raguz S, Fumagalli M, Da Costa M, Brown C, Popov N *et al*: **Chemokine Signaling via the CXCR2 Receptor Reinforces Senescence**. *Cell* 2008, **133**(6):1006 -- 1018.

78. Coppe JP, Patil CK, Rodier F, Sun Y, Munoz DP, Goldstein J, Nelson PS, Desprez PY, Campisi J: **Senescence-Associated Secretory Phenotypes Reveal Cell-Nonautonomous Functions of Oncogenic RAS and the p53 Tumor Suppressor**. *PLOS Biol* 2008, **6**(12):2853 -- 2868.

79. Kuilman T, Michaloglou C, Vredeveld LCW, Douma S, van Doom R, Desmet CJ, Aarden LA, Mooi WJ, Peeper DS: **Oncogene-Induced Senescence Relayed by**

an Interleukin-Dependent Inflammatory Network. *Cell* 2008, **133**(6):1019 -- 1031.

80. Herbig U, Jobling WA, Chen BP, Chen DJ, Sedivy JM: **Telomere Shortening Triggers Senescence of Human Cells through a Pathway Involving ATM, p53, and p21^{CIP1}, but Not p16^{INK4a}**. *J Mol Cell* 2004, **14**(4):501 -- 513.

81. Takai H, Smogorzewska A, de Lange T: **DNA Damage Foci at Dysfunctional Telomeres**. *Curr Biol* 2003, **13**(17):1549 -- 1556.

82. Kreiling JA, Tamamori-Adachi M, Sexton AN, Jeyapalan JC, Munoz-Najar U, Peterson AL, Manivannan J, Rogers ES, Pchelintsev NA, Adams PD *et al*: **Age-Associated Increase in Heterochromatic Marks in Murine and Primate Tissues**. *Aging Cell* 2011, **10**(2):292 -- 304.

83. Torella D, Rota M, Nurzynska D, Musso E, Monsen A, Shiraishi I, Zias E, Walsh K, Rosenzweig A, Sussman MA *et al*: **Cardiac Stem Cell and Myocyte Aging, Heart Failure, and Insulin-Like Growth Factor-1 Overexpression**. *Circ Res* 2004, **94**(4):514 -- 524.

84. Krishnamurthy J, Torrice C, Ramsey MR, Kovalev GI, Al-Regaiey K, Su L, Sharpless NE: **INK4a/ARF Expression is a Biomarker of Aging**. *J Clin Invest* 2004, **114**(9):1299 -- 1307.

85. Inuzuka Y, Okuda J, Kawashima T, Kato T, Niizuma S, Tamaki Y, Iwanaga Y, Yoshida Y, Kosugi R, Watanabe-Maeda K *et al*: **Suppression of Phosphoinositide 3-Kinase Prevents Cardiac Aging in Mice**. *Circulation* 2009, **120**(17):1695 -- 1703.

86. Zipes DP, Wellens HJ: **Sudden Cardiac Death**. *Circulation* 1998, **98**(21):2334 -- 2351.

87. Ferrari AU, Radaelli A, Centola M: **Invited Review: Aging and the Cardiovascular System**. *J Appl Physiol* 2003, **95**(6):2591 -- 2597.

88. O'Rourke MF, Nichols WW: **Aortic Diameter, Aortic Stiffness, and Wave Reflection Increase with Age and Isolated Systolic Hypertension**. *Hypertension* 2005, **45**(4):652 -- 658.

89. Goor D, Lillehei CW, Edwards JE: **The "Sigmoid Septum". Variation in the Contour of the Left Ventricular Outt**. *AJR Roentgenol* 1969, **107**(2):366 -- 376.

90. McLean MR, Goldberg PB, Roberts J: **An Ultrastructural Study of the Effects of Age on Sympathetic Innervation and Atrial Tissue in the Rat**. *J Mol Cell Cardiol* 1983, **15**(2):75 -- 92.

91. Rossi S, Baruffi S, Bertuzzi A, Miragoli M, Corradi D, Maestri R, Alinovi R, Mutti A, Musso E, Sgoifo A *et al*: **Ventricular Activation is Impaired in Aged Rat Hearts**. *Am J Physiol - Heart C* 2008, **295**(6):H2336 -- 2347.

92. Gerstenblith G, Frederiksen J, Yin FC, Fortuin NJ, Lakatta EG, Weisfeldt ML: **Echocardiographic Assessment of a Normal Adult Aging Population**. *Circulation* 1977, **56**(2):273 -- 278.

93. Lakatta EG, Zhou Y-Y, R-P X, Boluyt MO: **Aging of the Cardiovascular System**. In: *Heart Physiology and Pathophysiology.* Fourth edn. Edited by Sperelakis N, Kurachi Y, Terzic A, Cohen M: Academic Press; 2000: 737 -- 760.

94. de Jong S, van Veen TA, van Rijen HV, de Bakker JM: **Fibrosis and Cardiac Arrhythmias**. *J Cardiovasc Pharm* 2011, **57**(6):630 -- 638.

95. Spirito P, Maron BJ: **Relation Between Extent of Left Ventricular Hypertrophy and Occurrence of Sudden Cardiac Death in Hypertrophic Cardiomyopathy**. *J Am Coll Cardiol* 1990, **15**(7):1521 -- 1526.

96. Mitchell GF: **Increased Aortic Stiffness: An Unfavorable Cardiorenal Connection**. *Hypertension* 2004, **43**(2):151 -- 153.

97. Mitchell GF, Parise H, Benjamin EJ, Larson MG, Keyes MJ, Vita JA, Vasan RS, Levy D: **Changes in Arterial Stiffness and Wave Reflection with Advancing Age in Healthy Men and Women: the Framingham Heart Study**. *Hypertension* 2004, **43**(6):1239 -- 1245.

98. Lakatta EG, Levy D: **Arterial and Cardiac Aging: Major Shareholders in Cardiovascular Disease Enterprises: Part I: Aging Arteries: A "Set Up" for Vascular Disease**. *Circulation* 2003, **107**(1):139 -- 146.

99. Rodeheffer RJ, Gerstenblith G, Becker LC, Fleg JL, Weisfeldt ML, Lakatta EG: **Exercise Cardiac Output is Maintained with Advancing Age in Healthy Human Subjects: Cardiac Dilatation and Increased Stroke Volume Compensate for a Diminished Heart Rate**. *Circulation* 1984, **69**(2):203 -- 213.

100. Miller TR, Grossman SJ, Schectman KB, Biello DR, Ludbrook PA, Ehsani AA: **Left Ventricular Diastolic Filling and Its Association with Age**. *Am J Cardiol* 1986, **58**(6):531 -- 535.

101. Lakatta EG, Gerstenblith G, Angell CS, Shock NW, Weisfeldt ML: **Prolonged Contraction Duration in Aged Myocardium**. *J Clin Invest* 1975, **55**(1):61 -- 68.

102. Redfield MM, Jacobsen SJ, Borlaug BA, Rodeheffer RJ, Kass DA: **Age- and Gender-Related Ventricular-Vascular Stiffening: A Community-Based Study**. *Circulation* 2005, **112**(15):2254 -- 2262.

103. Fleg JL, Oconnor F, Gerstenblith G, Becker LC, Clulow J, Schulman SP, Lakatta EG: **Impact of Age on the Cardiovascular-Response to Dynamic Upright Exercise in Healthy-Men and Women**. *J Appl Physiol* 1995, **78**(3):890-900.

104. Wessells RJ, Bodmer R: **Cardiac Aging**. *Semin Cell Dev Biol 2*007, **18**(1):111 -- 116.

105. Chiamvimonvat N: **Diastolic Dysfunction and the Aging Heart**. *J Mol Cell Cardiol* 2002, **34**(6):607 -- 610.

106. Sakai M, Danziger RS, Staddon JM, Lakatta EG, Hansford RG: **Decrease with Senescence in the Norepinephrine-Induced Phosphorylation of Myofilament Proteins in Isolated Rat Cardiac Myocytes**. *J Mol Cell Cardiol* 1989, **21**(12):1327 -- 1336.

107. Xiao RP, Spurgeon HA, O'Connor F, Lakatta EG: **Age-Associated Changes in Beta-Adrenergic Modulation on Rat Cardiac Excitation-Contraction Coupling**. *J Clin Iinvest* 1994, **94**(5):2051 -- 2059.

108. Lakatta EG: **Cardiovascular Regulatory Mechanisms in Advanced Age**. *Physiol Rev* 1993, **73**(2):413 -- 467.

109. Effron MB, Bhatnagar GM, Spurgeon HA, Ruano-Arroyo G, Lakatta EG: **Changes in Myosin Isoenzymes, ATPase Activity, and Contraction Duration in Rat Cardiac Muscle with Aging can be Modulated by Thyroxine**. *Circ Res* 1987, **60**(2):238 -- 245.

110. O'Neill L, Holbrook NJ, Fargnoli J, Lakatta EG: **Progressive Changes From Young Adult Age to Senescence in mRNA for Rat Cardiac Myosin Heavy Chain Genes**. *Cardioscience* 1991, **2**(1):1 -- 5.

111. Reiser PJ, Portman MA, Ning XH, Moravec CS: **Human Cardiac Myosin Heavy Chain Isoforms in Fetal and Failing Adult Atria and Ventricles**. *Am J Physiol - Heart C* 2001, **280**(4):H1814 -- H1820.

112. Dibb KM, Rueckschloss U, Eisner DA, Isenberg G, Trafford AW: **Mechanisms Underlying Enhanced Cardiac Excitation Contraction Coupling Observed in the Senescent Sheep Myocardium**. *J Mol Cell Cardiol* 2004, **37**(6):1171 -- 1181.

113. Mace LC, Palmer BM, Brown DA, Jew KN, Lynch JM, Glunt JM, Parsons TA, Cheung JY, Moore RL: **Influence of Age and Run Training on Cardiac Na^+/Ca^{2+} Exchange**. *J Appl Physiol* 2003, **95**(5):1994 -- 2003.

114. Walker KE, Lakatta EG, Houser SR: **Age Associated Changes in Membrane Currents in Rat Ventricular Myocytes**. *Cardiovasc Res* 1993, **27**(11):1968 -- 1977.

115. Wei JY, Spurgeon HA, Lakatta EG: **Excitation-Contraction in Rat Myocardium: Alterations with Adult Aging**. *Am J Physiol* 1984, **246**(6 Pt 2):H784 -- 791.

116. Janczewski AM, Spurgeon HA, Lakatta EG: **Action Potential Prolongation in Cardiac Myocytes of Old Rats is an Adaptation to Sustain Youthful Intracellular Ca^{2+} Regulation**. *J Mol Cell Cardiol* 2002, **34**(6):641 -- 648.

117. Josephson IR, Guia A, Stern MD, Lakatta EG: **Alterations in Properties of L-Type Ca Channels in Aging Rat Heart**. *J Mol Cell Cardiol* 2002, **34**(3):297 -- 308.

118. Hart G: **Cellular Electrophysiology In Cardiac Hypertrophy and Failure**. *Cardiovasc Res* 1994, **28**(7):933 -- 946.

119. Cerbai E, Barbieri M, Li Q, Mugelli A: **Ionic Basis of Action Potential Prolongation of Hypertrophied Cardiac Myocytes Isolated from Hypertensive Rats of Different Ages**. *Cardiovasc Res* 1994, **28**(8):1180 -- 1187.

120. Rossi S, Baruffi S, Bertuzzi A, Mastorci F, Sgoifo A, Musso E, Corradi D, Maestri R, Brisinda D, Fenici R *et al*: **Susceptibility to Ventricular Arrhythmias In Aged Hearts**. *Conf Proc IEEE Eng Med Biol Soc,* **2007**:410 -- 414.

121. Jones SA, Lancaster MK, Boyett MR: **Ageing-Related Changes of Connexins and Conduction within the Sinoatrial Node**. *J Physiol* 2004, **560**(2):429 -- 437.

122. Spach MS, Heidlage JF, Dolber PC, Barr RC: **Electrophysiological Effects of Remodeling Cardiac Gap Junctions and Cell Size: Experimental and Model Studies of Normal Cardiac Growth**. *Circ Res* 2000, **86**(3):302 -- 311.

123. Dhein S, Hammerath SB: **Aspects of the Intercellular Communication in Aged Hearts: Effects of the Gap Junction Uncoupler Palmitoleic Acid**. *Naunyn-Schmiedebergs Arch Pharmacol* 2001, **364**(5):397 -- 408.

124. Stein M, Noorman M, van Veen TA, Herold E, Engelen MA, Boulaksil M, Antoons G, Jansen JA, van Oosterhout MF, Hauer RN *et al*: **Dominant Arrhythmia**

Vulnerability of the Right Ventricle in Senescent Mice. *Heart Rhythm* 2008, **5**(3):438 -- 448.

125. Yanni JF, Tellez JO, Dobrzynski H, Boyett MR: **Age-Dependent Changes In HCN4 And Nav1.5 in the Sinoatrial Node**. *J Mol Cell Cardiol* 2007, **42**:S15 -- S15.

126. Stein M, Noorman M, van Veen TAB, Herold E, Engelen MA, Boulaksil M, Antoons G, Jansen JA, van Oosterhout MFM, Hauer RNW *et al*: **Dominant Arrhythmia Vulnerability of the Right Ventricle in Senescent Mice**. *Heart Rhythm* 2008, **5**(3):438 -- 448.

127. Ashrafian H, Frenneaux MP: **Metabolic Modulation in Heart Failure: The Coming of Age**. *Cardiovasc Drug Ther* 2007, **21**(1):5 -- 7.

128. Gustafsson AB, Gottlieb RA: **Heart Mitochondria: Gates of Life and Death**. *Cardiovasc Res* 2008, **77**(2):334 -- 343.

129. Andrienko T, Kuznetsov AV, Kaambre T, Usson Y, Orosco A, Appaix F, Tiivel T, Sikk P, Vendelin M, Margreiter R *et al*: **Metabolic Consequences of Functional Complexes of Mitochondria, Myofibrils and Sarcoplasmic Reticulum in Muscle Cells**. *J Exp Biol* 2003, **206**(Pt 12):2059 -- 2072.

130. Halestrap AP: **Calcium, Mitochondria and Reperfusion Injury: A Pore Way to Die**. *Biochem Soc Trans* 2006, **34**(Pt 2):232 -- 237.

131. Gustafsson AB, Gottlieb RA: **Mechanisms of Apoptosis in the Heart**. *J Clin immunol* 2003, **23**(6):447 -- 459.

132. Chen Q, Vazquez EJ, Moghaddas S, Hoppel CL, Lesnefsky EJ: **Production of Reactive Oxygen Species by Mitochondria: Central Role of Complex III**. *J Biol Chem* 2003, **278**(38):36027 -- 36031.

133. Turrens JF: **Mitochondrial Formation of Reactive Oxygen Species**. *J Physiol* 2003, **552**(Pt 2):335 -- 344.

134. Staniek K, Nohl H: **H_2O_2 Detection from Intact Mitochondria as a Measure for One-Electron Reduction of Dioxygen Requires a Non-Invasive Assay System**. *Biochimica Et Biophysica Acta* 1999, **1413**(2):70 -- 80.

135. Giordano FJ: **Oxygen, Oxidative Stress, Hypoxia, and Heart Failure**. *J Clin Invest* 2005, **115**(3):500 -- 508.

136. Nordberg J, Arner ES: **Reactive Oxygen Species, Antioxidants, and the Mammalian Thioredoxin System**. *Free Radical Bio Med* 2001, **31**(11):1287 -- 1312.

137. Hudson EK, Tsuchiya N, Hansford RG: **Age-Associated Changes in Mitochondrial mRNA Expression and Translation in the Wistar Rat Heart**. *Mech Ageing Dev* 1998, **103**(2):179 -- 193.

138. Coleman R, Silbermann M, Gershon D, Reznick AZ: **Giant Mitochondria in the Myocardium of Aging and Endurance-Trained Mice**. *Gerontology* 1987, **33**(1):34 -- 39.

139. Muscari C, Finelli C, Stefanelli C, Flamigni F, Guarnieri C, Caldarera CM: **Age-Dependent Differences of ATP Breakdown and ATP-Catabolite Release in Ischemic and Reperfused Hearts**. *Mech Ageing Dev* 1993, **67**(1-2):1 -- 11.

140. Muscari C, Caldarera CM, Guarnieri C: **Age-Dependent Production of Mitochondrial Hydrogen Peroxide, Lipid Peroxides and Fluorescent Pigments in the Rat Heart**. *Basic Res Cardiol* 1990, **85**(2):172 -- 178.

141. Sohal RS, Sohal BH: **Hydrogen Peroxide Release by Mitochondria Increases During Aging**. *Mech Ageing Dev* 1991, **57**(2):187 -- 202.

142. Sohal RS, Agarwal S, Sohal BH: **Oxidative Stress and Aging in the Mongolian Gerbil (Meriones Unguiculatus)**. *Mech Ageing Dev* 1995, **81**(1):15 -- 25.

143. Sohal RS, Ku HH, Agarwal S, Forster MJ, Lal H: **Oxidative Damage, Mitochondrial Oxidant Generation and Antioxidant Defenses During Aging and in Response to Food Restriction in the Mouse**. *Mech Ageing Dev* 1994, **74**(1-2):121 -- 133.

144. Suh JH, Heath SH, Hagen TM: **Two Subpopulations of Mitochondria in the Aging Rat Heart Display Heterogenous Levels of Oxidative Stress**. *Free Radical Bio Med* 2003, **35**(9):1064 -- 1072.

145. Suh JH, Shigeno ET, Morrow JD, Cox B, Rocha AE, Frei B, Hagen TM: **Oxidative Stress in the Aging Rat Heart is Reversed by Dietary Supplementation with (R)-Alpha-Lipoic Acid**. *FASEB J* 2001, **15**(3):700 -- 706.

146. De Meyer GR, De Keulenaer GW, Martinet W: **Role of Autophagy in Heart Failure Associated with Aging**. *Heart Fail Rev* 2010, **15**(5):423 -- 430.

147. Gurusamy N, Das DK: **Is Autophagy a Double-Edged Sword for the Heart?** *Acta Physiol Hung* 2009, **96**(3):267 -- 276.

148. Brunk UT, Jones CB, Sohal RS: **A Novel Hypothesis of Lipofuscinogenesis and Cellular Aging Based on Interactions between Oxidative Stress and Autophagocytosis**. *Mutat Res* 1992, **275**(3-6):395 -- 403.

149. Dammrich J, Pfeifer U: **Cardiac Hypertrophy in Rats After Supravalvular Aortic Constriction. II. Inhibition of Cellular Autophagy in Hypertrophying Cardiomyocytes**. *Virchows Arch B* 1983, **43**(3):287 -- 307.

150. Nishida K, Kyoi S, Yamaguchi O, Sadoshima J, Otsu K: **The Role of Autophagy in the Heart**. *Cell Death Differ* 2009, **16**(1):31 -- 38.

151. Tanida I, Ueno T, Kominami E: **LC3 and Autophagy**. *Methods Mol Biol* 2008, **445**:77 -- 88.

152. Pankiv S, Clausen TH, Lamark T, Brech A, Bruun JA, Outzen H, Overvatn A, Bjorkoy G, Johansen T: **p62/SQSTM1 Binds Directly to ATG8/LC3 to Facilitate Degradation of Ubiquitinated Protein Aggregates by Autophagy**. *J Biol Chem* 2007, **282**(33):24131 -- 24145.

153. Bjorkoy G, Lamark T, Pankiv S, Overvatn A, Brech A, Johansen T: **Monitoring Autophagic Degradation of p62/SQSTM1**. *Methods Enzymol* 2009, **452**:181 -- 197.

154. Lim CC, Apstein CS, Colucci WS, Liao RL: **Impaired Cell Shortening and Relengthening with Increased Pacing Frequency Are Intrinsic to the Senescent Mouse Cardiomyocyte**. *J Mol Cell Cardiol* 2000, **32**(11):2075 -- 2082.

155. Isenberg G, Borschke B, Rueckschloss U: **Ca^{2+} Transients of Cardiomyocytes fom Senescent Mice Peak Late and Decay Slowly**. *Cell Calcium* 2003, **34**(3):271 -- 280.

156. Howlett SE, Grandy SA, Ferrier GR: **Calcium Spark Properties in Ventricular Myocytes Are Altered in Aged Mice**. *Am J Physiol - Heart C* 2006, **290**(4):H1566 -- 1574.

157. Xu A, Narayanan N: **Effects of Aging on Sarcoplasmic Reticulum Ca^{2+}-Cycling Proteins and Their Phosphorylation in Rat Myocardium**. *Am J Physiol 1*998, **275**(6 Pt 2):H2087 -- 2094.

158. Zhu XS, Altschafl BA, Hajjar RJ, Valdivia HH, Schmidt U: **Altered Ca^{2+} Sparks and Gating Properties of Ryanodine Receptors in Aging Cardiomyocytes**. *Cell Calcium* 2005, **37**(6):583 -- 591.

159. Nerbonne JM: **Studying Cardiac Arrhythmias in the Mouse -- A Reasonable Model for Probing Mechanisms?** *Trends Cardiovas Med* 2004, **14**(3):83 -- 93.

160. Vermeulen JT, McGuire MA, Opthof T, Coronel R, de Bakker JM, Klopping C, Janse MJ: **Triggered Activity and Automaticity in Ventricular Trabeculae of Failing Human and Rabbit Hearts**. *Cardiovasc Res* 1994, **28**(10):1547 -- 1554.

161. Bers DM: **Control of Cardiac Contraction by SR-Ca Release and Sarcolemmal-Ca Fluxes**. In: *Excitation-Contraction Coupling and Cardiac Contractile Force: Developments In Cardiovascular Medicine. Volume 122*, Edited by Bers DM. Dordrecht, Boston, London: Kluver Academic Publishers; 1991:149 -- 170.

162. Hasenfuss G: **Animal Models of Human Cardiovascular Disease, Heart Failure and Hypertrophy**. *Cardiovasc Res* 1998, **39**(1):60 -- 76.

163. Morimoto M: **General Physiology of Rabbits**. In: *Rabbit Biotechnology. Volume 3*, edn. Edited by Houdebine L, Fan J. Dordrecht; Heidelberg; London; New York: Springer; 2009 27 -- 35.

164. Gottwald M, Gottwald E, Dhein S: **Age-Related Electrophysiological and Histological Changes in Rabbit Hearts: Age-Related Changes in Electrophysiology**. *Int J Cardiol* 1997, **62**(2):97 -- 106.

165. Dressler MR, Butler DL, Boivin GP: **Effects of Age on the Repair Aability of Mesenchymal Stem Cells in Rabbit Tendon**. *J Orthop Res* 2005, **23**(2):287 -- 293.

166. Sklenka AM, Levy MS, Boivin GP: **Effect of Age on Collagen Fibril Diameter in Rabbit Patellar Tendon Repair**. *Comparative Med* 2006, **56**(1):8 -- 11.

167. von Holst D, Hutzelmeyer H, Kaetzke P, Khaschei M, Schonheiter R: **Social Rank, Stress, Fitness, and Life Expectancy in Wild Rabbits**. *Naturwissenschaften* 1999, **86**(8):388 -- 393.

168. Hayashi H, Wang C, Miyauchi Y, Omichi C, Pak HN, Zhou S, Ohara T, Mandel WJ, Lin SF, Fishbein MC *et al*: **Aging-Related Increase to Inducible Atrial Fibrillation in the Rat Model**. *J Cardiovasc Electr* 2002, **13**(8):801 -- 808.

169. Alings AM, Bouman LN: **Electrophysiology of the Ageing Rabbit and Cat Sinoatrial Node -- a Comparative Study**. *Eur Heart J* 1993, **14**(9):1278 -- 1288.

170. Alings AM, Abbas RF, Bouman LN: **Age-Related Changes in Structure and Relative Collagen Content of the Human and Feline Sinoatrial Node. a Comparative Study**. *Eur Heart J* 1995, **16**(11):1655 -- 1667.

171. Strait JB, Lakatta EG: **Aging-Associated Cardiovascular Changes and Their Relationship to Heart Failure**. *Heart Fail Clin* 2012, **8**(1):143 -- 164.

172. Chimenti C, Kajstura J, Torella D, Urbanek K, Heleniak H, Colussi C, Di Meglio F, Nadal-Ginard B, Frustaci A, Leri A *et al*: **Senescence and Death of Primitive Cells and Myocytes Lead to Premature Cardiac Aging and Heart Failure**. *Circ Res* 2003, **93**(7):604 -- 613.

Chapter 2: Electromechanical and Structural Alterations in the Aging Rabbit Heart and Aorta

This chapter has been published*: Am J Physiol - Heart C*, 2012. **302**(8): p. H1625 -- 1635

The author contributed to this manuscript by performing *in vivo* hemodynamics, aortic stiffness studies, echocardiography, histology and Sirius Red staining (fibrosis), and assisting with *in vivo* electrophysiology.

Leroy L. Cooper*[1,2], Katja E. Odening*[1], Min-Sig Hwang[3,4], Leonard Chaves[1], Lorraine Schofield[1], Chantel A. Taylor[1], Anthony S. Gemignani[5], Gary F. Mitchell[6], John R. Forder[3,7], Bum-Rak Choi[1], and Gideon Koren[1]

[1]Cardiovascular Research Center, Division of Cardiology, Rhode Island Hospital, Warren Alpert Medical School of Brown University, Providence, RI, USA

[2]Department of Molecular Pharmacology, Physiology, and Biotechnology, Brown University, Providence, RI, USA

[3]McKnight Brain Institute, University of Florida, Gainesville, FL, USA

[4]Department of Neuroscience, University of Florida, Gainesville, FL, USA

[5]Division of Cardiology, Rhode Island Hospital, Warren Alpert Medical School of Brown University, Providence, RI, USA

[6]Cardiovascular Engineering, Inc., Norwood, MA, USA

[7]Department of Radiology, University of Florida, Gainesville, FL, USA

*These authors contributed equally.

Address for reprint requests and other correspondence: Gideon Koren, Cardiovascular Research Center, Rhode Island Hospital, Brown University School of Medicine, 1 Hoppin Street, West Coro-5, Providence, RI 02903 (e-mail: Gideon_Koren@Brown.edu).

Keywords: cardiac electrophysiology, cardiac hemodynamics, optical mapping, high-field magnetic resonance imaging (MRI)

2.1 Abstract

Aging increases the risk for arrhythmias and sudden cardiac death (SCD). We aimed at elucidating aging-related electrical, functional, and structural changes in the heart and vasculature that account for this heightened arrhythmogenic risk. Young (5 – 9 months) and old (3.5 – 6 years) female NZW rabbits were subjected to *in vivo* hemodynamic, electrophysiologic, and echocardiographic studies as well as *ex vivo* optical mapping, high-field magnetic resonance imaging (MRI), and histochemical experiments. Aging increased aortic stiffness (baseline PWV: young, 3.54 ± 0.36 vs. old, 4.35 ± 0.28 m/s, $p<0.002$) and diastolic (EDPVR: 3.28 ± 0.5 vs. 4.95 ± 1.5 mmHg/ml, $p<0.05$) and systolic (ESPVR: 20.56 ± 4.2 vs. 33.14 ± 8.4 mmHg/ml, $p<0.01$) myocardial elastances in old rabbits. Electrophysiological and optical mapping studies revealed age-related slowing of ventricular and His-Purkinje conduction (HV interval: 23 ± 2.5 vs. 31.9 ± 2.9 ms, $p<0.0001$), altered conduction anisotropy, and a greater inducibility of VF (3/12 vs. 7/9, $p<0.05$) in old rabbits. Histochemical studies confirmed an aging-related increased fibrosis in the ventricles. MRI showed a deterioration of the free-running Purkinje fiber network in ventricular and septal walls in old hearts as well as aging-related alterations of the myofibrillar orientation and myocardial sheet structure that may account for this slowed conduction velocity. Aging leads to parallel stiffening of the aorta and the heart, including an increase in systolic stiffness and contractility and diastolic stiffness. Increasingly anisotropic conduction velocity due to fibrosis and altered myofibrillar orientation and myocardial sheet structure may contribute to the pathogenesis of VF in old hearts. The aging rabbit model represents a useful tool for elucidating age-related

changes that predispose the aging heart to arrhythmias and sudden cardiac death (SCD).

2.2 Introduction

Aging is associated with an increased incidence of cardiac arrhythmias and is a known independent risk factor for sudden cardiac death (SCD) [1]. Multiple factors may influence age-related SCD, including structural and electrical changes in the heart. Aging results in increased fibrosis and reduced cellular coupling in the cardiac muscle [2, 3] and the specialized conduction system [4], which slows activation and conduction velocity throughout both the ventricle [5] and the His-Purkinje system [4, 6-8]. Age-related alterations in anisotropic conduction velocity with a preferentially reduced transverse conduction provide a substrate for reentrant arrhythmias and exert a pro-arrhythmic effect by decreasing the threshold for ventricular fibrillation in various animal models of aging such as rabbits, dogs, and mice [5, 9-11].

In addition to direct electrophysiologic effects, the effects of aging on cardiac mechanical function and vascular structure may contribute to increased arrhythmogenic risk. Indeed, it is known that in humans aging is associated with increased arterial stiffness and pulse pressure, which are associated with an increased susceptibility to various cardiac events including arrhythmia [12-14].

In light of the many environmental confounders associated with aging in humans, elucidation of major causes and underlying mechanisms of SCD has proven difficult.

Studies in humans generally provide only statistical associations [15, 16], which require subsequent validation in experimental models for a more thorough examination of the causal relations between aging and increased incidence of SCD. It is known that the rabbit's action potential shape and its ionic composition are similar to humans [17, 18]. Hence, we examined aging-related changes in cardiac electrophysiological, mechanical, and structural features in a rabbit model, and we also related sequelae of vasculature aging to structural and electrophysiological alterations in the myocardium, thereby providing a more thorough assessment of pathophysiological alterations that may render the aging heart more susceptible to arrhythmia and sudden cardiac death.

2.3 Methods

Animal Ethical Statement

All animal studies were performed in accordance with the local guidelines of the institutions and only after approval by the Institutional Animal Care and Use Committee in accordance with the *Guide for the Care and Use of Laboratory Animals* published by the U.S. National Institutes of Health (NIH Publication No. 85-23, revised 1996).

Aortic Pullback and Pulse Wave Velocity (PWV)

PWV was assessed via aortic pullback as previously described [19, 20]. Briefly, under fluoroscopic guidance, a 3F dual pressure-volume catheter (Millar Instruments,

Houston, TX, USA) was inserted through a 3F sheath via the right carotid artery and advanced to the proximal aorta. Additionally, a 2F pressure catheter (Millar Instruments, Houston, TX, USA) was inserted via the femoral artery and advanced retrogradely to the proximal aorta. An incremental 10-cm pullback of the femoral pressure catheter was performed, with proximal and distal pressures recorded at 2-cm intervals. With the catheters in their final locations, PWV was subsequently assessed in young and old rabbits during a graded intravenous (IV) infusion of phenylephrine at 2-10 µg/kg/min. The carotid artery was tied, the femoral artery repaired, and animals were survived after the study. Data was analyzed off-line with proprietary software (NIHem, Cardiovascular Engineering, Norwood, MA, USA). In brief, proximal and distal pressures were signal averaged using the electrocardiographic R-wave as a fiducial point. The foot-to-foot transit time was ascertained from signal-averaged waveforms. Transit distance was derived from linear fitting of the pullback data as previously described [20].

In Vivo Hemodynamic Studies

Young (5-9 months, n=6) and old (4-6 years, n=6) female NZW rabbits were sedated with ketamine/xylazine (25 mg/kg/3.75 mg/kg IM), intubated and ventilated with supplemental oxygen (2-4 %). During the procedure, the rabbits were anesthetized with continuous IV infusion of ketamine and xylazine (5mg/kg/hr and 4.5mg/kg/hr) as described [21]. Using the right carotid artery, a 3F dual pressure-volume catheter (Millar Instruments, Houston, TX, USA) was inserted through a 3F sheath via the right carotid artery and advanced into the LV under fluoroscopic guidance. Using 4 to 5 segments,

the electrical impedance was measured within the LV and data recorded with LabChart7 Software (ADInstruments, Sidney, Australia) and MPVS Ultra Control Software (Millar Instruments, Houston, TX, USA) as high-fidelity, instantaneous LV pressure-volume loops during steady state, inferior vena cava (IVC) occlusion, and saline calibration. To reduce preload to acquire systolic and diastolic pressure-volume relations, the IVC was occluded by physically compressing the inferior vena cava by applying pressure in the subxiphoid right lateral region of the abdomen. To obtain absolute volumes, blood resistivity was measured using approximately 1 mL of heparinized blood and a Rho cuvette, and parallel conductance was determined by the hypertonic saline method [22]. The saline calibration was confirmed with echocardiography. Data was analyzed off-line with PVAN Ultra software (Millar, Houston, TX, USA).

Echocardiographic Studies

Transthoracic echocardiography was performed in sedated young (5-9 months, n=5) and old (4-6 years, n=5) female NZW rabbits (ketamine/xylazine 25 mg/kg/3.75 mg/kg IM). A 7.5-mHz probe and long axis and M-mode views were used. Analysis included LV and septal wall thickness, LV lumen diameter during systole and diastole, and LV fractional shortening and ejection fraction. Analyses were performed by an experienced echocardiographer blinded to the age.

In VIvo Electrophysiological Studies (EPS)

Young (aged 5-7 months, n=6) and old (aged 3.5-5.5 years, n=8) female NZW rabbits were subjected to transvenous EPS as described [23]. Briefly, rabbits were anesthetized with ketamine/xylazine (25 mg/kg/3.75 mg/kg IM) and buprenorphine (0.03 mg/kg SQ), intubated, and ventilated with isoflurane (1–2%, FiO_2 0.5). Steerable 4F decapolar and 4F quadripolar EP catheters (Irvine Biomedical, Irvine, CA, USA) were inserted in the right femoral and right jugular veins through 4F sheaths and placed in the right atrium and ventricle, guided by fluoroscopy and pacing thresholds. Signals from the His-bundle were obtained with the ventricular EP catheter (RV base). During the procedure, 12-lead surface, two intra-atrial, and five intra-ventricular ECG signals were recorded continuously using the EP-Bard-System Software OS2/warp (kindly provided by Bard, Lowell, MA, USA), filtered with a bandwidth of 30–250 Hz (intracardiac signals) and 0.01–100 Hz (surface ECG). EPS were performed at a stimulation cycle length (CL) of 200 ms and 240 ms. The following electrophysiological parameters were analyzed as previously described [23]: Sinus node recovery time (SNRT) was evaluated at pacing drive rates of 200ms and 240ms after 200 beats and the heart-rate corrected SNRT (SNRT minus sinus cycle length) was calculated. Atrium to His (AH) and His to ventricle (HV) intervals that reflect conduction from the atrium to the proximal His bundle (AH) and from the His bundle via Purkinje fibers to the ventricle (HV) were measured. Antegrade and retrograde Wenckebach CL (AVWCL/VAWCL) were characterized as the longest CL resulting in Wenckebach AV block. Atrial effective refractory period (AERP), AV-nodal/His-Purkinje effective refractory period (AVN/His-ERP), and ventricular effective refractory periods in RV apex and septal RV base position (VERPapex, VERPbase) were analyzed by progressively shortening the S2-interval in

10-ms steps after 8-beat S1 trains. To evaluate potential aging-effects on QT duration, we applied the following previously established heart rate correction formulas for the expected QT interval under isoflurane anesthesia [24]: WT, QTexpected (QTexp) = 0.4 x RR + 92. The QTi was defined as the percentage of the observed vs. the expected QT. EPS were performed at baseline and during isoproterenol (ISO) infusion (0.10 - 0.25 μg/min to increase the spontaneous heart rate to 120%).

Ex vivo Optical Mapping

To further characterize electrophysiological changes in aging, we performed optical mapping studies of young (age 6-9 months, n=6-7) and old (age 3.5-6 years, n=8-9) female rabbits. Heart preparation and retrograde perfusion were performed as previously described [25]. Briefly, hearts were stained with a voltage sensitive dye, di-4 ANEPPS (Invitrogen, Carlsbad). 5 μM blebbistatin was added to the perfusate to reduce motion artifacts [26]. Fluorescence signals were recorded using a CMOS camera (100x100 pixels, 1000 f/s, 25x25 mm^2 field of view).

To measure and characterize anisotropic propagation, the center of the left ventricular epicardium was stimulated with a concentric bipolar electrode (Harvard Apparatus) at 350 ms cycle length to generate an elliptical activation pattern from the stimulus site. Activation time-point at each site was determined from the local action potential upstroke using $(dF/dt)_{max}$ and mapped using a custom designed software based on Interactive Data Language (IDL 6.3, Research Systems, Inc.), as previously described [25]. Longitudinal and transverse conduction velocities were calculated by determining

the major axis of conduction and estimating conduction along the direction of eigen vectors as previously described [25].

The spatial organization of wave propagations in VF was analyzed using cross correlation and correlation length analysis as described [25]. Briefly, the reference channel was selected at the center of LV free wall and correlation between reference, and the rest pixels were calculated and mapped. Higher correlation along the fiber orientation indicates activation during VF has preferential conduction along the fibers as previously described [25]. The correlation lengths along the longitudinal and the transverse direction were calculated, and the ratio of longitudinal/transverse was used for statistical test.

Sirius Red Staining

Rabbit hearts were excised from young (5 – 6 months, n=3) and old (4 – 6 years, n=3) female rabbits, fixed with 10% formalin, and embedded in paraffin. The hearts were cut in 4-chamber view orientation at 5 μm thickness, deparaffinized, and stained with picro-Sirius red for 1 h at RT. After washes, sections on the slides were dehydrated in 100% ethanol and xylene, and mounted in SHUR/Mount toluene-based liquid media (Triangle Biomedical Sciences, Inc., Durham, NC).

Analysis of Fibrosis

Sections stained with Sirius Red were visualized with an Eclipse TE2000 microscope (Nikon, Melville, NY) and a 4x objective under white and polarized light, and the images were captured using Elements software (Nikon). The total and fibrotic areas were evaluated by capturing digital RGB images of the LV and septum wall. Analysis was performed using Adobe Photoshop software (Adobe Systems Corporation, San Jose, CA) and ImageJ software with the Otsu thresholding method (US National Institutes of Health, Bethesda, MD) as previously described and modified in [27]. The mean area of fibrosis was calculated by comparing total area (white light) and fibrotic area (polarized light) for young and old rabbit sections.

Magnetic Resonance Imaging (MRI)

To assess structural correlates to age-related changes in the conduction system, hearts from young female (aged 6 months, n=4) and old rabbits (age 5 years, n=3) were excised and quickly fixed in 10% formalin solution. Two days prior to MRI, fixed hearts were transferred to phosphate buffered saline (PBS) solution to wash out residual fixative. Fluorocarbon solution (FC-43, Fluorinert, 3M, St. Paul, MN) was used to prevent dehydration and eliminate proton-signal from the surrounding fluid [28].

The hearts were examined using a 17.6 T / 89 mm vertical wide-bore magnet (Oxford Instruments, Inc., Oxford, UK) connected to a Bruker spectrometer console running Paravision 4 software (Bruker Instruments, Billerica, MA). The RF coil used for the in

vitro imaging was a commercial birdcage coil (Bruker Instruments, Billerica, MA), diameter = 25 mm, length = 35 cm. The temperature in the magnet was maintained at 19 - 20°C. Three dimensional high resolution MR image data were collected using a fast gradient echo pulse sequence, achieving a voxel resolution of 35 μm x 35 μm x 82 μm. Imaging parameters were TR = 150 ms, TE = 18.5 ms, 1 average, sampling bandwidth = 20 k. Total acquisition time was 7 hrs 30 min. The subsequent high angular resolution diffusion microscopy (HARDM) using 21 directions was performed using a standard multislice PGSE pulse sequence, achieving an in-plane resolution of 60 μm x 60 μm with a slice thickness of 600 μm. Diffusion sensitizing factor (b-value) was 1000 s/mm^2 using Δ = 13.4 ms and δ = 1.8 ms. Imaging parameters were TR = 3000 ms, TE = 25.1 ms, 1 average. Total acquisition scan time for each HARDM experiment was 7 hrs 40 min. The pilot images with three orthogonal planes were collected at intervals during the experiment to determine if the isolated heart imbedded in the dense FC-43 solution moved during these long scans.

Data Analysis: Volume rendering of the 3D MR data sets were performed using ImageJ (ver. 1.41, http://rsbweb.nih.gov/ij/) that enabled appropriate virtual sectioning in any direction and geometrical image registration with the HARDM data sets. The tensor processing of HARDM data sets was performed using fanDTasia™ (©2008, Barmpoutis, http://www.cise.ufl.edu/~abarmpou/) [29].

Explanation of the HARDM imaging interpretation: A diffusion tensor can be visualized as the intersection of two orthogonal ellipses, with the largest ellipse representing the preferential (or least restricted) direction of diffusion. The ellipse that is orthogonal to the

largest ellipse is described by two additional vectors, which reflect diffusion barriers in this plane. If diffusion is isotropic (without barriers to diffusion), all three vectors that describe the ellipses are equal, and the volume that reflects the probability of water diffusion is represented by a sphere. If diffusion is restricted in one or more directions it is referred to as anisotropic, and there are differences between the magnitudes of the three vectors. The term “eigen” is used to indicate that the calculated value is characteristic of the diffusion – eigen-vector is defined as the orientation of diffusion, and eigen-value reflects the rate of water diffusion. The orientation that is preferential, or least restricted, is known as the principle eigen-vector. The rate of diffusion that corresponds to the principle eigenvector is known as the principle eigen-value. The assignment of secondary and tertiary eigen-vectors is dependent upon the magnitude of the corresponding eigen-values, and is made according to decreasing magnitude. Therefore, the principle, secondary, and tertiary eigen-values are ordered in decreasing magnitude, and the corresponding eigen-vectors reflect their direction. Previous work investigating diffusion in the heart suggests that the primary eigen-vector reflects the orientation of the cardiomyofibers [30], and that the myocardial sheet structure proposed by LeGrice et al. [31] may be reflected by the tertiary eigen-vector [30]. A 3 x 3 diffusion tensor matrix, describing the three-dimensional translational diffusion of water molecules in each voxel, was calculated from the HARDM data set, and the three (primary, secondary, and tertiary) eigen-vectors and eigen-values were obtained [32, 33].

Statistical analysis

All data was normally distributed. We used Student's unpaired and paired *t*-tests to compare the means of two groups. Analysis was performed with Prism 4 for Windows (Graphpad, San Diego, CA). All data are presented as means ± standard deviation.

2.4 Results

In vivo Hemodynamics and Pulse Wave Velocity (PWV)

We first investigated pulse wave velocity (PWV) as an indicator of aortic stiffness. **Figure 2.1A** depicts the initial placement of the two catheters used during aortic pullback. **Figures 2.1B** and **2.1C** show old and young representative pressure tracings from the proximal pressure catheter in the aortic root and the distal femoral catheter at the femoral catheter's most distal point (10 cm). Baseline PWV and PWV under phenylephrine were significantly higher in old rabbits as compared to young rabbits (baseline: young, 3.54 ± 0.36 vs. old, 4.35 ± 0.28 m/s, $p<0.002$ and phenylephrine: 4.3 ± 0.8 vs. 5.8 ± 0.7 m/s, $p<0.01$) (**Figures 2.1D** and **2.1E**) indicating that stiffening of the aorta occurs with aging. **Figure 2.1F** depicts the relation between PWV and mean arterial pressure (MAP) in essentially non-overlapping groups of young and old rabbits at baseline and during phenylephrine. Old rabbits tended to have lower MAP at baseline (young, 60.2 ± 7.5 vs. old, 53.2 ± 8.1, $p=0.152$); whereas, MAP was similar under PE infusion (young, 95.8 ± 11.6 vs. old, 98.7 ± 19.3, n.s.). Phenylephrine slowed heart rates in both young and old animals: young (baseline, 115 ± 20 vs. PE, 75 ± 13, paired *t*-test, $p<0.001$) and old (125 ± 13 vs. 85 ± 22, paired *t*-test, $p<0.01$).

Secondly, we investigated the aging-effect on LV stiffness. During IVC occlusion, the slopes of the end systolic pressure-volume relations (ESPRV) and end diastolic pressure-volume relations (EDPVR) were significantly altered in old as compared to young rabbit hearts as illustrated in **Figures 2.2A** and **2.2B**. ESPRV was significantly higher in old rabbits (20.56 ± 4.2 vs. 33.14 ± 8.4 mm Hg/ml, $p<0.01$) (**Figure 2.2C**), indicating an increased systolic stiffness and contractility in the aging heart. EDPRV was also significantly higher in old rabbits (3.28 ± 0.5 vs. 4.95 ± 1.5 mm Hg/ml, $p<0.05$) (**Figure 2.2D**, $p<0.05$), indicating an increased diastolic stiffness and hence reduced compliance of the aging rabbit heart. Additionally, we observed a proportional, linear relation between PWV and ESPVR (**Figure 2.2E**) indicating a parallel stiffening and remodeling of the aging heart and aorta. In contrast, no correlation was observed between PWV and EDPVR.

Echocardiographic Studies

Echocardiography data showed a 30% increase in wall thickness of the interventricular septum of old rabbits as well as a trend towards a thicker posterior wall, consistent with concentric hypertrophy (**Table 1**). Moreover, old rabbits had an increased LV mass (young, n=7, 8.26 ± 0.55 vs. old, n=5, 12.11 ± 1.48, $p<0.05$), but left ventricular mass to body weight ratio was not changed with aging. No differences were observed between old and young rabbits in regard to ejection fraction, fractional shortening, LV diastolic diameter, LV systolic diameter (**Table 1**).

In vivo Electrophysiological Studies (EPS)

During *in vivo* EPS the heart rate was significantly slower in old rabbits (184 ± 4 vs. 166 ± 6 beats/min, $p<0.05$) at baseline and slower during isoproterenol exposure (212 ± 17 vs. 200 ± 11 beats/min, $p<0.05$), but isoproterenol significantly increased heart rate in both, young and old rabbits ($p<0.05$ each, paired t-test). In line with the slower heart rate in old rabbits, *in vivo* EPS revealed longer heart rate corrected sinus node recovery time (cSNRT) in old rabbits at baseline (78.4 ± 23.4 vs. 126.0 ± 24.1 ms, $p<0.05$) and after sympathetic stimulation (70.0 ± 13.6 vs. 109.0 ± 29.5 ms, $p<0.05$ each).

Figures 2.3A and **2.3B** depict representative alterations in QRS morphology and duration in old rabbits, demonstrating classical right bundle branch block (RBBB) features with an rR' QRS morphology in V1 and a broad S in V5, V6 along with the typically seen inverted T-wave in V1. We observed this classical complete RBBB morphology in 4/8 old rabbits, the other three old rabbits had incomplete RBBB-like QRS patterns. In contrast, all young rabbits had normal QRS patterns in leads V1-V6 as shown in **Figure 2.3A**. These age-related changes in QRS resulted in significantly prolonged QRS complex durations in old rabbits ($p<0.01$; **Figure 2.3D**). Moreover, we observed a trend towards longer PQ intervals in old rabbits (78.0 ± 1.6 vs. 82.4 ± 8.7 ms, $p=0.295$, **Figure 2.3C**). Heart rate corrected QT indices did not differ between old and young rabbits (**Figure 2.3E**). *In vivo* EPS revealed prolonged HV intervals in old rabbits (HV: 23 ± 2.5 vs. 31.9 ± 2.9 ms, $p<0.0001$, **Figure 2.3F, G, I**), indicating a slowed conduction particularly through the His-Purkinje system in old rabbits. However,

AH intervals (**Figure 2.3H**), AV Wenckebach cycle length (AVWCL: 163.3 ± 15.1 vs. 165.7 ± 17.2 ms) and AV nodal effective refractory periods (AVNERP: 110 ± 15.8 vs. 106.7 ± 13.7 ms) did not differ between both age groups, indicating a lack of age-related changes in the AV nodal conduction.

Ventricular effective refractory periods (VERP) in the RV apex and base did not differ between old and young rabbits (VERP240 apex, 140.0 ± 8.9 vs. 147.5 ± 14.9 ms; VERP base: 150 ± 22.8 vs. 155 ± 16 ms). However, the isoproterenol-induced shortening of the VERP was more pronounced in young rabbits where a significant shortening occurred in both of the apex and the base (VERP240apex-Iso, young, ms, 128.3 ± 14.7, $p<0.05$ vs. baseline; VERP240base-Iso, ms, 136.7 ± 13.7, $p<0.05$ vs. baseline) while in old rabbits the VERP only shortened in the base (VERP240apex-Iso, old, ms 141.3 ± 17.3; VERP240base-Iso, ms, 137.1 ± 12.8, $p<0.05$ vs. baseline).

Tissue Anisotropy and VF Inducibility

We further investigated conduction velocity (CV) changes and VF inducibility of young and old hearts using optical mapping. Activation maps under sinus rhythm show marked delay in old heart (**Figures 2.4 A – C**) and the total activation time from the field of view was longer in line with widening QRS complex in old hearts (see **Figure 2.3**). However, APD (young, 210.39 ± 15.55 vs. old, 206.18 ± 19.57) and APD dispersion did not differ between young and old hearts (**Figures 2.4 D – F**). **Figures 2.4G** and **2.4H** show typical examples of elliptical activation patterns during LV stimulation. In the aging heart, the anisotropic conduction became more exaggerated: in the old heart CV_L = 0.828 ±

0.053 ms / CT_T = 0.280 ± 0.078 ms; whereas, in the young heart CV_L = 0.767 ± 0.091 ms / CV_T = 0.348 ± 0.047 ms. **Figure 2.4I** shows box plots of the distribution of longitudinal and transverse CV (CV_L/CV_T), with an increase of the CV_L/CV_T ratio and a greater variation mostly in old hearts (p<0.05), suggesting that conduction in the transverse direction is hindered with age compared to longitudinal direction.

We further investigated whether changes in tissue anisotropy in aging can cause different wave dynamics in VF. VF was inducible in most old hearts (7 out of 9) and only a few young hearts (3 of 12) by ramp pacing protocol (systematic decrease in stimulation cycle length). Typical examples of VF signals from young and old hearts are shown in **Figures 2.5A** and **2.5B**. Since transverse conduction is hampered in aging hearts, we hypothesized that conduction blocks across the transverse direction may provide a substrate for VF maintenance. The superimposed traces along transverse direction in old hearts (lower panels of **Figures 2.5C** and **2.5D**) also show asynchronous membrane potential (V_m) oscillations, indicating anomalies in transverse conduction in old hearts may contribute to VF maintenance. To quantify abnormal conduction in transverse direction in VF, we applied cross correlation analysis (with correlation of V_m oscillations between different pixels in VF). The center of field of view was selected as reference and correlation between the rest of the field of view was calculated and mapped in **Figures 2.5C** and **2.5D** (upper panels). In line with CV_L/CV_T measurements, old hearts show lower correlation along the transverse direction, resulting in more elongated elliptical correlation maps.

Fibrosis in the Aging Heart

Histochemical experiments revealed an age-related increase of total (5.60 ± 0.1 vs. 11.01 ± 0 1.3 %, $p<0.01$) and interstitial fibrosis (defined as total fibrosis minus fibrosis around the epicardium, valves, and large vessels) (2.82 ± 0.5 vs. 6.97 ± 0.8 %, $p<0.01$) in the LV and interventricular septum (**Figure 2.6**).

Structural Changes in the Aging Heart

In line with the increased wall thickness of the interventricular septum assessed *in vivo* by echocardiography, we observed a significant increase in interventricular septum thickness in the young (n=4) and old (n=3) rabbit hearts using MR imaging (3.87 ± 0.08 vs. 4.81 ± 0.60 mm, $p<0.05$). Moreover, volume rendered transverse images of the apical half of the LV suggest that the free-running Purkinje fiber network in the LV cavity is significantly altered with aging (**Figures 2.7A** and **2.7B**). Young hearts have a higher complexity in the geometry of free-running fibers than hearts from older animals. In addition, young hearts have free-running fibers that are significantly larger in diameter (0.2 ± 0.01 vs. 0.14 ± 0.018 mm, $p<0.05$).

Results of HARDM are presented in **Figures 2.7C** and **2.7D,** which show typical, representative tensor component (D_{yz}) maps of hearts from a young and an old rabbit. The heart from the young animal shows a conspicuous stripe pattern in the interseptum and freewall (**Figure 2.7C**). This pattern is less apparent in the heart from the older animal (**Figure 2.7D**). A volume rendered image of the interventricular septum shows that the stripe pattern has a longitudinal direction and appears to exist in the basal half of the LV. **Figures 2.7E** and **2.7F** compare the primary eigen vector and the tertiary

eigen vector in the mid-interventricular septum of a young heart and an old heart. These correspond to the myocardial fiber orientation and the orientation of the myocardial sheet structure, respectively [34, 35]. These transmural patterns are less distinct in the old heart, and the orientation of the tertiary eigen vectors are dramatically altered as well.

2.5 Discussion

In this study we reveal age-related functional, electrical, and morphological changes in the heart and the aorta, such as an increased aortic stiffness that is associated with decreased diastolic and systolic compliance, increased fibrosis and altered myofibrillar orientation and myocardial sheet structure in the septum, slowed CV and increased CV anisotropy in the ventricle and the His-Purkinje conduction system and Purkinje fiber network deterioration. Thus, this study provides a detailed assessment of various components of ventricular and vascular aging that may contribute to heightened arrhythmogenic risk with advancing age.

Aging and Structural and Functional Changes in the Heart and Aorta

We show age-related alterations in diastolic and systolic mechanical function as previously shown in humans [36, 37]. The end-diastolic elastance (E_{ed}) is increased in old rabbits indicating a decreased diastolic compliance as previously described in older humans with a reduced LV filling rate [38-40] and an age-related increase in operant E_{ed}

[41]. Moreover, we observed an age-related increase in end-systolic elastance (E_{es}), indicating that myocardial stiffness and contractility are also increased during systole. We hypothesize that changes in ventricular stiffness associated with cardiac remodeling are coupled to arterial remodeling during the aging process. It is well known that arterial stiffness, wave reflections, and systolic and pulse pressures all increase with aging in humans [40, 42]. We confirmed that in the rabbit model PWV, and hence, aortic stiffness also increases with aging. In humans <50 years of age, the PWV typically ranges from 5 to 7 m/s; whereas, in humans >60 years of age, PWV ranges from 8 to 11 m/s or higher [42, 43], which is considerably higher than PWV values observed during aortic pullback experiments in our rabbits. For these studies, however, baseline measures were acquired while the rabbits were anesthetized with ketamine and xylazine, which considerably lowered blood pressure. At baseline, old rabbits tend to have lower MAP yet higher PWV, and under α_1-adrenergic stimulation, young and old rabbits have similar MAP while old rabbits have much higher PWV. Additionally, the relative difference in PWV between young and old was more comparable between humans and rabbits when evaluated at the higher pressures generated by α_1-adrenergic stimulation. Since it has been shown that higher resting heart rate and an acute increase in heart rate are associated with higher PWV, lower heart rate cannot explain higher PWV during phenylephrine infusion [42, 44-47]. Moreover, we were able to show a positive, linear relation between aortic stiffness and cardiac stiffness during systole, whereas no relation existed between aortic and diastolic cardiac stiffness, suggesting that aortic stiffness lead to systolic stiffening of the aging heart.

In rabbits, aging increased LV wall thickness but did not alter systolic LV function as assessed by ejection fraction, which is similar to the pattern observed in aging humans in the absence of hypertension or cardiovascular disease [40]. We observe a simultaneous increase in aortic and diastolic stiffness, increase systolic contractility and elastance, and maintenance of the ejection fraction with age, which reinforces this idea that ventricular performance is coupled with arterial function. Hence, when we correlate both systolic and diastolic indices of ventricular function with aortic PWV, we observed that only systolic stiffness is strongly associated with progressive aortic stiffness with age, suggesting that an age-related concentric remodeling of the left ventricle in response to stiffening of the aorta maintains ejection fraction in the presence of hypertrophy and diastolic dysfunction.

Aging and electrophysiological and structural properties of the His Purkinje system

We show aging-related impaired sinus node function and slowed atrio-ventricular conduction, similarly as in humans [4, 7, 8]. But while it has been demonstrated by various groups that aging prolongs PQ interval durations mainly by slowing of conduction through the AV node and proximal His bundle due to increased fibrosis in the specialized conduction system [4, 7, 8], we revealed a pronounced slowing of conduction particularly through the distal His-Purkinje system resulting in prolonged HV intervals and broader QRS complexes. Similarly, in comprehensive electrophysiological studies prolonged HV intervals were described in older individuals [6]. However, so far,

the mechanisms underlying this impaired conduction through the distal His-Purkinje system remained unclear. Using high resolution MRI, we revealed that alterations in His-Purkinje function were associated with morphological changes in the Purkinje system consisting of a thinned reticular network with fewer connections and thinner individual free-running Purkinje fibers. Whether age-related morphological changes in the human Purkinje system similar to those that we have described in the rabbit might underlie slowed conduction in humans remains to be investigated.

Tensor component maps of young hearts derived from HARDM data show a conspicuous stripe pattern in the interventricular septum and freewall, which becomes less apparent in hearts from older animals. This stripe pattern has a longitudinal direction and appears to exist in the basal half of the LV. Considering that a basal end of these longitudinal stripes is proximal to the membraneous interventricular septum from where the left bundle originates [48, 49], the stripe patterns visible by endogenous MR contrast could represent projections from the left bundle that forms the fan-like structure in the subendocardium of the interventricular septum. Combined analysis of the two MR modalities (MRM & HARDM) may provide a powerful tool to understand and monitor alterations in myofibrillar orientation, myocardial sheet structure, and the cardiac conduction network that occur as a result of aging.

Aging and structural and electrophysiological properties of the ventricle

Similar to observations in aging humans, we show that ventricular stiffness and wall thickness increase in the aging rabbit heart. Myocardial sheet structure reorientation

has been shown to contribute to myocardial wall thickening in rats [50]. Here, we show that increased wall thickness and alterations of myofibrillar and myocardial sheet orientation are both positively associated with age. Whether these age-related changes in myofibrillar and myocardial sheet orientation directly contribute to ventricular stiffness, however, remains to be investigated. Moreover, alterations in cell excitation and calcium handling also contribute to the age-related changes in the electrophysiological properties of the ventricle. It has been shown that cardiomyocytes from aging animals have longer action potentials primarily due to increased inward L-type current and reduced outward potassium currents [51, 52]. Also, several studies in murine models have shown changes in calcium handling proteins, such as sarco/endoplasmic reticulum Ca^{2+}-ATPase (SERCA), phospholamban, L-type calcium channel, ryanodine receptor, sodium-calcium exchanger [51, 53-58]. Also, functional changes in calcium handling, particular with regard to SERCA, have been associated with both systolic and diastolic dysfunction [56, 57, 59]. These alterations suggest that age-related cellular and molecular changes are plausible culprits behind the slowing of conduction velocity as well as triggered activity associated with the aging pro-arrhythmogenic phenotype.

Several reports have suggested that fibrosis in aging may increase the anisotropy of the ventricular muscle and may play an important role in the initiation and maintenance of VF through conduction blocks along the transverse direction [60-63]. Using epicardial optical mapping, we revealed an increase in anisotropic conduction. Increased conduction anisotropy was associated with a higher VF-inducibility rate and a changed spatial organization of wave propagations during VF in old rabbits suggesting that increased conduction velocity anisotropy provided a pro-arrhythmogenic substrate.

Similarly, age-related reductions in transverse conduction velocity have been described in rabbits [5], mice [10], and dogs [9] and were attributed to increased fibrosis and reduced intercellular coupling in old myocardium. Using HARDM, we have shown that not only increased fibrosis but also alterations of the myofibrillar orientation and myocardial sheet structure accompany age-related slowing of ventricular conduction velocity and increased conduction anisotropy. Moreover, these age-related changes in myocardial sheet and fiber orientation likely provide a structural substrate for reentrant arrhythmias, thereby increasing susceptibility to ventricular fibrillation.

Conclusion

In summary, we have provided a detailed assessment of the impact of aging on the electromechanical structure and function of the rabbit heart. The rabbit model shows a parallel age-related increase in aortic and ventricular stiffness, as is seen in older humans. Moreover, aging slows conduction velocity throughout the His-Purkinje system and changes the morphology of the Purkinje network. The old rabbit heart also has an increased ventricular conduction anisotropy probably due to fibrosis, changed myofibrillar orientation and myocardial sheet structure, which provides a pro-arrhythmogenic substrate and thereby contributes to pathogenesis of VF in old hearts. Thus, the aging rabbit model represents a useful tool for elucidating age-related changes that predispose the aging heart to arrhythmia and sudden cardiac arrest.

2.6 Acknowledgements

We would like to thank Paul Jeng, Divyang Patel, and Ohad Ziv for their support, assistance with data analysis, and preparation of figures.

2.7 Figures and Table

Figure 2.1: Aortic pulse wave velocity (PWV) in young and old rabbits.

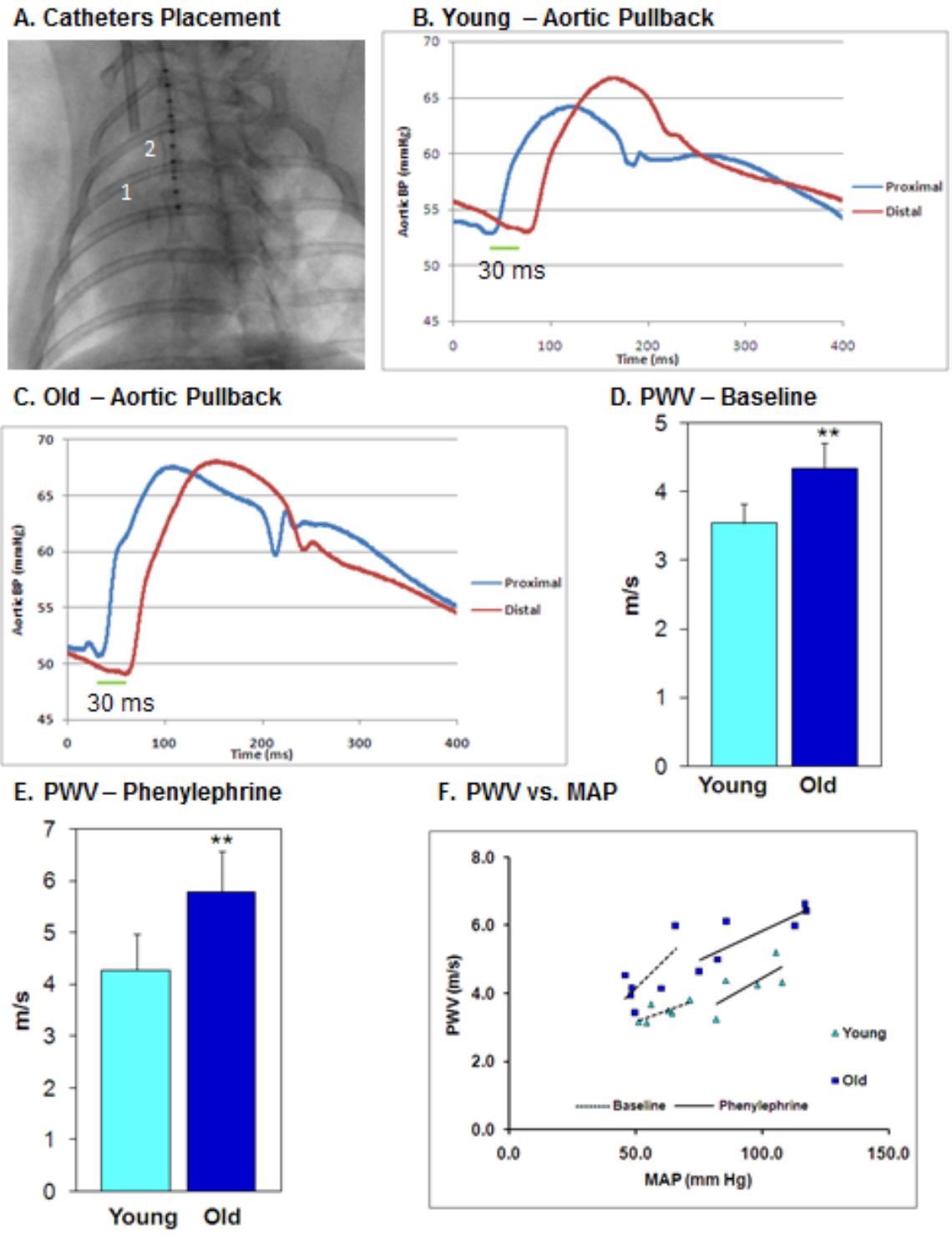

A. Fluoroscopic image of the placement of the two catheters. **B.** and **C.** show representative pressure tracings from young and old hearts at the end of the aortic during pullback procedure (proximal at 0 cm; distal at 10 cm). **D.** and **E.** PWV in at baseline (n=6 young and n=6 old rabbits) and with phenylephrine (n=5 young and n=6 old rabbits), respectively. ***p*<0.01. All values are shown as mean ± SD. **F.** PWV vs. mean arterial pressure (MAP) of old and young rabbits at baseline and with phenylephrine. Data points represent individual rabbits of each group.

Figure 2.2: LV hemodynamic parameters and relation to PWV in young and old rabbits.

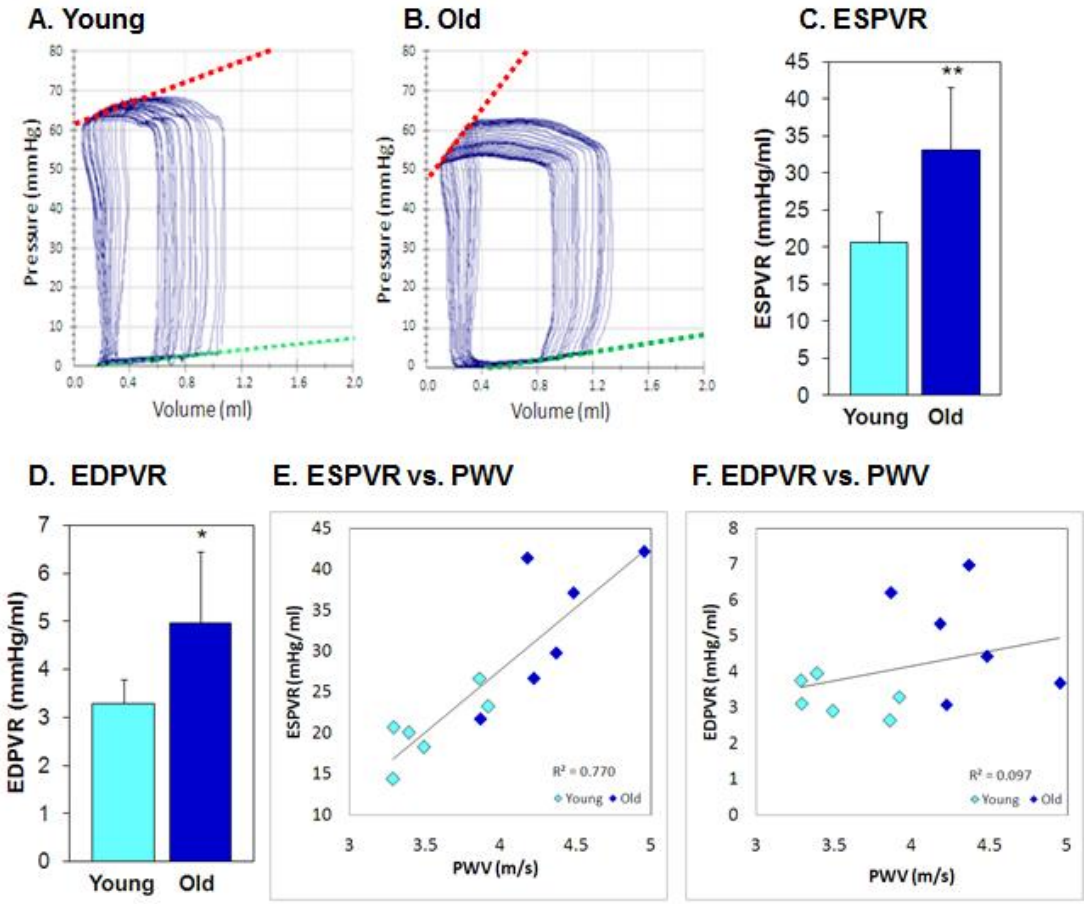

A. and **B.** show representative pressure-volume (PV) loops of individual young and old rabbits during occlusion of the inferior vena cava. **C.** End systolic pressure-volume relationship (ESPRV, red dashed line) in n=6 young and n=6 old rabbits. ***p*<0.01. **D.** End diastolic pressure-volume relationship (EDPVR, green dashed line) in n=6 young and n=6 old rabbits. **p*<0.05. **E.** ESPVR vs. PWV in n=6 young and n=6 old rabbits, linear relationship: y = 15.28x - 33.40, R^2 = 0.770. **F.** EDPVR vs. PWV in n=6 young and n=6 old rabbits, no correlation: y = 0.819x + 0.889, R^2 = 0.097. All values are shown as mean ± SD.

Figure 2.3: ECG parameters in young and old rabbits.

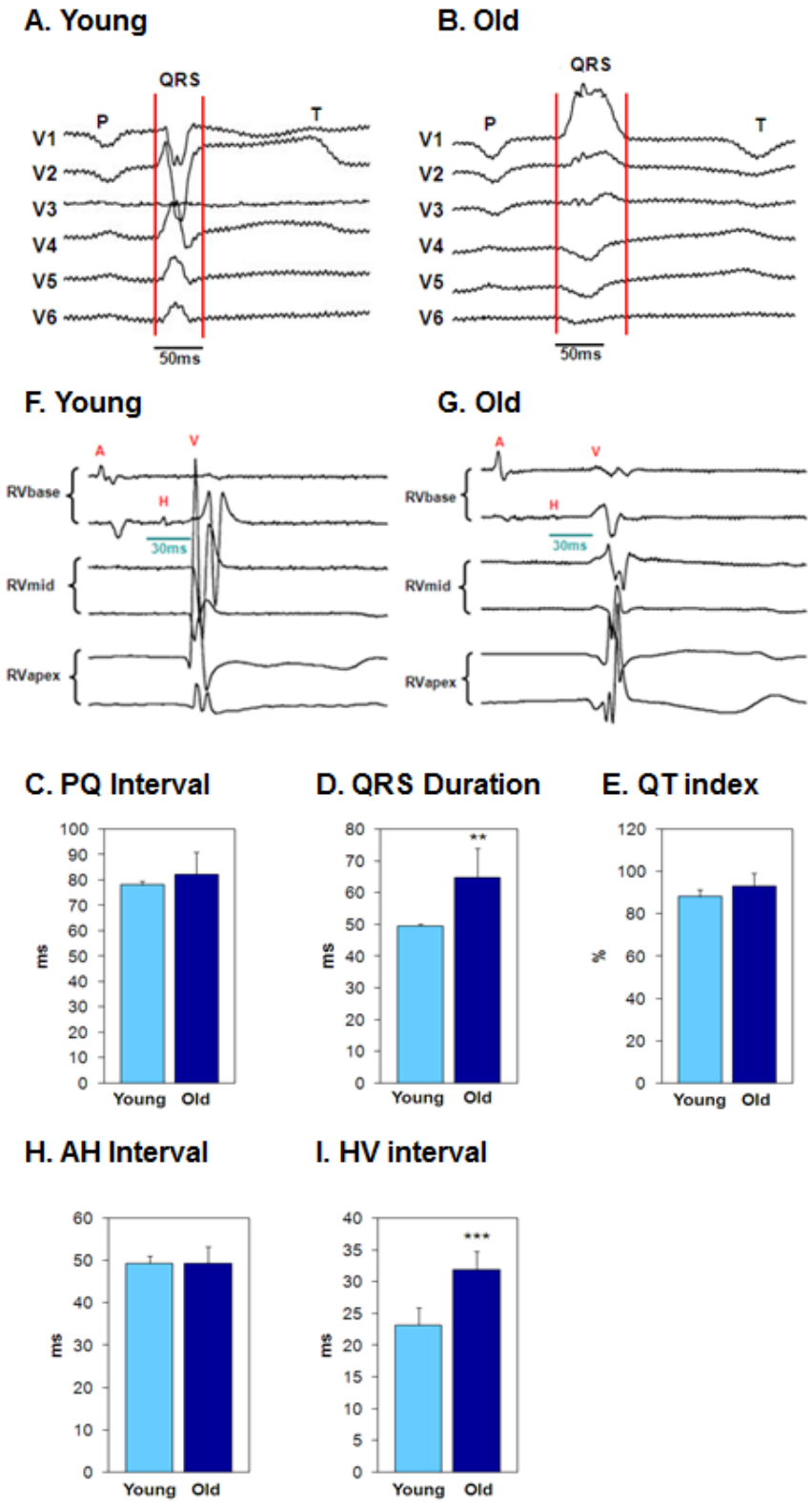

A. and **B.** show representative ECG traces (chest leads V1-V6) of individual young and old rabbits, demonstrating classical RBBB features along with the typically seen inverted T-wave in V1. P= P wave, QRS complex, T= T wave. **C.** PQ interval duration in n=8 young and n=6 old rabbits. **D.** QRS duration in n=8 young and n=6 old rabbits. ** $p<0.01$. **E.** Heart rate corrected QT index (QT_i) in n=8 young and n=6 old rabbits. All values are shown as mean ± SD. **F.** and **G.** show representative intracardiac ECG traces (RV apex, mid, and base position) of individual young and old rabbits. A= atrium, H= His electrogram, V= ventricle. **H.** Duration of AH intervals, which reflect conduction from the atrium to the proximal His bundle, in n=8 young and n=6 old rabbits. **I.** Duration of HV intervals, which reflect conduction from the His bundle via Purkinje fibers to the ventricle, in n=8 young and n=6 old rabbits. *** $p<0.0001$. All values are shown as mean ± SD. *The author contributed to this experiment as a supportive role.*

Figure 2.4: Optical mapping in young and old hearts.

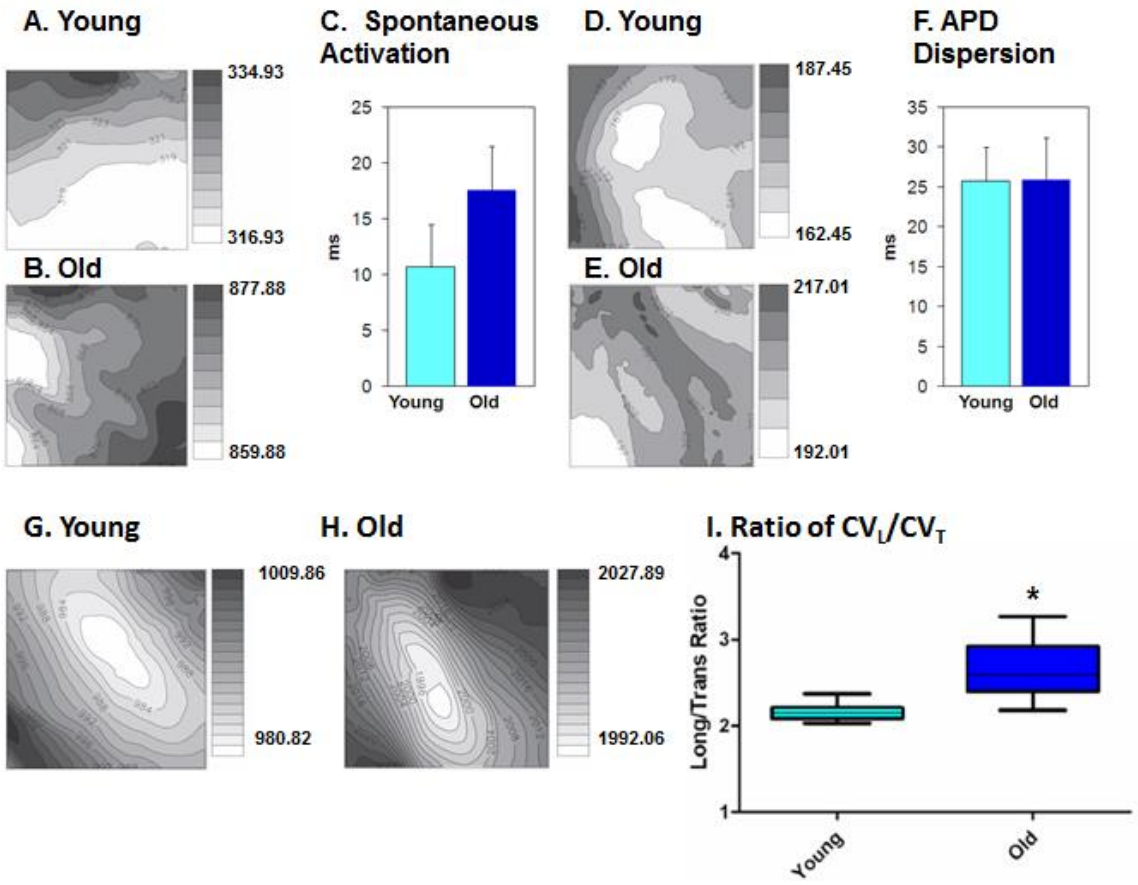

A. – C. Representative maps and graph of spontaneous activation from the LV in n=6 young and n=9 old hearts. Isochronal lines are drawn 2 ms intervals and brighter color indicate earlier activation. *p=NS*. **D. – F.** Representative action potential dispersion maps and graph in n=6 young and n=8 old hearts. *p=NS*. **G** and **H.** Representative activation maps and graph from LV center stimulation. **I.** Ratio of CV_L/CV_T in n=7 young and n=9 old hearts.*$p<0.05$; all values are shown as mean ± SD. *This experiment was not performed by the author.*

Figure 2.5: VF in young and old hearts.

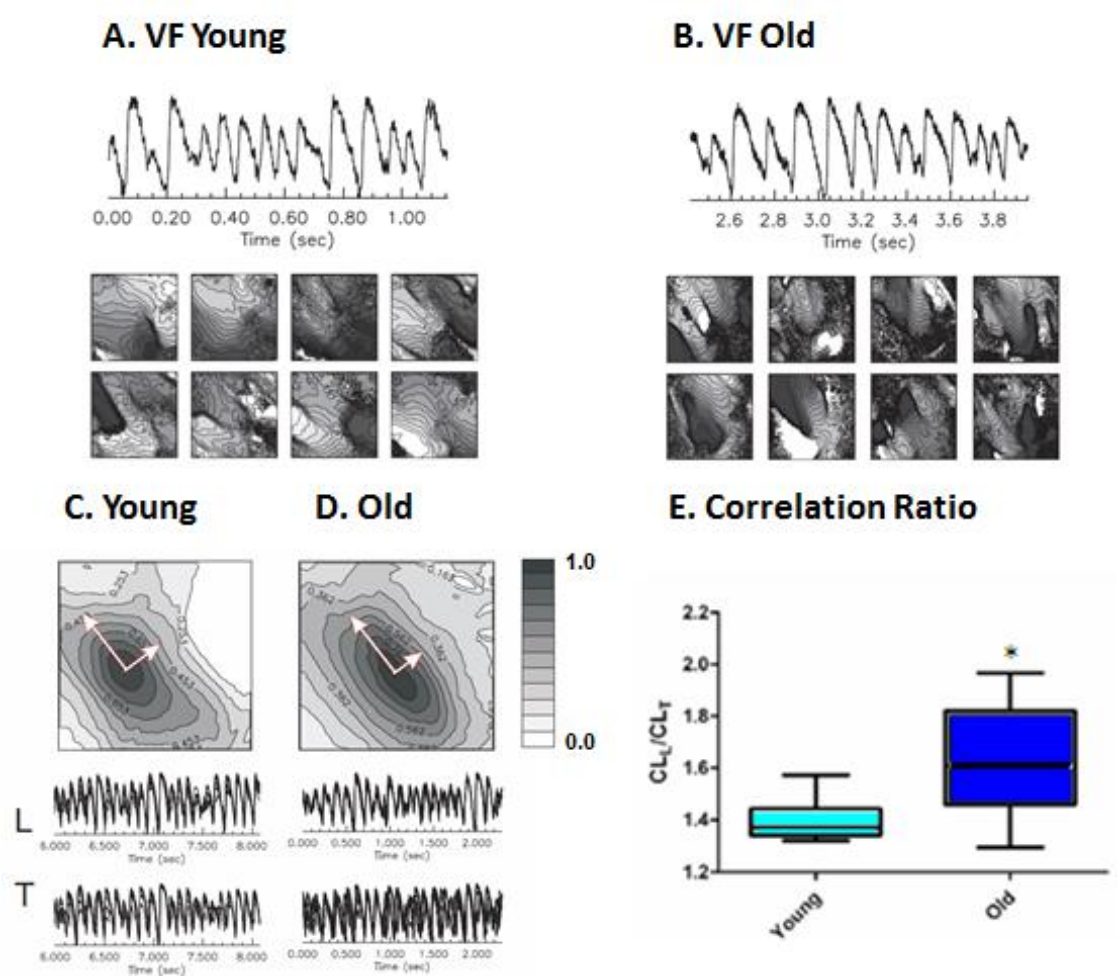

A. and **B.** Representative series of activation maps of hearts during VF from the LV in n=3 young and n=7 old hearts. Isochronal lines are drawn at 2 ms intervals, brighter colors indicate earlier activation. **C.** and **D.** Cross-correlation of propagating waves in the longitudinal (L) and transverse (T) directions of individual young and old rabbit hearts during VF. **E.** Box graphs of correlation length ratio (CL_L/CL_T) in n=3 young and n=7 old rabbit hearts. *p<0.05; all values are shown as mean ± SD. *This experiment was not performed by the author.*

Figure 2.6: Fibrosis analysis in young and old hearts.

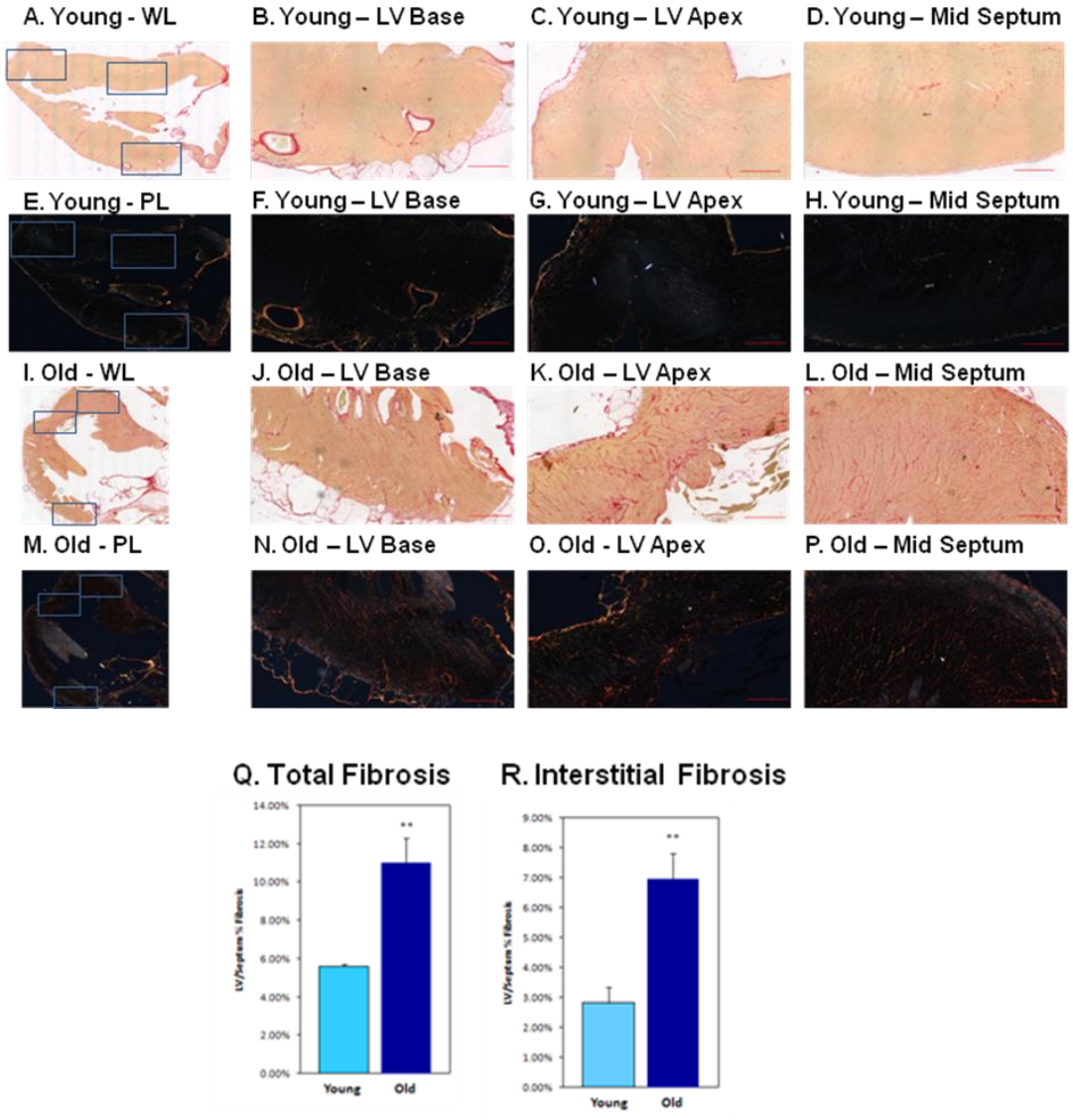

A. – P. show representative Sirius red stainings of the LV and septum of young hearts under white and polarized light. **Q.** and **R.** show total and interstitial fibrosis as a percentage of the LV and the septum in young (n=3) and old (n=3) rabbit hearts (one section of LV and septum per heart). ***p*<0.01; all scale bars = 1,000 µm. All values are shown as mean ± SD.

Figure 2.7: MRI parameters in the young and old heart.

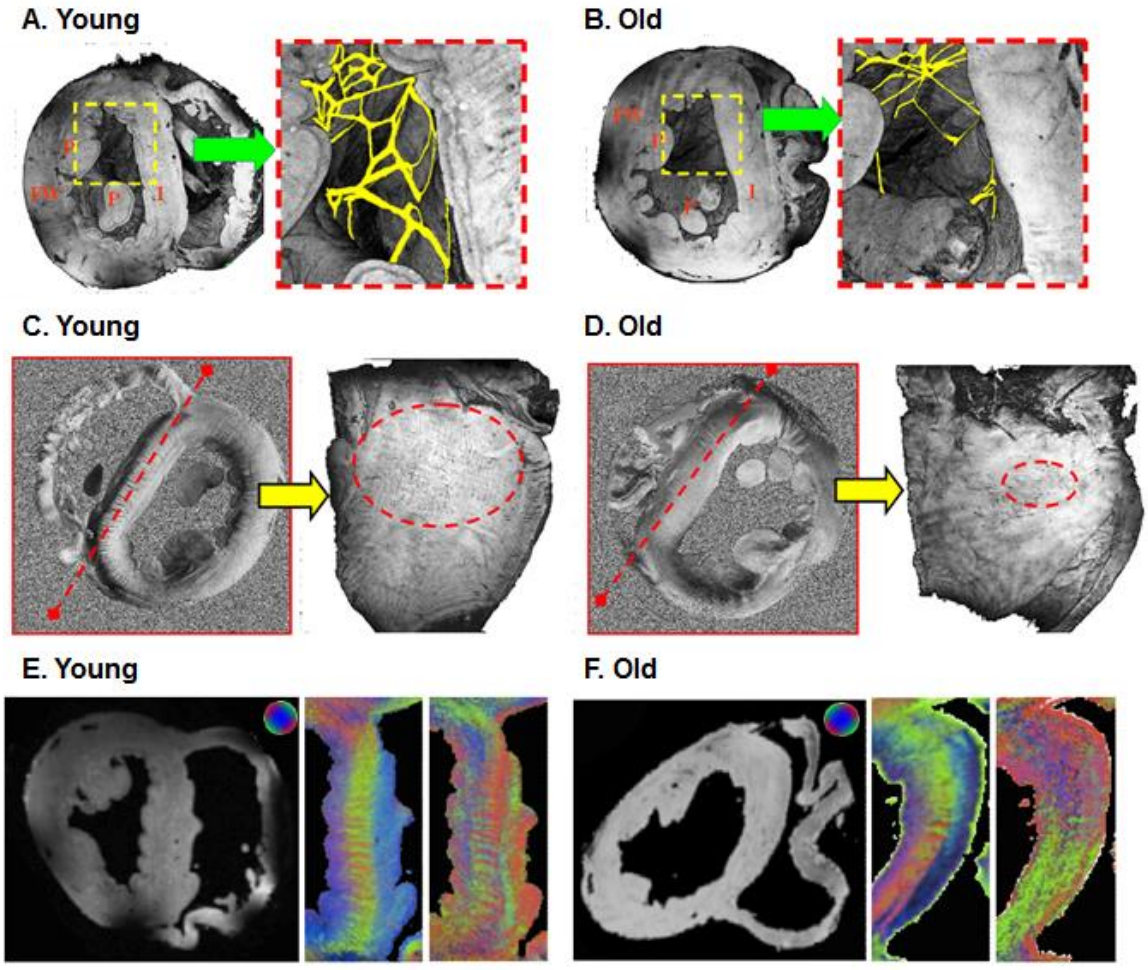

A. and **B.** Representative volume rendered transverse images and manual segmentation (magnified) of the free-running Purkinje fiber network in the LV of an individual young and old rabbit heart. Lines and arrows in the green and red boxes indicate where virtual sectioning occurred in the long axis planes. Interventricular septum thickness is approximately 3.93 mm (young) and 4.82 mm (old). I: interventricular septum, P: papillary muscle, FW: free wall. **C.** and **D.** Representative tensor component (Dyz) map from high angular resolution diffusion microscopy and a volume rendered image of the interventricular septum of an individual young and old

rabbit heart. Dotted lines (red) indicate where sectioning occurred and dotted circles confine regions where the stripe pattern is observed. **E.** and **F.** The primary eigen vector and the tertiary eigen vector maps of the left interventricular septum of a young and old rabbit hearts. The primary eigen vector shows the preferential direction of water diffusion, and is known to follow cardiomyofibers and conducting fiber tracts. Note the rotation of the color wheel orientation in Panels E and F. The color wheel located at the top of each panel reflects the directional orientation of the respective eigen-vectors. Blue represents eigen-vectors that are through-plane (e.g, traveling out the page), while the colors red and green reflect in-plane orientations. Septal images have been rotated to allow comparison, and the color wheels have been rotated to the same extent to maintain the correct orientation for directionality. *This experiment was not performed by the author.*

Table 2.1: Echocardiography of young and old rabbits.

Table 1: Echocardiographic Data						
	IVS (mm)	PW (mm)	LVD (mm)	LVS (mm)	FS (%)	EF (%)
Young (n= 5)	2.66 (±0.39)	2.77 (±0.44)	13.51 (±2.02)	9.37 (±2.18)	30.86 (±10.29)	65.25 (±13.60)
Old (n= 5)	3.47 (±0.66) *	3.36 (±0.58)	13.50 (±2.58)	9.62 (±2.51)	29.41 (±6.30)	64.16 (±8.97)

Comparison of the interventricular septum (IVS) thickness, *p<0.05; All other comparisons, p=NS. EF, ejection fraction; FS, fractional shortening; IVS, intraventricular septum thickness; LVD, diastolic diameter of the left ventricle; LVS, systolic diameter of the left ventricle; PW, posterior wall thickness. *The author acquired echocardiography images, which were analyzed by a reader blinded to age.*

2.8 References

1. Kannel WB, Cupples LA, D'Agostino RB: **Sudden Death Risk in Overt Coronary Heart Disease: the Framingham Study**. *Am Heart J* 1987, **113**(3):799 -- 804.
2. Eghbali M, Robinson TF, Seifter S, Blumenfeld OO: **Collagen Accumulation In Heart Ventricles as a Function of Growth and Aging**. *Cardiovasc Res* 1989, **23**(8):723 -- 729.
3. Rossi S, Baruffi S, Bertuzzi A, Miragoli M, Corradi D, Maestri R, Alinovi R, Mutti A, Musso E, Sgoifo A *et al*: **Ventricular Activation is Impaired in Aged Rat Hearts**. *Am J Physiol - Heart C* 2008, **295**(6):H2336 -- 2347.
4. Gottwald M, Gottwald E, Dhein S: **Age-Related Electrophysiological and Histological Changes in Rabbit Hearts: Age-Related Changes in Electrophysiology**. *Int J Cardiol* 1997, **62**(2):97 -- 106.
5. Dhein S, Hammerath SB: **Aspects of the Intercellular Communication in Aged Hearts: Effects of the Gap Junction Uncoupler Palmitoleic Acid**. *Naunyn-Schmiedebergs Arch Pharmacol* 2001, **364**(5):397 -- 408.
6. Taneja T, Mahnert BW, Passman R, Goldberger J, Kadish A: **Effects of Sex and Age on Electrocardiographic and Cardiac Electrophysiological Properties in Adults**. *Pacing Clin Electrophysiol* 2001, **24**(1):16 -- 21.
7. Fleg JL, Das DN, Wright J, Lakatta EG: **Age-Associated Changes in the Components of Atrioventricular Conduction in Apparently Healthy Volunteers**. *J Gerontol* 1990, **45**(3):M95 -- 100.

8. Schmidlin O, Bharati S, Lev M, Schwartz JB: **Effects of Physiological Aging on Cardiac Electrophysiology in Perfused Fischer 344 Rat Hearts**. *Am J Physiol* 1992, **262**(1 Pt 2):H97 -- 105.

9. Koura T, Hara M, Takeuchi S, Ota K, Okada Y, Miyoshi S, Watanabe A, Shiraiwa K, Mitamura H, Kodama I *et al*: **Anisotropic Conduction Properties in Canine Atria Analyzed by High-Resolution Optical Mapping: Preferential Direction of Conduction Block Changes from Longitudinal to Transverse with Increasing Age**. *Circulation* 2002, **105**(17):2092 -- 2098.

10. Stein M, Noorman M, van Veen TA, Herold E, Engelen MA, Boulaksil M, Antoons G, Jansen JA, van Oosterhout MF, Hauer RN *et al*: **Dominant Arrhythmia Vulnerability of the Right Ventricle in Senescent Mice**. *Heart Rhythm* 2008, **5**(3):438 -- 448.

11. Stein M, Boulaksil M, Jansen JA, Herold E, Noorman M, Joles JA, van Veen TA, Houtman MJ, Engelen MA, Hauer RN *et al*: **Reduction of Fibrosis-Related Arrhythmias by Chronic Renin-Angiotensin-Aldosterone System Inhibitors in an Aged Mouse Model**. *Am J Physiol - Heart C* 2010, **299**(2):H310 -- 321.

12. Mitchell GF, Vasan RS, Keyes MJ, Parise H, Wang TJ, Larson MG, D'Agostino RB, Sr., Kannel WB, Levy D, Benjamin EJ: **Pulse Pressure and Risk of New-Onset Atrial Fibrillation**. *JAMA* 2007, **297**(7): 709 -- 715.

13. Mitchell GF: **Arterial Stiffness and Wave Reflection: Biomarkers of Cardiovascular Risk**. *Artery Res* 2009, **3**(2):56 -- 64.

14. Mitchell GF, Hwang SJ, Vasan RS, Larson MG, Pencina MJ, Hamburg NM, Vita JA, Levy D, Benjamin EJ: **Arterial Stiffness and Cardiovascular Events the Framingham Heart Study**. *Circulation* 2010, **121**(4):505 -- 511.

15. Zheng ZJ, Croft JB, Giles WH, Mensah GA: **Sudden Cardiac Death in the United States, 1989 to 1998**. *Circulation* 2001, **104**(18):2158 -- 2163.

16. Schatzkin A, Cupples LA, Heeren T, Morelock S, Kannel WB: **Sudden-Death in the Framingham Heart-Study - Differences in Incidence and Risk-Factors by Sex and Coronary-Disease Status**. *Am J Epidemiol* 1984, **120**(6):888 -- 899.

17. Salata JJ, Jurkiewicz NK, Jow B, Folander K, Guinosso PJ, Jr., Raynor B, Swanson R, Fermini B: **IK of Rabbit Ventricle is Composed of Two Currents: Evidence for IKs**. *Am J Physiol* 1996, **271**(6 Pt 2):H2477 -- 2489.

18. Varro A, Lathrop DA, Hester SB, Nanasi PP, Papp JG: **Ionic Currents and Action Potentials in Rabbit, Rat, and Guinea Pig Ventricular Myocytes**. *Basic Res Cardiol* 1993, **88**(2):93 -- 102.

19. Mitchell GF, Pfeffer MA, Westerhof N, Pfeffer JM: **Measurement of Aortic Input Impedance in Rats**. *Am J Physiol* 1994, **267**(5 Pt 2):H1907-1915.

20. Mitchell GF, Pfeffer MA, Finn PV, Pfeffer JM: **Comparison of Techniques for Measuring Pulse-Wave Velocity in the Rat**. *J Appl Physiol* 1997, **82**(1):203 -- 210.

21. Yershov AL, Jordan BS, Fudge JM, Dubick MA: **Influence of the Mode of Ventilation on Ketamine/Xylazine Requirements on Rabbits**. *Vet Anaesth Analg* 2007, **34**(3):157 -- 163.

22. Pacher P, Nagayama T, Mukhopadhyay P, Bátkai S, Kass DA: **Measurement of Cardiac Function Using Pressure–Volume Conductance Catheter Technique in Mice and Rats**. *Nat Protoc* 2008, **3**:1422 -- 1434.

23. Odening KE, Kirk M, Brunner M, Ziv O, Lorvidhaya P, Liu GX, Schofield L, Chaves L, Peng X, Zehender M *et al*: **Electrophysiological Studies of Transgenic Long QT Type 1 and Type 2 Rabbits Reveal Genotype-Specific Differences in Ventricular Refractoriness and His Conduction**. *Am J Physiol - Heart C* 2010, **299**(3):H643 -- 655.

24. Brunner M, Peng X, Liu GX, Ren XQ, Ziv O, Choi BR, Mathur R, Hajjiri M, Odening KE, Steinberg E *et al*: **Mechanisms of Cardiac Arrhythmias and Sudden Death in Transgenic Rabbits with Long QT Syndrome**. *J Clin Invest* 2008, **118**(6):2246 -- 2259.

25. Choi BR, Liu T, Lavasani M, Salama G: **Fiber Orientation and Cell-Cell Coupling Influence Ventricular Fibrillation Dynamics**. *J Cardiovasc Electrophysiol* 2003, **14**(8):851 -- 860.

26. Fedorov VV, Lozinsky IT, Sosunov EA, Anyukhovsky EP, Rosen MR, Balke CW, Efimov IR: **Application of Blebbistatin as an Excitation-Contraction Uncoupler for Electrophysiologic Study of Rat and Rabbit Hearts**. *Heart Rhythm* 2007, **4**(5):619 -- 626.

27. Andersen A, Nielsen JM, Peters CD, Schou UK, Sloth E, Nielsen-Kudsk JE: **Effects of Phosphodiesterase-5 Inhibition by Sildenafil in the Pressure Overloaded Right Heart**. *Eur J Heart Fail* 2008, **10**(12):1158 -- 1165.

28. Benveniste H, Blackband S: **MR Microscopy and High Resolution Small Animal MRI: Applications in Neuroscience Research**. *Prog Neurobiol* 2002, **67**(5):393 -- 420.

29. Barmpoutis A, Vemuri B: **A Unified Framework for Estimating Diffusion Tensors of Any Order with Symmetric Positive-Definite Constraints**. In: *I S Biomed Imaging 2010*; 2010: 1385 -- 1388.

30. Helm PA, Tseng HJ, Younes L, McVeigh ER, Winslow RL: ***Ex Vivo* 3D Diffusion Tensor Imaging and Quantification of Cardiac Laminar Structure**. *Magn Reson Med* 2005, **54**(4):850 -- 859.

31. LeGrice IJ, Smaill BH, Chai LZ, Edgar SG, Gavin JB, Hunter PJ: **Laminar Structure of the Heart: Ventricular Myocyte Arrangement and Connective Tissue Architecture in the Dog**. *Am J Physiol* 1995, **269**(2 Pt 2):H571 -- 582.

32. Basser PJ: **Focal Magnetic Stimulation of an Axon**. *IEEE Trans Biomed Eng* 1994, **41**(6):601 -- 606.

33. Basser PJ, Mattiello J, LeBihan D: **MR Diffusion Tensor Spectroscopy and Imaging**. *Biophys J* 1994, **66**(1):259 -- 267.

34. Hsu EW, Muzikant AL, Matulevicius SA, Penland RC, Henriquez CS: **Magnetic Resonance Myocardial Fiber-Orientation Mapping with Direct Histological Correlation**. *Am J Physiol* 1998, **274**(5 Pt 2):H1627 -- 1634.

35. Scollan DF, Holmes A, Winslow R, Forder J: **Histological Validation of Myocardial Microstructure Obtained from Diffusion Tensor Magnetic Resonance Imaging**. *Am J Physiol* 1998, **275**(6 Pt 2):H2308 -- 2318.

36. Miller TR, Grossman SJ, Schectman KB, Biello DR, Ludbrook PA, Ehsani AA: **Left Ventricular Diastolic Filling and Its Association with Age**. *Am J cardiol* 1986, **58**(6):531 -- 535.

37. Rodeheffer RJ, Gerstenblith G, Becker LC, Fleg JL, Weisfeldt ML, Lakatta EG: **Exercise Cardiac-Output Is Maintained with Advancing Age in Healthy-Human Subjects - Cardiac Dilatation and Increased Stroke Volume Compensate for a Diminished Heart-Rate**. *Circulation* 1984, **69**(2):203 -- 213.

38. Schulman SP, Lakatta EG, Fleg JL, Lakatta L, Becker LC, Gerstenblith G: **Age-Related Decline in Left-Ventricular Filling at Rest and Exercise**. *Am J Physiol* 1992, **263**(6):H1932 -- H1938.

39. Benjamin EJ, Levy D, Anderson KM, Wolf PA, Plehn JF, Evans JC, Comai K, Fuller DL, Sutton MS: **Determinants of Doppler Indexes of Left-Ventricular Diastolic Function in Normal Subjects (the Framingham Heart-Study)**. *Am J Cardiol* 1992, **70**(4):508 -- 515.

40. Lakatta EG, Levy D: **Arterial and Cardiac Aging: Major Shareholders in Cardiovascular Disease Enterprises - Part II: the Aging Heart In Health: Links to Heart Disease**. *Circulation* 2003, **107**(2):346 -- 354.

41. Borlaug BA, Lam CSP, Roger VL, Rodeheffer RJ, Redfield MM: **Contractility and Ventricular Systolic Stiffening in Hypertensive Heart Disease Insights Into the Pathogenesis of Heart Failure With Preserved Ejection Fraction**. *J Am Coll Cardiol* 2009, **54**(5):410 -- 418.

42. Mitchell GF, Parise H, Benjamin EJ, Larson MG, Keyes MJ, Vita JA, Vasan RS, Levy D: **Changes in Arterial Stiffness and Wave Reflection with Advancing**

Age in Healthy Men and Women - the Framingham Heart Study. *Hypertension* 2004, **43**(6):1239 -- 1245.

43. Rogers WJ, Hu YL, Coast D, Vido DA, Kramer CM, Pyeritz RE, Reichek N: **Age-Associated Changes in Regional Aortic Pulse Wave Velocity**. *J Am Coll Cardiol* 2001, **38**(4):1123 -- 1129.

44. Mahmud A, Feely J: **Acute Effect of Caffeine on Arterial Stiffness and Aortic Pressure Waveform**. *Hypertension* 2001, **38**(2):227 -- 231.

45. Kingwell BA, Cameron JD, Gillies KJ, Jennings GL, Dart AM: **Arterial Compliance May Influence Baroreflex Function in Athletes and Hypertensives**. *Am J Physiol* 1995, **268**(1 Pt 2):H411 -- 418.

46. Avolio A, Jones D, Tafazzoli-Shadpour M: **Quantification of Alterations in Structure and Function of Elastin in the Arterial Media**. *Hypertension* 1998, **32**(1):170 -- 175.

47. Lantelme P, Khettab F, Custaud MA, Rial MO, Joanny C, Gharib C, Milon H: **Spontaneous Baroreflex Sensitivity: Toward an Ideal Index of Cardiovascular Risk in Hypertension?** *J Hypertens* 2002, **20**(5):935 -- 944.

48. Bosch X, Theroux P, Roy D, Moise A, Waters DD: **Coronary Angiographic Significance of Left Anterior Fascicular Block During Acute Myocardial Infarction**. *J Am Coll Cardiol* 1985, **5**(1):9 -- 15.

49. Mortara A, Sleight P, Pinna GD, Maestri R, Prpa A, La Rovere MT, Cobelli F, Tavazzi L: **Abnormal Awake Respiratory Patterns Are Common in Chronic Heart Failure and May Prevent Evaluation of Autonomic Tone by Measures of Heart Rate Variability**. *Circulation* 1997, **96**(1):246 -- 252.

50. Chen JJ, Liu W, Zhang HY, Lacy L, Yang XX, Song SK, Wickline SA, Yu X: **Regional Ventricular Wall Thickening Reflects Changes in Cardiac Fiber and Sheet Structure During Contraction: Quantification with Diffusion Tensor MRI**. *Am J Physiol - Heart C* 2005, **289**(5):H1898 -- H1907.

51. Josephson IR, Guia A, Stern MD, Lakatta EG: **Alterations in Properties of L-Type Ca Channels in Aging Rat Heart**. *J Mol Cell Cardiol* 2002, **34**(3):297 -- 308.

52. Walker KE, Lakatta EG, Houser SR: **Age Associated Changes in Membrane Currents in Rat Ventricular Myocytes**. *Cardiovasc Res* 1993, **27**(11):1968 -- 1977.

53. Slack JP, Grupp IL, Dash R, Holder D, Schmidt A, Gerst MJ, Tamura T, Tilgmann C, James PF, Johnson R *et al*: **The Enhanced Contractility of the Phospholamban-Deficient Mouse Heart Persists with Aging**. *J Mol Cell Cardiol* 2001, **33**(5):1031 -- 1040.

54. Li Q, Wu S, Li SY, Lopez FL, Du M, Kajstura J, Anversa P, Ren J: **Cardiac-Specific Overexpression of Insulin-Like Growth Factor 1 Attenuates Aging-Associated Cardiac Diastolic Contractile Dysfunction and Protein Damage**. *Am J Physiol - Heart C* 2007, **292**(3):H1398 -- 1403.

55. Lim CC, Liao R, Varma N, Apstein CS: **Impaired Lusitropy-Frequency in the Aging Mouse: Role of Ca^{2+}-Handling Proteins and Effects of Isoproterenol**. *Am J Physiol* 1999, **277**(5 Pt 2):H2083 -- 2090.

56. Schmidt U, del Monte F, Miyamoto MI, Matsui T, Gwathmey JK, Rosenzweig A, Hajjar RJ: **Restoration of Diastolic Function in Senescent Rat Hearts**

Through Adenoviral Gene Transfer of Sarcoplasmic Reticulum Ca^{2+}-ATPase. *Circulation* 2000, **101**(7):790 -- 796.

57. Xu A, Narayanan N: **Effects of Aging on Sarcoplasmic Reticulum Ca^{2+}-Cycling Proteins and Their Phosphorylation in Rat Myocardium**. *Am J Physiol* 1998, **275**(6 Pt 2):H2087 -- 2094.

58. Zhu X, Altschafl BA, Hajjar RJ, Valdivia HH, Schmidt U: **Altered Ca^{2+} Sparks and Gating Properties of Ryanodine Receptors in Aging Cardiomyocytes**. *Cell Calcium* 2005, **37**(6):583 -- 591.

59. Froehlich JP, Lakatta EG, Beard E, Spurgeon HA, Weisfeldt ML, Gerstenblith G: **Studies of Sarcoplasmic Reticulum Function and Contraction Duration in Young Adult and Aged Rat Myocardium**. *J Mol Cell Cardiol* 1978, **10**(5):427 -- 438.

60. Kondo T, Yamaki M, Kubota I, Tachibana H, Tomoike H: **Electrophysiologic Effects of Sodium Channel Blockade on Anisotropic Conduction and Conduction Block in Canine Myocardium: Preferential Slowing of Longitudinal Conduction by Flecainide Versus Disopyramide or Lidocaine**. *J Am Coll Cardiol* 1997, **29**(7):1639 -- 1644.

61. Mizumaki K, Fujiki A, Tani M, Misaki T: **Effects of Acute Ischemia on Anisotropic Conduction in Canine Ventricular Muscle**. *Pacing Clin Electrophysiol* 1993, **16**(8):1656 -- 1663.

62. Zipes DP, Jalife J (eds.): **Cardiac Electrophysiology: From Cell to Bedside**. Philadelphia WB Saunders; 1990.

63. Tsuboi N, Kodama I, Toyama J, Yamada K: **Anisotropic Conduction Properties of Canine Ventricular Muscles. Influence of High Extracellular K+ Concentration and Stimulation Frequency**. *Jpn Circ J* 1985, **49**(5):487 -- 498.

Appendix A: Supplemental Data for *Chapter 2*

This brief appendix presents unpublished data tables as a supplement to *Chapter 2,* which has been published.

The author contributed to this appendix by performing *in vivo* hemodynamics, aortic stiffness studies, and calculations herein.

Leroy L. Cooper*[1,2], Katja E. Odening*[1], Min-Sig Hwang[3,4], Leonard Chaves[1], Lorraine Schofield[1], Chantel A. Taylor[1], Anthony S. Gemignani[5], Gary F. Mitchell[6], John R. Forder[3,7], Bum-Rak Choi[1], and Gideon Koren[1]

[1]Cardiovascular Research Center, Division of Cardiology, Rhode Island Hospital, Warren Alpert Medical School of Brown University, Providence, RI, USA

[2]Department of Molecular Pharmacology, Physiology, and Biotechnology, Brown University, Providence, RI, USA

[3]McKnight Brain Institute, University of Florida, Gainesville, FL, USA

[4]Department of Neuroscience, University of Florida, Gainesville, FL, USA

[5]Division of Cardiology, Rhode Island Hospital, Warren Alpert Medical School of Brown University, Providence, RI, USA

[6]Cardiovascular Engineering, Inc., Norwood, MA, USA

[7]Department of Radiology, University of Florida, Gainesville, FL, USA

*These authors contributed equally.

A.1 Additional Hemodynamic Parameters

Using previously calculated parameters from the cardiac hemodynamic and aortic stiffness assessment, we calculated three additional parameters: preload recruitable stroke work (PRSW), arterial elastance (E_a), and arterial-ventricular coupling efficiency (AVCE):

Table A.1: Additional Hemodynamic Parameters

	Young	Old	*p*-value
PRSW (mmHg)	35.82 ± 11.02	43.64 ± 9.97	0.2265
E_a (mmHg/ml)	60.96 ± 14.02	53.21 ± 8.06	0.2677
E_{es} (mmHg/ml)	20.56 ± 4.20	33.14 ± 8.35	**0.0081
AVCE, E_a/E_{es}	3.04 ± 0.79	1.71 ± 0.53	**0.0063

All values are mean ± SD; n=6 per group; ***p*<0.01.

In ***Chapter 2*****,** we showed an age-related increase in the slope of the end systolic pressure-volume relation (ESPVR) and the end diastolic pressure-volume relation (EDPVR). This led us to conclude that aging in the rabbit was associated with greater cardiac contractility (steeper ESPVR) and greater diastolic stiffness (steeper EDPVR).

We also showed a significant increase in cardiac fibrosis in the aging rabbit. It has been shown that the ESPVR is susceptible to changes in preload and afterload; whereas, PRSW (the relation between stroke work and end-diastolic volume) is more reproducible and independent of load [1-3]. Therefore, we calculated PRSW as an additional parameter to assess systolic performance. Contrary to E_{es}, we showed that PRSW was not statistically altered with age, which suggests that cardiac aging of the rabbit heart is not associated with increased systolic contractility. Yet, a major limitation of this study is the low sample size, and although a trend toward an age-associated increase in PRSW exists, further study with adequate statistical power would be required to resolve this discrepancy. Additionally, Burkhoff and Sagawa have shown using an analytical model that PRSW is not entirely linear [4]. Also, stroke work is sensitive to changes in E_a as well as to diastolic pressure in the presence of diastolic dysfunction (as observed in old rabbits as a higher EDPVR) [4].

We also calculated E_a and arterial-ventricular coupling efficiency (AVCE or E_a/E_{es}) for young and old rabbits as a measure of global arterial load and an estimation of the relative coupling between the vascular systems and heart, respectively [5]. We were unable to detect statistical differences in the E_a between young and old rabbits; however, we observed lower AVCE in older animals. These data show that we were unable to resolve differences in E_a under ketamine/xylazine anesthesia in small groups of young and old rabbits. Additionally, higher AVCE in younger animals suggests that young rabbits may have a more robust response to anesthesia that tends to maximize stroke work at the expense of cardiac efficiency. Moreover, since older rabbits have higher E_{es}, the anesthesia-induced increase in E_a has less of an effect on the coupling

ratio. Young and old rabbits had comparable E_a under anesthesia; whereas, old rabbits had significantly higher PWV, indicating increased aortic stiffness. This contrast emphasizes the limitation of using E_a as a measure of arterial stiffness. E_a depends on many factors, including peripheral resistance (R_t) and cardiac cycle length (CL) [6]. We observed no age-related differences in R_t (36.02 ± 17.11 vs. 29.12 ± 7.53 mmHg/ml/s, p=0.3878) or CL (0.57 ± 0.13 vs. 0.54 ± 0.09 s, p=0.6750). Hence, when we estimated E_a as $Ea' \sim R_t/CL$ [4, 6], the values were highly correlated (E_a vs. E_a', R^2 = 0.919), and Ea' also did not differ between young and old rabbit hearts (p=0.0503).

In conclusion, we found evidence that older animals have stiffer aortas (PWV) and stiffer hearts in systole (ESPVR) and diastole (EDPVR). The markedly elevated coupling ratios observed under anesthesia suggest that both groups of animals were operating far from the optimum value, suggesting that E_a was markedly altered by anesthesia effects. The point estimate for PRSW was higher in older animals, although the difference could not be estimated with adequate precision in this small sample.

A.2 Heart Weight to Body Weight Ratio

Heart and body weights were obtained before optical mapping and used to calculate heart weight to body weight ratio as an estimation of age-associated hypertrophy. However, with a small sample size, the heart weight to body weight ratio was not significantly different with age, and we proceeded with more sensitive methods to detect hypotrophy (e.g., echocardiography and high-field MRI).

Table A.2: Heart Weight to Body Weight Ratio

	Young	Old	*p*-value
Heart Weight (HW, g)	8.90 ± 1.24	11.14 ± 2.87	0.2022
Body weight (BW, kg)	4.34 ± 0.40	4.72 ± 0.36	0.3991
HW:BW × 1000	2.06 ± 0.22	2.40 ± 0.74	0.4360

All values are mean ± SD; n=4 per group. All *p*-values are NS.

A.3 References

1. Feneley MP, Skelton TN, Kisslo KB, Davis JW, Bashore TM, Rankin JS: **Comparison of Preload Recruitable Stroke Work, End-Systolic Pressure-Volume and Dp/Dtmax-End-Diastolic Volume Relations as Indexes of Left-Ventricular Contractile Performance in Patients Undergoing Routine Cardiac-Catheterization**. *J Am Coll Cardiol* 1992, **19**(7):1522 -- 1530.

2. Glower DD, Spratt JA, Snow ND, Kabas JS, Davis JW, Olsen CO, Tyson GS, Sabiston DC, Rankin JS: **Linearity of the Frank-Starling Relationship in the Intact Heart - the Concept of Preload Recruitable Stroke Work**. *Circulation* 1985, **71**(5):994 -- 1009.

3. Kass DA, Midei M, Graves W, Brinker JA, Maughan WL: **Use of a Conductance (Volume) Catheter and Transient Inferior Vena-Caval Occlusion for Rapid-Determination of Pressure-Volume Relationships in Man**. *Catheter Cardio Diag* 1988, **15**(3):192 -- 202.

4. Burkhoff D, Sagawa K: **Ventricular Efficiency Predicted by an Analytical Model**. *Am J Physiol* 1986, **250**(6 Pt 2):R1021 -- 1027.

5. Kass DA: **Age-Related Changes in Venticular-Arterial Coupling: Pathophysiologic Implications**. *Heart Fail Rev* 2002, **7**(1):51 -- 62.

6. Kelly RP, Ting CT, Yang TM, Liu CP, Maughan WL, Chang MS, Kass DA: **Effective Arterial Elastance as Index of Arterial Vascular Load in Humans**. *Circulation* 1992, **86**(2):513 -- 521.

Chapter 3: Cellular Senescence and Pathological Hypertrophy Do Not Contribute to the Cellular, Pro-arrhythmic Phenotype Associated with Normal Aging in a Rabbit Model of Cardiac Aging

This chapter presents unpublished data.

The author contributed to this manuscript by performing *in situ* hybridization, immunofluorescence, immunoblotting and *β*-galactosidase assays, and qPCRs. The author also served as the co-mentor to Ezinne J. Ihenachor, a Brown University undergraduate student volunteer, who performed molecular analysis of hypertrophy under the direction of the author and his advisor.

Leroy L. Cooper[1,2], Ezinne J. Ihenachor[1,3], and Gideon Koren[1,2]

[1]Cardiovascular Research Center, Division of Cardiology, Rhode Island Hospital, Warren Alpert Medical School of Brown University, Providence, RI, USA

[2]Department of Molecular Pharmacology, Physiology, and Biotechnology, Brown University, Providence, RI, USA

[3]Division of Biology and Medicine, Health and Human Biology, Brown University, Providence, RI, USA

Keywords: cellular senescence, telomere dysfunction, DNA damage, and *β*-galactosidase

3.1 Abstract

We, and others, have shown that the age-related changes to the heart provide a substrate for deadly arrhythmias. Nonetheless, much remains unknown about the mechanisms that underlie the age-related, pro-arrhythmic triggers in the mammalian heart at the cellular and molecular level and how they are related to increased incidence of sudden cardiac death (SCD). Both cellular senescence and pathological hypertrophy have been implicated in increased arrhythmic risk. However, the putative link connecting organismal aging, cellular aging, and arrhythmia remains ambiguous and controversial. We seek to quantify senescence and pathological hypertrophy in young and old cardiac tissues and to address the hypothesis that these two processes provide sufficient trigger for arrhythmias in the aging heart, which contributes to the increased risk of sudden cardiac death. To that end, we performed various molecular biological and biochemical assays – including telomere dysfunction–induced foci (TIF) assay, *β*-galactosidase assay, immunoblotting, and qPCR – in order to quantify markers of cellular senescence and pathological hypertrophy in young (5 – 9 months) and old (4 – 6 years) rabbit heart tissue. The results did not reveal any significant differences between tissues from young and old rabbit hearts in any markers of cellular senescence nor did we observe any differences in molecular markers of pathological hypertrophy. We conclude that in the aging rabbit heart, cellular senescence and pathological hypertrophy do not play a role in the cellular pro-arrhythmic phenotype associated with normal aging in the absence of pathology.

3.2 Introduction

Accounting for approximately 50% of deaths related to heart disease, sudden cardiac death (SCD) is a leading cause of death in the United States. Thus, understanding the mechanisms that underlie SCD could lead to preventative and therapeutic strategies that would increase life expectancy and quality of life among a growing and susceptible population. The aging heart is characterized by an increase in fibrosis in the conduction system associated with slowing of the conduction velocity (CV) and increased incidence of conduction block [1-4]. It is likely that these morphologic changes exert a pro-arrhythmic effect by decreasing the threshold for ventricular fibrillation (VF) and by providing a substrate for deadly arrhythmias [5, 6]. Yet, much remains unknown about the processes that underlie the age-related, pro-arrhythmic changes in the mammalian heart at the cellular and molecular level and how they are related to increased incidence of SCD.

Cellular senescence is marked by terminal growth arrest, resistance to apoptosis and altered gene expression; however, these cells remain biologically active in their tissue niche [7]. Herein lies their potential to have various deleterious effects to an organ and entire organism. Cellular senescence is a process that has a putative link connecting organismal aging, cellular aging, and heart disease, but its role remains ambiguous and controversial although *in vivo* data have demonstrated that senescent cells accumulate with advancing cardiac and organismal age [8, 9]. Thus far, many age-associated, pathological cellular and molecular studies of the heart have focused on proliferating cells in the vasculature, “young” cardiomyocytes, and cardiac stem cells in the heart.

Minamino *et al.* found senescent vascular endothelial cells within human atherosclerotic lesions; this senescence was induced by telomere shortening, which they believe contributes to atherogenesis [10]. In addition, Torella *et al.* found that senescence, DNA damage, and death of cardiomyocytes and cardiac stem cells from mice hearts increased with age leading to heart failure [9]. More recently, it has been shown that suppression of phosphoinositide-3-kinase prevented expression of senescence markers and preserved cardiac function preventing heart failure in mice [11]. Yet, in an attempt to connect cellular senescence and cardiac aging, these studies show the presence of senescence cells that contribute to heart failure but have not thoroughly addressed mechanisms of cardiac arrhythmias and the age-associated alterations that occur at the cellular level.

Pathological hypertrophy is the enlargement of the myocardium in response to stress associated with increased wall thickness and/or increased chamber luminal dimensions, marked by a switch to fetal gene expression in rodents [12, 13]. Pathological hypertrophy has been connected to increased arrhythmic risk, and the extent of left ventricular hypertrophy has been used as an indicator of SCD risk [14, 15]. In addition, pressure-overload left ventricular hypertrophy is associated with increased rate of reactive oxygen species (ROS), resulting in oxidative damage to the heart [16-18]. Increased ROS production could contribute to cellular remodeling by activation of protein kinases sensitive to redox modification, which could further lead to cardiomyocyte death and accelerate decompensation of myocardium from hypertrophy to failure [19]. ROS may also oxidase receptors and ion channels modulating their activities leading to cardiomyocyte contractile dysfunction [19] and altering or promoting

substrate and triggers for arrhythmia. Hypertrophy has also been shown to affect mitochondria and the sarcoplasmic reticulum (SR). Sordahl *et al.* found that during the early phase of hypertrophy, mitochondria and SR have reduced rates of calcium binding, and the mitochondria have increased respiratory function; however, this is reversed then downregulated during decompensation and failure [20]. Clearly by affecting ROS production, mitochondrial function, and calcium cycling, hypertrophy has the potential to increase arrhythmic risk.

Previous studies have attempted to address the link between cellular aging and myocardial aging, but they have not thoroughly addressed cardiac arrhythmia and have failed to examine the age-associated alterations that occur in senescent cardiofibroblasts which play an integral role in the pathophysiology of myocardial senescence. Senescent cells hypertrophy [7], and since hypertrophy can induce mechanical and, more interestingly oxidative stress onto the heart leading to genotoxic damage, theoretically, these two processes may be connected in their contributions to increased triggers and/or modulation of pro-arrhythmic substrate. In order to bridge the gap between organ dysfunction and cellular aging, this investigation seeks to provide both molecular biological and biochemical evidence in order to examine the hypothesis that cellular senescence and pathological hypertrophy in the aging heart are important components that provide trigger for arrhythmias in the aging heart.

3.3 Methods

Animal Ethical Statement

All animal work was performed in accordance with the local guidelines of the institutions and only after approval by the Institutional Animal Care and Use Committee in accordance with the *Guide for the Care and Use of Laboratory Animals* published by the U.S. National Institutes of Health (NIH Publication No. 85-23, revised 1996).

Cell Isolation

Ventricular myocytes were isolated from young (5-9 months) and old (4-6 years) female, New Zealand White rabbits (Millbrook Breeding Labs, Amherst, MA, USA) as previously described [21, 22]. The rabbits were anaesthetized with ketamine (60 mg·kg^{-1}), xylazine (15 mg·kg^{-1} IM) and buprenorphine (0.03 mg·kg^{-1} SQ), and sodium pentobarbital (150 mg·kg^{-1}, IV). Hearts were quickly excised after thoracotomy and retrogradely perfused on a Langendorff apparatus with solution containing collagenase I (Roche Applied Science, Indianapolis, IN, USA) at 37°C. Cell solution was centrifuged at 20*g* for 5 min., and the resulting pellet containing cardiomyocytes was suspended in PBS solution. The supernatant was further centrifuged at 1,000*g* for 5 min., and the resulting pellet was suspended in DMEM/F12 media and plated onto cover glass and incubated at 37°C for 3 – 4 days or until 60 – 70 % confluence before assay. Late-passage human lung fibroblasts (HLF) (courtesy of the Sedivy lab) were quickly thawed, suspended in DMEM/F12 media, plated onto cover glass, and incubated at 37°C until 60 -- 70 % confluence before assay.

Tissues

Rabbit hearts were excised from young (5-9 months) and old (4-6 years) female, New Zealand White rabbits (Millbrook Breeding Labs, Amherst, MA, USA) as previously described [21, 22]. The rabbits were anaesthetized with ketamine (60 $mg \cdot kg^{-1}$), xylazine (15 $mg \cdot kg^{-1}$ IM) and buprenorphine (0.03 $mg \cdot kg^{-1}$ SQ), and sodium pentobarbital (150 $mg \cdot kg^{-1}$, IV). Hearts were quickly excised after thoracotomy. Tissue from the left ventricle was rapidly frozen with liquid nitrogen for biochemistry. For histological analysis, heart tissue was encapsulated in optimal cutting temperature (OCT, Andwin Scientific) compound solution or fixed in formalin for several days then encapsulated in paraffin.

Telomere Dysfunction–Induced Foci (TIF) Assay (ImmunoFISH Assay)

Sample Preparation: ImmunoFISH of rabbit tissue, rabbit cardiomyocytes and cardiofibroblasts, and cultured, late-passaged human lung fibroblasts (HLF, positive controls) were performed as described previously [23, 24]. Rabbit tissues in OCT were cut into 6 µm thick sections with a cryotome and immediately fixed for 20 min. with freshly prepared 4% paraformaldehyde dissolved in PBS. Rabbit tissues in paraffin were cut into 6 µm thick sections with a microtome, deparafinized, and rehydrated. Antigen retrieval was performed by microwave treatment (800 W for 15 min. in Target Retrieval Solution (Dako)), followed by 30 min. cooling in buffer. Cells (HLF, cardiomyocytes, and cardiofibroblasts) were washed in PBS then fixed with freshly prepared 4% paraformaldehyde dissolved in PBS for 5 min.

Samples were permeabilized for 20 min. with PBST (PBS with 0.2% Triton-X100), and then incubated in blocking buffer (4% BSA in PBS) for 1 h at room temperature. After

blocking, samples were incubated with a mouse monoclonal anti-53BP1 (or γH2AX) antibody (1:500 – 1,000) in 4% BSA-PBST for 2 h, washed three times with PBS, and then incubated with a goat anti-mouse Alexa-488-conjugated secondary antibody (Invitrogen Molecular Probes; Carlsbad, CA; 1:1000) for 1 h in 4% BSA-PBST. Afterwards, samples were washed with PBS, fixed again for 20 min. with 4% paraformaldehyde in PBS, and incubated with 0.25 mM glycine (in PBS) for 20 min. Samples were dehydrated sequentially by placing them in increasing amounts of ethanol (70, 90, and 100% ethanol for 3 min.). Samples were air dried on the slides then incubated for 5 min. at 80°C in hybridization buffer containing 0.5 μg/ml $(C_3TA_2)_3$-Cy3 labeled peptide nucleic acid (PNA) telomeric probe (courtesy of the Sedivy Laboratory, Applied Biosystems, Foster City, CA), 70% formamide (Sigma, St. Louis, MO), 12 mM Tris–HCl (pH 8.5), 5 mM KCl, 1 mM $MgCl_2$, 0.001% Triton X-100 and 2.5 mg/ml acetylated BSA (Sigma). In the same buffer, the samples were further incubated at room temperature for 14 h in a humidified chamber. The slides were washed three times in 70% formamide/2 × SSC (0.3 M NaCl, 30 mM Na-citrate, pH 7) for 10 min, followed by a 10 min wash with 2 × SSC, followed by a 10 min wash with PBS. Sections were incubated for 1 h with a donkey anti-goat antibody Alexa-488-conjugated (Invitrogen Molecular Probes; 1:1000). After three 5 min washes with PBS, nuclei were counterstained with 0.1 μg/ml DAPI for 5 min. Microscopy analysis was performed as previously described [23, 24] using 200 – 500 nuclei scored for each rabbit.

Immunofluorescence for Senescence in Tissue – Modification of TIF assay (above)

Fixation, permeabilization and blocking of samples were performed as described above. After blocking, sections were incubated with a mouse monoclonal anti-53BP1 (1:500 – 1,000) in 4% BSA-PBST for 2 h, washed three times with PBS, and then incubated with a goat anti-mouse Alexa-488-conjugated secondary antibody (Invitrogen Molecular Probes; Carlsbad, CA; 1:1,000) for 1 h in 4% BSA-PBST. Afterwards, tissue sections were washed with PBS, and incubated in blocking buffer (4% BSA in PBS) for 1 h at room temperature. Sections were incubated with a goat polyclonal anti-TRF1 antibody (1:500 – 1,000) in 4% BSA-PBST for 2 h, washed three times with PBS, and then incubated with a donkey anti-goat Cy3-conjugated secondary antibody (Invitrogen Molecular Probes; Carlsbad, CA; 1:1000) for 1 h in 4% BSA-PBST. After three 5 min. washes with PBS, nuclei were counterstained with 0.1 µg/ml DAPI for 5 min. and visualized with an epi-fluorescence scope.

β-galactosidase Assay

β-galactosidase staining was performed with modifications as previously performed by Dimri *et al.* and Debacq-Chainiaux *et al*. [25, 26]. Tissue sections were washed in PBS, fixed for 1 min. at room temperature in 2% formaldehyde/0.2% glutaraldehyde (in 1X PBS), washed, and incubated at 37°C with no CO_2 with fresh *β*-galactosidase staining solution (40 mM citric acid/Na phosphate buffer, 5 mM $K_4[Fe(CN)_6]\cdot 3H_2O$, 5 mM $K_3[Fe(CN)_6]$, 150 mM sodium chloride, 2 mM magnesium chloride and 1 $mg\cdot ml^{-1}$ X-gal) at pH 6 and pH 4 overnight.

RNA Isolation and cDNA Synthesis

Tissue from mid LV free wall (100 mg) was homogenized in 1 ml of TRIzol. Samples were incubated at room temperature for 5 min. 260 µl of chloroform was added to each sample and vortexed for 10 seconds. The samples were incubated at room temperature for 5 min., centrifuged at 11,700 g for 15 min. at 4^{o} C, and the top aqueous phase containing total RNA was removed. 700 µl of isopropyl alcohol was added to each sample to precipitate RNA. The samples were briefly mixed end over end, incubated at room temperature for 10 min., and centrifuged at 11,700 g for 10 min. at 4^{o} C. The supernatant was removed, 1.4 ml of 75% ethanol (made with diethylpyrocarbonate (DEPC)-treated water) was added, and the samples were vortexed and centrifuged at 7,500 g for 5 min. at 4^{o} C. The supernatant was removed, and the RNA was allowed to air dry for 5 min., and then re-dissolved in DEPC water. The nucleic acid concentration of the RNA was determined using the NANODROP 2000c Spectrophometer (ThermoScientific). DNAse treatment was performed to remove DNA contamination in the RNA sample. 0.1 volume 10X TURBO DNAse buffer and 1 µl TURBO DNAse (Life Technologies) was added to RNA and shaken gently. The RNA samples were then incubated at 37^{o} C for 20 min. 0.1 volume of DNAse inactivation reagent was resuspended and added to the above mixtures. The mixtures were then incubated for 5 min. at room temperature. The mixtures were centrifuged at 10,000 g for 1.5 min., and the RNA was transferred into a fresh tube. Nucleic acid concentration was determined once again post DNAse treatment. Reverse transcription was performed to produce cDNA libraries. 2X master mix was made as follows: 3.2 µl of nuclease-free water, 2 µl reverse-transcription buffer, 0.8 µl of dNTP mix, 2 µl of random primers, 1 µl reverse transcriptase, and 1µl of RNAse inhibitor. RNA for primer testing (from a young rabbit

sample) was diluted to 200 ng/µl and RNA from young and old hearts was diluted to 200 ng/µl as well. 10 µl of RNA (200 ng/µl) was added to 10 µl of 2X master mix (resulting in 100 ng/µl cDNA assuming 1:1 conversion) for both purposes. Reverse transcriptions were performed using the T3000 Thermocycler (Biometra).

Forward/reverse Primer Design and Conventional PCR

In order to perform PCR amplification, primer sets (and fluorescence probes) were designed for each candidate gene. Ensembl Genome Browser (www.ensembl.org) was used to obtain exon sequences for each candidate gene, and IDT DNA primer design tool (Integrated DNA Technologies, Coralville, IA) was used to yield several primer/probe sets for each candidate gene. Two primer sets were selected for each candidate gene for subsequent testing. Conventional PCR (cPCR) was performed to select specific primers for analysis of gene expression. TaqMan-based PCR reactions were used to amplify cDNA using forward and reverse primer sets for each candidate gene. 1 µl cDNA (100 ng/µl), 1 µl of forward primer, 1 µl of reverse primer, 25 µl of TaqMan polymerase, and 22 µl of water was combined for a final 50 µl reaction mixture for each forward/reverse primer pair. 20 µl of each cPCR product was run on a 2% agarose gel. The fluorescently labeled primer/probes for quantitative PCR (qPCR) were ordered based on the relative brightness of these pairs and correct amplicon size (**Table 3.1**).

Quantitative PCR (qPCR) for Primer/probe Efficiency and Analysis of Gene Expression

The efficiencies of selected primer/probe sets for each gene were determined (**Table 3.1**) to accurately calculate fold change of gene expression ($\Delta\Delta$ C_T). TaqMan-based qPCR using 100 ng, 50 ng, 25 ng, and 10 ng of cDNA was performed in triplicate for each primer set using ABI 7900 (BioRad). GAPDH control and no template or no primers were used as positive and negative controls, respectively. Standard curves were constructed using DNA quantity plotted against the mean C_T values on a logarithmic scale. The slope of the resulting linear regression was used to calculate efficiency (eff) using the equation as follows: $eff=10^{(-1/slope)} -1$.

To calculate relative change in gene expression, each of the candidate genes was quantified using TaqMan-based qPCR using 23.5 – 112.5 ng of DNA and ABI 7900 HT (Applied Biosystems) thermocycler. qPCR reactions were done in triplicate. Fold change of gene expression was calculated as $\Delta\Delta$ C_T corrected for primer efficiency.

Western Blotting

Antibodies against atrial natriuretic peptide (ANP, Thermo Fisher, Waltham, MA, USA), tumor necrosis factor-α (TNFα, Thermo Fisher), and desmin (Thermo Fisher) were used to determine respective protein levels by immunoblotting. Tissue homogenates proteins (20-30 µg) were resolved on a 4–20 % gel via SDS-PAGE, transferred onto nitrocellulose membranes, and probed with mouse monoclonal antibodies specific for these proteins (1:1,000) and subsequently probed with a donkey anti-mouse secondary antibody (1:10,000), Thermo Fisher). Blots were developed with SuperSignal West Pico and Femto (Thermo Fisher), and quantified and analyzed by using GeneSnap

(Syngene, Cambridge, UK) and ImageJ (US National Institutes of Health, Bethesda, MD, USA) softwares.

Statistical Analysis

Data are presented as mean ± SEM of *n* measured cells or rabbits. Statistical comparisons between groups were performed with Student's *t* test. Differences were considered statistically significant at $P < 0.05$.

3.4 Results

Young Cardiofibroblasts but not Cardiomyocytes Show Evidence of Cellular Senescence (Replicative)

We first established the TIF assay in cells using HLF (positive controls), and cardiomyocytes and cardiofibroblast in young rabbits. We performed the TIF assay six times with only cardiofibroblasts and twice with both cardiofibroblasts and cardiomyocytes all originating from young left ventricular area of rabbit hearts. For this assay, telomeres were marked via Cy3-PNA probes and appear red, and dsDNA breaks were marked via an anti-53BP1 antibody (cross-linked with Alexa fluor 488) and are depicted as the larger green foci. **Figure 3.1** depicts representative cells after ImmnoFISH assay as merged maximum projected deconvolved images and arrows point to areas of co-localization of 53BP1 foci (dsDNA breaks) and telomeres. Cells are classified senescent per the criteria outlined by Herbig *et al.*: colocalization of 53BP1 foci at the site of telomere in two or more planes, and at least 50 % of the 53BP1 foci

co-localize with telomeres [23]. Panel A of **Figure 3.1** shows the nucleus of a representative HLF with three 53BP1 foci that are all colocalized with telomeres (TIF positive). About 25% of HLF are TIF positive. Panels B and C of **Figure 3.1** depict the nuclei of a TIF negative and TIF positive rabbit cardiofibroblast. In Panel B, only one 53BP1 foci is colocalized with a telomere (33%, TIF negative); however, one of the two 53BP1 foci is colocalized with a telomere in Panel C (50%, TIF positive). Thus, a small population of cardiofibroblasts (<5 %) is senescent; however, no isolated cardiomyocytes were TIF positive. Panel D of **Figure 3.1** depicts two rabbit cardiomyocytes at lower magnification in order to show none of the nuclei have 53PB1 foci. These data suggest that cardiofibroblasts (*in vitro*), but not cardiomyocytes (acutely isolated), undergo replicative senescence under these experimental conditions.

Lack of Increasing Markers of Senescence with Age In Vivo

Flash-frozen tissue sections (or immediately fixed tissues) are representative of the *in vivo* state of the heart [27]. We used the TIF assay to quantify the amount of cellular senescence in the rabbit LV heart tissue due to increasing age, which is depicted as deconvolved maximum projection images in **Figure 3.2**, and colocalization of 53BP1 foci and telomere in nuclei are shown in the merge subpanels for each group. Panel A shows representative nuclei of HLFs, which have ~25% TIF positive cells. However, in Panels B – E, no 53BP1 foci (or evidence of dsDNA breakage) are present as depicted in DAPI + FITC subpanels. Thus, using both frozen and paraffin-embedded sections, we were unable to observe any marker of dsDNA breakage using both 53BP1 and γH2AX in rabbit heart tissue. TIF assays in tissues using frozen sections were repeated eight

times; paraffin sections were only used once. These data suggest that replicative senescence is absent *in vivo* in cardiac tissue.

Lysosomal β-galactosidase Staining but not SA β-galactosidase Increases with Age

To measure senescence that is not specifically associated with telemetric dysfunction, SA-*β*-galactosidase assays (at pH 6) were performed (4X) on frozen tissue sections from young and old rabbits (**Figure 3.3 D – F**). Panel D depicts HLFs (positive controls) which are almost 100% positive for *β*-galactosidase activity (as indicated by the blue precipitate) under these conditions specific to senescence. Panels E and F, however, are absent of the blue precipitate and therefore absent of *β*-galactosidase activity at pH 6 in young and old rabbit heart tissues. Thus, we did not find positive evidence of cellular senescence via this method in the rabbit heart tissue. Concurrently, we performed the assays at pH 4, which is specific to lysosomal *β*-galactosidase activity at optimal pH conditions (**Figure 3.3 A – C**). Panel A depicts HLFs (positive controls), where 20 – 25% were positive for *β*-galactosidase activity (as indicated by the blue precipitate). Panels B and C of **Figure 3.3** show representative images of young and old rabbit heart tissues assayed for lysosomal *β*-galactosidase activity. As evidenced by more areas of blue precipitate in Panel C when compared to Panel B of **Figure 3.3**; therefore, we found that lysosomal *β*-galactosidase staining increased with age in the rabbit heart (**Figure 3.3, G**), suggesting that lysosomes (or autophagosomes) are accumulating in the aging heart.

Furthermore, qPCR analysis confirmed that cellular senescence was not increased in the aging rabbit heart tissues as evidenced by the lack of upregulation of senescence genes at the transcript level. **Figure 3.4** shows that relative steady-state levels of p21, p53, and Rb1 transcripts were insignificant leading to negligible fold changes ($\Delta\Delta C_T$) with respect to age: 0.993, 1.006, and 1.000, respectively. Using qPCR, we were unable to determine age-related changes in steady-state levels of p16 due to low levels of the transcript. At the protein level, **Figure 3.5** shows an age-associated increase in p53 protein expression of about 35%, indicating that p53 is only upregulated post-transcriptionally in the aging heart. We were unable to determine age-related changes of p16, Rb1, and p21 at the protein level with Western blotting using multiple antibodies, which all resulted in either no bands or several non-specific bands.

Markers of Pathological Hypertrophy are Not Present in the Aging Rabbit Heart

Previously, we have shown that the septal and posterior wall of the rabbit heart becomes enlarged with age [28]; however, molecular characterization of the hypertrophy is unknown. Thus, we also examined if molecular evidence of pathological hypertrophy is associated with cardiac aging at both the transcript and protein levels. **Figure 3.6** shows that relative steady-state levels of ANP, Desmin, βMHC, and TNFα transcripts were insignificant leading to negligible fold changes ($\Delta\Delta C_T$) with respect to age: 0.996, 0.996, 0.997, and 1.000, respectively. Reinforcing this, we also did not observe any significant changes in protein expression levels of hypertrophic markers (**Figure 3.7**), including ANP, Desmin, and TNFα. These data indicate that the

hypertrophy associated with normal aging in the rabbit model is not pathological in nature.

3.5 Discussion

Here, we show via molecular biological and biochemical techniques that markers of cellular senescence and pathological hypertrophy are not present with increasing age in the rabbit model of cardiac aging. There were no significant differences in expression of any markers of cellular senescence between tissues from young and old rabbit hearts, and we showed that expression of molecular markers of pathological hypertrophy were unchanged with respect to age in the rabbit heart. We believe that cellular senescence and pathological hypertrophy do not play a role in the cellular pro-arrhythmic phenotype associated with normal aging.

No Evidence of Cellular Senescence in the Aging Rabbit Heart In Vivo

Although a small population of cultured isolated rabbit cardiofibroblasts were positive for senescence (**Figure 3.1**), it has been shown that cell culturing conditions can elicit false positives mainly due to oxidative stress (as reviewed in [29]); thus, in vitro observation are not directly generalizable to the *in vivo* state. Using both TIF and SA-*β*-galactosidase assays (**Figures 3.2** and **3.3 D – F),** we did not find evidence of dsDNA damage or cellular senescence in young and old tissues indicating that cellular senescence likely is not present *in vivo* in the rabbit heart to a measurable degree as evidenced using these methods. These findings are in direct contrast to Inuzuka *et al.*

who found that the number of cells (both cardiac myocytes and nonmyocytes) positive for SA-*β*-galactosidase activity increased 7-fold with aging in mice [11]. Our findings, however, are more in line with the Jeyepalan *et al*. study in a baboon model of aging where, in skeletal muscle, DNA damage to telomeres occurred in less than 3% of nuclei. Interestingly, they did not observe an age-associated increased of TIF foci indicating that cellular senescence via telemetric dysfunction did not increase with aging in skeletal muscle tissue [24]. This, along with our findings, further reinforces that in post-mitotic cells (like cardiomyocytes) and in quiescent cells (like cardiofibroblasts) replicative senescence like does not occur *in vivo*.

In addition, it has been shown that multiple markers of senescence, such as $p27^{Kip1}$, p53, $p16^{INK4a}$, and p19 [30], increase with age, and particularly in the heart [9, 11] in rodent models of aging via PCR and western blotting; however, we have not found similar results in our aging rabbit heart tissues (**Fig. 3.3**). Although we found that p53 protein increases with age, confirming a positive result for the presence of cellular senescence requires two or more concurrently expressed molecular markers of senescence. Moreover, we were unable to determine age-associated changes in other senescence markers at the protein level; yet, the steady-state levels of senescence gene expression were unchanged with age. Additionally, p53 is involved in a myriad of cellular processes including stress response, DNA repair, cell-cycle arrest, autophagy and apoptosis [31-33], so alternative above-mentioned interpretations for age-related upregulation of p53 are reasonable. These data from the rabbit heart tissue indicate that the process of cellular senescence is not a contributing factor to deleterious effects of normal cardiac aging.

No Evidence of Pathological Hypertrophy in the Aging Rabbit Heart

In our previous study presented in ***Chapter 2***, we showed that the ventricular wall of the aging rabbit hearts becomes less compliant and hypertrophies [28]. It is clear that decompensated cardiac hypertrophy can progress toward heart failure, which is correlated with age and associated with a significant increased risk of incidence of cardiac arrhythmias [34-36]. Here, however, we have shown that the mild cardiac hypertrophy observed in the rabbit heart is not associated with classic pathological hypertrophic markers (i.e., reversion to the cardiac fetal gene program) at the transcript and protein levels (**Figures 3.4** and **3.5**). Contrary to aging rodent models [11, 37-39], these data are consistent with human data of normal aging [35, 40] indicating that the molecular program of the heart does not revert to fetal gene expression and is absent of pathological hypertrophy. Thus, we believe that the hypertrophy associated in the rabbit aging model is a physiological consequence associated with normal aging and is not pathological in nature *en route* to heart failure. These data further reinforce the notion that our aging rabbit model is an appropriate, generalizable model for human cardiac function in normal aging and non- pathological conditions.

Reduced Autophagy as an Alternative Process That Could Underlie the Aging, Pro-Arrhythmic Phenotype at the Cellular Level

Autophagy is an important process that removes and recycles damaged organelle, proteins, and macromolecules via a lysosomal process to ensure cell survival and function (reviewed in [41] and [42]). However, with age, autophagy also declines leading

to the accumulation of cellular protein aggregates, which can inhibit essential molecular processes and cell functions [43, 44]. Although we did not observe an age-related increase in senescence, **Figure 3.2 A – C** shows an increase in lysosomal *β*-galactosidase staining in the aging rabbit heart tissue. These data suggest that aging upregulates the expression and/or increases the activity of lysosomal *β*-galactosidase under these conditions or that aging decreases autophagy as evidenced by the downregulation of processes downstream of lysosomal *β*-galactosidase activity. A downregulation of autophagy marked by the accumulation of the protein within arrested lysosomes and autophagosomes has been shown in both skeletal and cardiac muscle fibers [45, 46]. Thus, we believe a thorough examination of autophagy with the aging heart and how it may alter substrate and trigger relationship warrants further study as autophagy likely plays an important role in the cardiac remodeling associated with aging that contributes to a pro-arrhythmic phenotype.

Conclusion

These data indicate that cellular senescence and pathological hypertrophy are not involved in the age-related, arrhythmogenic phenotype associated with normal aging in the rabbit model. Since we observed increased lysosomal β-galactosidase staining with increasing age in the rabbit heart, decreased autophagy is an alternative process that we hypothesize is of an important research interest that may underlie the various mechanisms that alter both substrate and trigger and enhances age-related cardiac dysfunction and arrhythmic risk.

3.6 Figures and Table

Figure 3.1: TIF assay shows evidence of cellular senescence in isolated rabbit cardiofibroblasts but not in cardiomyocytes.

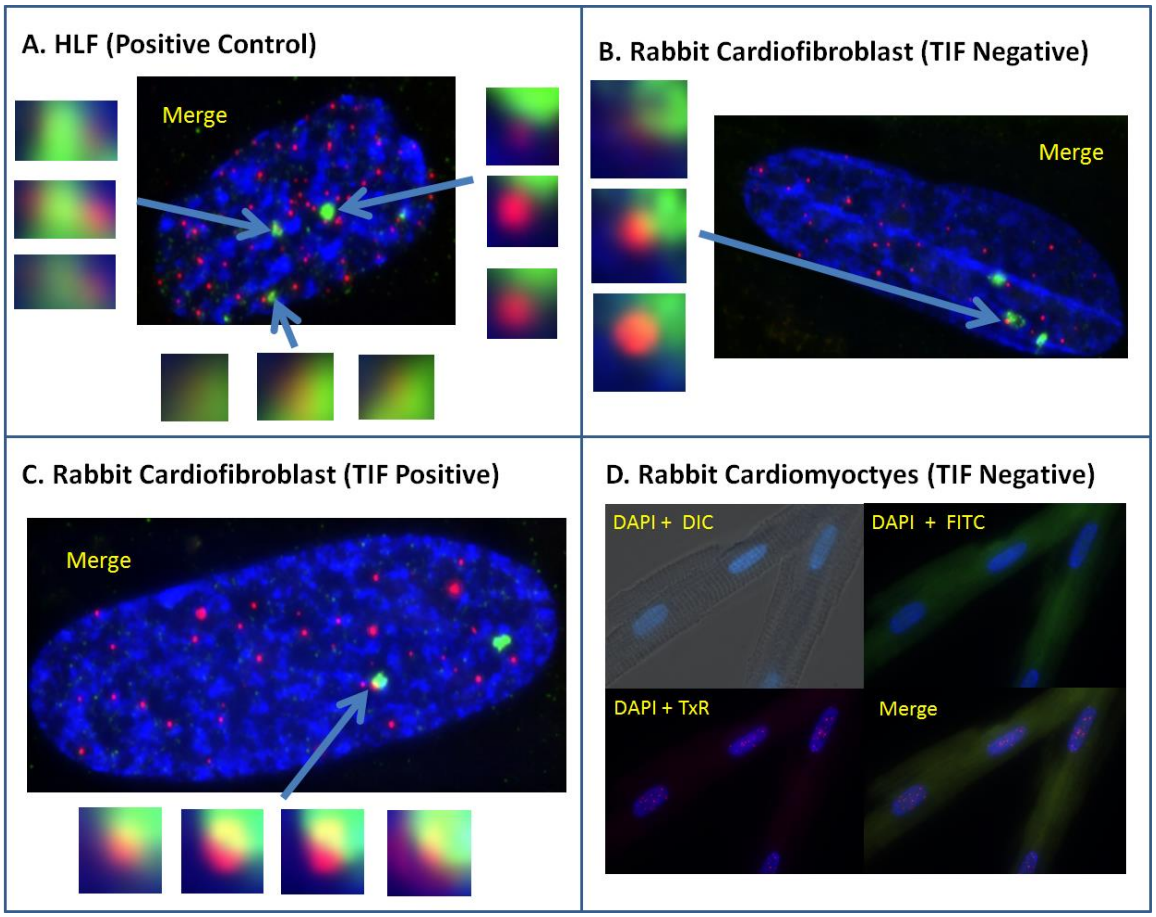

A – D. Representative images as maximum projections of deconvolved of TIF assay performed with human lung fibroblasts (HLF) and cardiofibroblasts and cardiomyocytes from young rabbit hearts. Cells were processed by immunoFISH to visualize 53BP1 foci (green) and telomeres (red). DNA was counterstained with DAPI (blue). Arrows point to enlarged images of the 53BP1/telomere signal in different planes at 0.5 um.

Figure 3.2: TIF assay in young and old rabbit heart tissue shows no staining of dsDNA breakage (53BP1 foci), thus no evidence of cellular senescence *in vivo.*

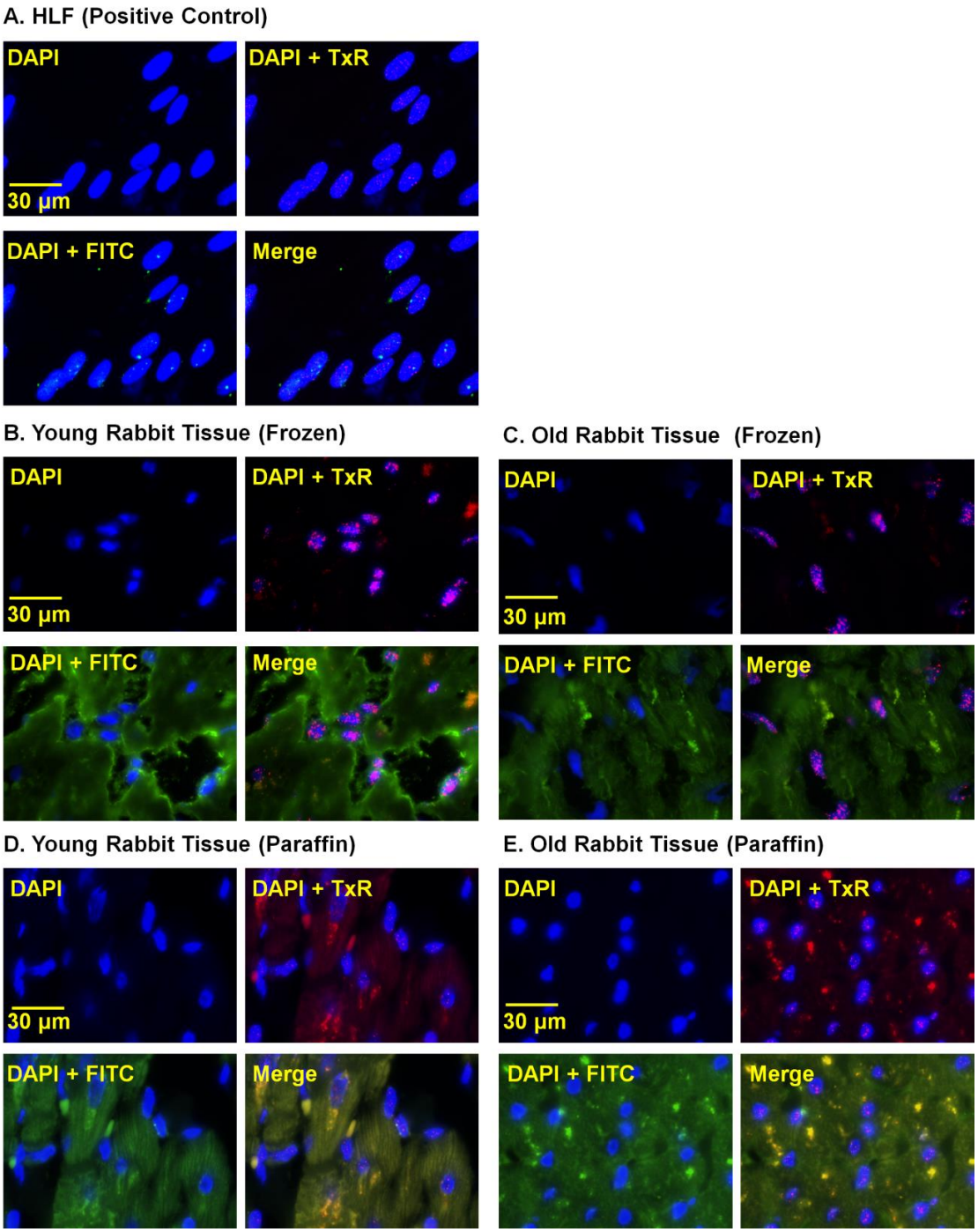

A – E. Representative images as maximum projections of decovolved of TIF assay performed with human lung fibroblasts (HLF) and young and old rabbit LV heart tissues

in OCT and paraffin, respectively. Cells and tissues were processed by immunoFISH to visualize 53BP1 foci (green) and telomeres (red). DNA was counterstained with DAPI (blue).

Figure 3.3: Lysosomal *β*-galactosidase staining, but not senescence-associated *β*-galactosidase staining, increases with age in the rabbit heart.

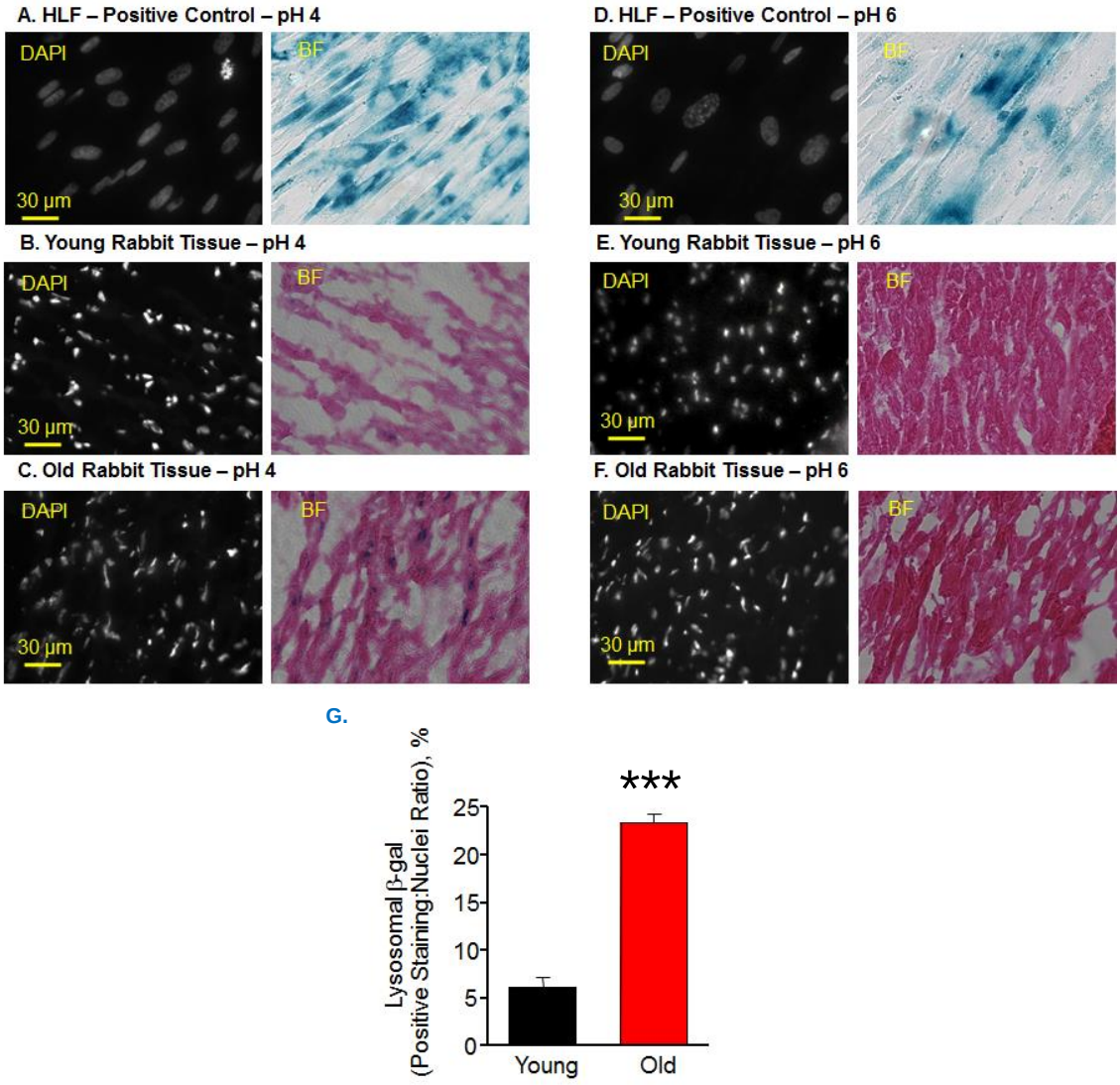

A. – C. Representative images of lysosomal *β*-galactosidase staining (pH 4) performed with HLF and young and old rabbit heart tissues, respectively. **D. – F.** Representative images of SA *β*-galactosidase staining (pH 6) performed with HLF and young and old rabbit heart tissues, respectively; no positive staining *β*- galactosidase staining. **G.** Graphic representation for lysosomal *β*- galactosidase staining data. ***$P < 0.01$. $n = 3 – 4$ rabbits and 314 – 575 cells from 3 – 4 sections per rabbit; all values are ± SEM.

Figure 3.4: Gene expression of senescence markers does not increase with age in rabbit heart tissue.

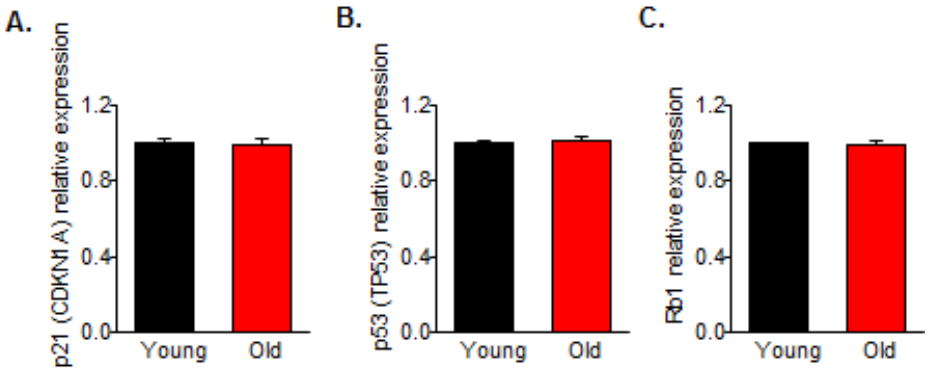

A. –- C. qPCR analysis showing relative expression of p21, p53, and Rb1 in young and old rabbit LV heart tissues. Age-related fold Δ p21, p53, and Rb1 are 0.993, 1.006, and 1.000, respectively. *P*=NS. *n* = 4 rabbits; all values are ± SEM.

Figure 3.5: p53 protein expression increases with age in the rabbit heart.

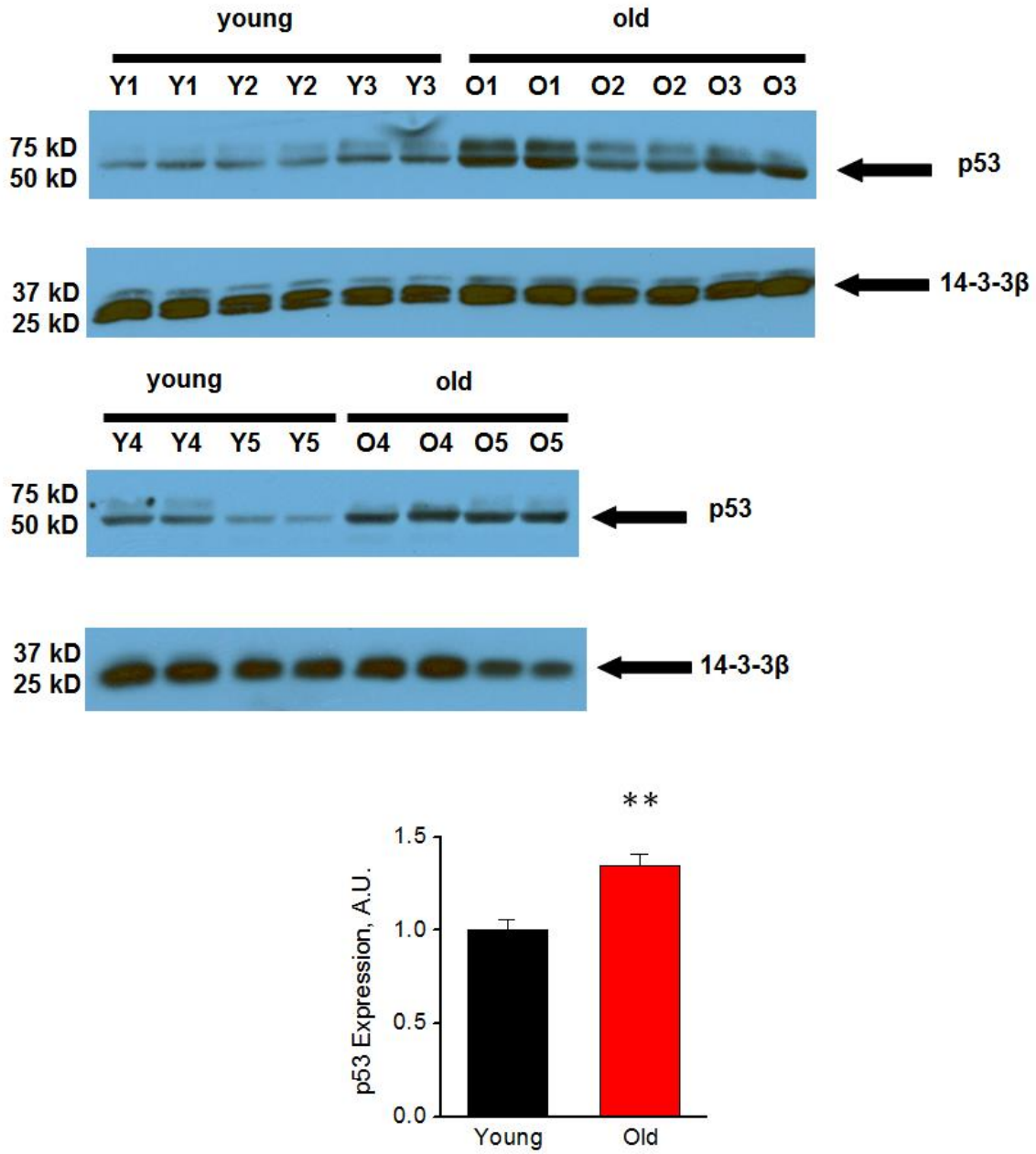

Average normalized OD data for the relative protein expression of p53 protein. 30 µg of protein was used from LV heart tissue. Protein expression was normalized to 14-3-3*β*. ***P <0.01*. *n* = 5 rabbits; all values are ± SEM.

Figure 3.6: Gene expression of hypertrophy markers does not increase with age in rabbit heart tissue.

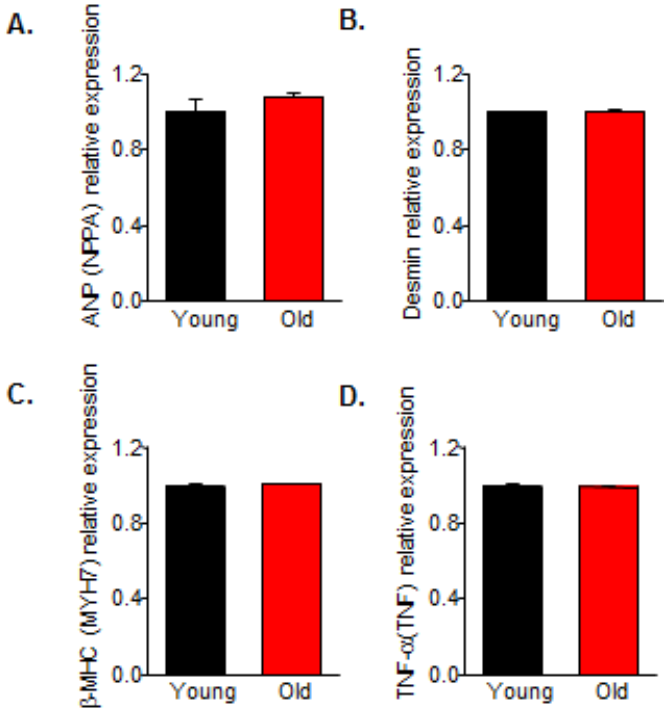

A. –- D. qPCR analysis showing relative expression of ANP, Desmin, βMHC, and TNFα in young and old rabbit LV heart tissue. Age-related fold Δ ANP, Desmin, βMHC, and TNFα are 0.996, 0.996, 0.997, and 1.000, respectively. *P*=NS. *n* = 4 rabbits; all values are ± SEM. *This experiment was not performed by the author.*

Figure 3.7: Protein expression of hypertrophy markers does not increase with age in rabbit heart tissue.

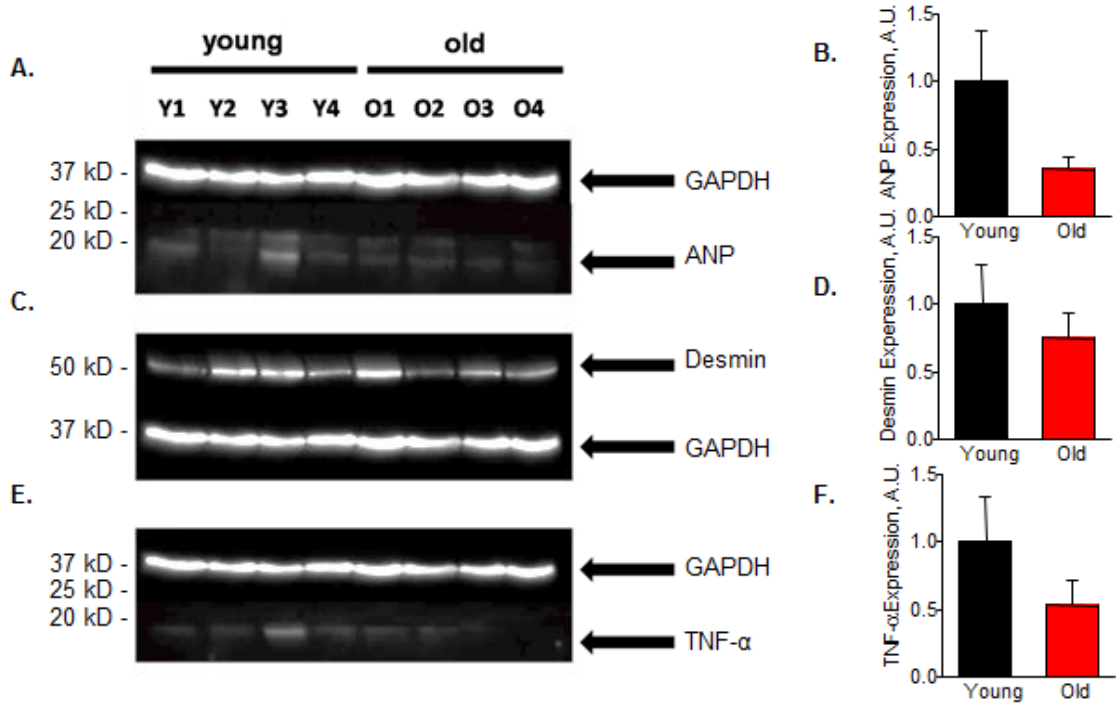

A – F. Average normalized OD data for the relative protein expression of ANP, Desmin, and TNFα. 30 µg of protein was used from LV heart tissue. Protein expression was normalized to GAPDH. *P*=NS. *n* = 4 rabbits; all values are ± SEM. *This experiment was not performed by the author.*

Table 3.1: Primers used for qPCR following reverse transcription

	Primer/probe Sequences (5'-3')	Efficiency
p53	Forward: AAGTCTCAGCACATGACGG Probe: CCCCACCTCAGCATCTCATCCG Reverse: TCTGTCATCCAAATACTCCGC	86.48%
p21	Forward: CTGTCGCTGACCTGCAC Probe: CGCCGTTTCCGACCCTAGAGA Reverse: GCGTTTGGAGTGGTAGAAATC	77.67%
Rb1	Forward: GTGAGCATCGAATCATGGAATC Probe: ACAGTCAAAGGACAGAGAGGGACCA Reverse: TTTTGGAGAGGAAGGTTGAGAG	79.36%
ANP	Forward: TTTGCTGGATCACTTGGAGG Probe: CAGCTTCATCTTCAAAAGGCATCCTGTC Reverse: ACTCTGCTCACTTAGTGCTTG	79.40%
TNF-α	Forward: GCTACATCACCGAACCTCTG Probe: CCTAAGGGAGTTGTGTTGGTAACCGC Reverse: TTATTTCTCGCCACTGACCAG	78.90%
Desmin	Forward: GAATACCGACACCAGATCCAG Probe: TGAGGGCATCAATCTCGCAGGTG Reverse: CCGCATCAGGGAATCGTTAG	96.10%
ß-MHC	Forward: CCAATGAGAACAAGACCCCAG Probe: AGCACCAGGAAGGCATCCATGA Reverse: CAGGACCCCATTACAGCG	81.20%
GAPDH	Forward: TCGGAGTGAACGGATTTGG Probe: TCTGGCAAAGTGGATGTTGTCGC Reverse: ATGGGTGGAATCATACTGGAAC	85.02%
SRP14	Forward: AAGGAAAGGTTCTGTGGGG Probe: TCACTTCTTTGGAGCTCACCACGG Reverse: CAACAGGTTTGAATAGGCCATC	74.49%

3.7 References

1. Hayashi H, Wang C, Miyauchi Y, Omichi C, Pak HN, Zhou S, Ohara T, Mandel WJ, Lin SF, Fishbein MC *et al*: **Aging-Related Increase to Inducible Atrial Fibrillation in the Rat Model**. *J Cardiovasc Electr* 2002, **13**(8):801-808.
2. Alings AM, Bouman LN: **Electrophysiology of the Ageing Rabbit and Cat Sinoatrial Node--A Comparative Study**. *Eur Heart J* 1993, **14**(9):1278 --1288.
3. Alings AM, Abbas RF, Bouman LN: **Age-Related Changes in Structure and Relative Collagen Content of the Human and Feline Sinoatrial Node. A Comparative Study**. *Eur Heart J* 1995, **16**(11):1655 -- 1667.
4. Strait JB, Lakatta EG: **Aging-Associated Cardiovascular Changes and Their Relationship to Heart Failure**. *Heart Fail Clin* 2012, **8**(1):143 -- 164.
5. Stein M, Noorman M, van Veen TA, Herold E, Engelen MA, Boulaksil M, Antoons G, Jansen JA, van Oosterhout MF, Hauer RN *et al*: **Dominant Arrhythmia Vulnerability of the Right Ventricle in Senescent Mice**. *Heart Rhythm* 2008, **5**(3):438 -- 448.
6. Dhein S, Hammerath SB: **Aspects of the Intercellular Communication in Aged Hearts: Effects of the Gap Junction Uncoupler Palmitoleic Acid**. *Naunyn-Schmiedebergs Arch Pharmacol* 2001, **364**(5):397 -- 408.
7. Campisi J, di Fagagna FD: **Cellular Senescence: When Bad Things Happen to Good Cells**. *Nat Rev Mol Cell Bio* 2007, **8**(9):729 -- 740.
8. Chimenti C, Kajstura J, Torella D, Urbanek K, Heleniak H, Colussi C, Di Meglio F, Nadal-Ginard B, Frustaci A, Leri A *et al*: **Senescence and Death of Primitive**

Cells and Myocytes Lead to Premature Cardiac Aging and Heart Failure. *Circ Res* 2003, **93**(7):604 -- 613.

9. Torella D, Rota M, Nurzynska D, Musso E, Monsen A, Shiraishi I, Zias E, Walsh K, Rosenzweig A, Sussman MA *et al*: **Cardiac Stem Cell and Myocyte Aging, Heart Failure, and Insulin-Like Growth Factor-1 Overexpression**. *Circ Res* 2004, **94**(4):514 -- 524.

10. Minamino T, Miyauchi H, Yoshida T, Ishida Y, Yoshida H, Komuro I: **Endothelial Cell Senescence in Human Atherosclerosis: Role of Telomere in Endothelial Dysfunction**. *Circulation* 2002, **105**(13):1541 -- 1544.

11. Inuzuka Y, Okuda J, Kawashima T, Kato T, Niizuma S, Tamaki Y, Iwanaga Y, Yoshida Y, Kosugi R, Watanabe-Maeda K *et al*: **Suppression of Phosphoinositide 3-Kinase Prevents Cardiac Aging in Mice**. *Circulation* 2009, **120**(17):1695 -- 1703.

12. Frey N, Olson EN: **Cardiac Hypertrophy: the Good, the Bad and the Ugly**. *Annu Rev Physiol* 2003, **65**:45 -- 79.

13. McMullen JR, Jennings GL: **Differences between Pathological and Physiological Cardiac Hypertrophy: Novel Therapeutic Strategies to Treat Heart Failure**. *Clin Exp Pharmacol* 2007, **34**(4):255 -- 262.

14. Spirito P, Maron BJ: **Relation between Extent of Left Ventricular Hypertrophy and Occurrence of Sudden Cardiac Death in Hypertrophic Cardiomyopathy**. *J Am Coll Cardiol* 1990, **15**(7):1521 -- 1526.

15. Benjamin EJ, Levy D: **Why is Left Ventricular Hypertrophy So Predictive of Morbidity and Mortality?** *Am J Med Sci* 1999, **317**(3):168 -- 175.

16. Sugden PH, Clerk A: **Cellular Mechanisms of Cardiac Hypertrophy**. *Mol Med* 1998, **76**(11):725-746.

17. Chien KR: **Stress Pathways and Heart Failure**. *Cell* 1999, **98**(5):555 -- 558.

18. Dhalla NS, Temsah RM, Netticadan T: **Role of Oxidative Stress in Cardiovascular Diseases**. *J Hypertens* 2000, **18**(6):655 -- 673.

19. Li JM, Gall NP, Grieve DJ, Chen MY, Shah AM: **Activation of NADPH Oxidase During Progression of Cardiac Hypertrophy to Failure**. *Hypertension* 2002, **40**(4):477 -- 484.

20. Sordahl LA, McCollum WB, Wood WG, Schwartz A: **Mitochondria and Sarcoplasmic Reticulum Function in Cardiac Hypertrophy and Failure**. *Am J Physiol* 1973, **224**(3):497-- 502.

21. Brunner M, Peng XW, Liu GX, Ren XQ, Ziv O, Choi BR, Mathur R, Hajjiri M, Odening KE, Steinberg E *et al*: **Mechanisms of Cardiac Arrhythmias and Sudden Death in Transgenic Rabbits with Long QT Syndrome**. *J Clin Invest* 2008, **118**(6):2246 -- 2259.

22. Liu GX, Choi BR, Ziv O, Li WY, de Lange E, Qu ZL, Koren G: **Differential Conditions for Early After-Depolarizations and Triggered Activity in Cardiomyocytes Derived from Transgenic LQT1 and LQT2 Rabbits**. *J Physiol* 2012, **590**(5):1171 -- 1180.

23. Herbig U, Jobling WA, Chen BP, Chen DJ, Sedivy JM: **Telomere Shortening Triggers Senescence of Human Cells through a Pathway Involving ATM, p53, and p21^{CIP1}, but Not p16^{INK4a}**. *Mol Cell* 2004, **14**(4):501 -- 513.

24. Jeyapalan JC, Ferreira M, Sedivy JM, Herbig U: **Accumulation of Senescent Cells in Mitotic Tissue of Aging Primates**. *Mech Ageing Dev* 2007, **128**(1):36 -- 44.

25. Debacq-Chainiaux F, Erusalimsky JD, Campisi J, Toussaint O: **Protocols to Detect Senescence-Associated Beta-Galactosidase (SA-Beta gal) Activity, a Biomarker of Senescent Cells in Culture and *in Vivo***. *Nat Protoc* 2009, **4**(12):1798 -- 1806.

26. Dimri GP, Lee X, Basile G, Acosta M, Scott G, Roskelley C, Medrano EE, Linskens M, Rubelj I, Pereira-Smith O *et al*: **A Biomarker That Identifies Senescent Human Cells in Culture and in Aging Skin *in Vivo***. *Proc Natl Acad Sci USA* 1995, **92**(20):9363 -- 9367.

27. Herbig U, Ferreira M, Condel L, Carey D, Sedivy JM: **Cellular Senescence in Aging Primates**. *Science* 2006, **311**(5765):1257.

28. Cooper LL, Odening KE, Hwang MS, Chaves L, Schofield L, Taylor CA, Gemignani AS, Mitchell GF, Forder JR, Choi BR *et al*: **Electromechanical and Structural Alterations in the Aging Rabbit Heart and Aorta**. *Am J Physiol - Heart C* 2012, **302**(8):H1625 --1635.

29. Halliwell B: **Oxidative Stress in Cell Culture: An Under-Appreciated Problem?** *FEBS Lett* 2003, **540**(1-3):3 -- 6.

30. Krishnamurthy J, Torrice C, Ramsey MR, Kovalev GI, Al-Regaiey K, Su L, Sharpless NE: **Ink4a/Arf Expression is a Biomarker of Aging**. *J Clin invest* 2004, **114**(9):1299-1307.

31. Levine AJ: **p53, the Cellular Gatekeeper for Growth and Division**. *Cell* 1997, **88**(3):323 -- 331.

32. Riley T, Sontag E, Chen P, Levine A: **Transcriptional Control ofHuman p53-Regulated Genes**. *Nat Rev Mol Cell Bio* 2008, **9**(5):402 -- 412.

33. Vazquez A, Bond EE, Levine AJ, Bond GL: **The Genetics of the p53 Pathway, Apoptosis and Cancer Therapy**. *Nat Rev Drug Discov* 2008, **7**(12):979 -- 987.

34. Kitzman DW, Gardin JM, Gottdiener JS, Arnold A, Boineau R, Aurigemma G, Marino EK, Lyles M, Cushman M, Enright PL *et al*: **Importance of Heart Failure with Preserved Systolic Function in Patients ≥ 65 Years of Age. CHS Research Group. Cardiovascular Health Study**. *Am J Cardiol* 2001, **87**(4):413-419.

35. Barry SP, Davidson SM, Townsend PA: **Molecular Regulation of Cardiac Hypertrophy**. *Int J Biochem Cell B* 2008, **40**(10):2023 -- 2039.

36. Pogwizd SM, Bers DM: **Calcium Cycling in Heart Failure: The Arrhythmia Connection**. *J Cardiovasc Electr* 2002, **13**(1):88 -- 91.

37. Sadoshima J, Jahn L, Takahashi T, Kulik TJ, Izumo S: **Molecular Characterization of the Stretch-Induced Adaptation of Cultured Cardiac Cells: an in Vitro Model of Load-Induced Cardiac Hypertrophy**. *J Biol Chem* 1992, **267**(15):10551 -- 10560.

38. Izumo S, Nadal-Ginard B, Mahdavi V: **Protooncogene Induction and Reprogramming of Cardiac Gene Expression Produced by Pressure Overload**. *Proc Natl Acad Sci USA* 1988, **85**(2):339 -- 343.

39. Rajabi M, Kassiotis C, Razeghi P, Taegtmeyer H: **Return to the Fetal Gene Program Protects the Stressed Heart: a Strong Hypothesis**. *Heart Fail Rev* 2007, **12**(3-4):331 -- 343.

40. Pandya K, Kim HS, Smithies O: **Fibrosis, Not Cell Size, Delineates Beta-Myosin Heavy Chain Reexpression During Cardiac Hypertrophy and Normal Aging *in Vivo***. *Proc Natl Acad Sci USA* 2006, **103**(45):16864 -- 16869.

41. De Meyer GR, De Keulenaer GW, Martinet W: **Role of Autophagy in Heart Failure Associated with Aging**. *Heart Fail Rev* 2010, **15**(5):423 -- 430.

42. Gurusamy N, Das DK: **Is Autophagy a Double-Edged Sword for the Heart?** *Acta Physiol Hung* 2009, **96**(3):267 -- 276.

43. Brunk UT, Jones CB, Sohal RS: **A Novel Hypothesis of Lipofuscinogenesis and Cellular Aging Based on Interactions between Oxidative Stress and Autophagocytosis**. *Mutat Res* 1992, **275**(3-6):395 -- 403.

44. Dammrich J, Pfeifer U: **Cardiac Hypertrophy in Rats After Supravalvular Aortic Constriction. II. Inhibition of Cellular Autophagy in Hypertrophying Cardiomyocytes**. *Virchows Arch B* 1983, **43**(3):287 -- 307.

45. Klionsky DJ, Abdalla FC, Abeliovich H, Abraham RT, Acevedo-Arozena A, Adeli K, Agholme L, Agnello M, Agostinis P, Aguirre-Ghiso JA *et al*: **Guidelines for the Use and Interpretation of Assays for Monitoring Autophagy**. *Autophagy* 2012, **8**(4):445 -- 544.

46. Tanaka Y, Guhde G, Suter A, Eskelinen EL, Hartmann D, Lullmann-Rauch R, Janssen PML, Blanz J, von Figura K, Saftig P: **Accumulation of Autophagic**

Vacuoles and Cardiomyopathy in LAMP2-Deficient Mice. *Nature* 2000, **406**(6798):902 -- 906.

Chapter 4: Redox Modification of Ryanodine Receptors by Mitochondria-Derived Reactive Oxygen Species Contributes to Aberrant Ca^{2+} Handling in Aging Rabbit Hearts

This content of this chapter was submitted to *The Journal of Physiology* and is currently under revision.

The author contributed to this manuscript by performing all calcium, ROS, TMRE imaging confocal experiments, and Western blotting experiments.

Leroy L. Cooper[1,2], Weiyan Li[1], Yi Chun Lu[1], Jason Centracchio[1], Radmila Terentyeva[1], Gideon Koren[1,2], and Dmitry Terentyev[1]

[1]Cardiovascular Research Center, Division of Cardiology, Rhode Island Hospital, Warren Alpert Medical School of Brown University, Providence, RI, USA

[2]Department of Molecular Pharmacology, Physiology, and Biotechnology, Brown University, Providence, RI, USA

Address for reprint requests and other correspondence: Dmitry Terentyev, Cardiovascular Research Center, Rhode Island Hospital, Brown University School of Medicine, 1 Hoppin Street, West Coro-5, Providence, RI 02903 (e-mail: dmitry_terentyev@brown.edu).

Keywords: ryanodine receptor, aging, sarcoplasmic reticulum, mitochondria, reactive oxygen species, and redox modification

4.1 Abstract

Aging is associated with blunted response to sympathetic stimulation and an increased risk of arrhythmia and sudden cardiac death. Aberrant calcium (Ca^{2+}) handling is an important contributor to the electrical and contractile dysfunction associated with aging. Yet, the specific molecular mechanisms underlying abnormal Ca^{2+} handling in the aging heart remain poorly understood. In this study, we used ventricular myocytes isolated from young (5-9 months) and old (4-6 years) rabbit hearts to test the hypothesis that changes in Ca^{2+} homeostasis are caused by post-translational modification of ryanodine receptors (RyR) by mitochondria-derived reactive oxygen species (ROS) generated in the aging heart. Changes in parameters of Ca^{2+} handling were determined by measuring cytosolic and intra-sarcoplasmic reticulum (SR) Ca^{2+} dynamics in intact and permeabilized ventricular myocytes using confocal microscopy. We also measured age-related changes in ROS production and mitochondria membrane potential using a ROS-sensitive dye 5-(and-6) chloromethyl-2',7'-dichlorodihydrofluoroscein diacetate (DCFDA) and the voltage-sensitive fluorescent indicator, tetramethylrhodamine ethyl ester (TMRE), respectively. In permeabilized myocytes, aging did not change SERCA activity and spark frequency but decreased spark amplitude and SR Ca^{2+} load suggesting increased RyR activity. Treatment with dithiothreitol (DTT) antioxidant reduced RyR-mediated SR Ca^{2+} leak in permeabilized myocytes from old rabbit hearts to the level comparable to young. Moreover, myocytes from old rabbits had more depolarized mitochondria membrane potential and increased rate of ROS production; both parameters were enhanced after β-adrenergic stimulation (30 nM isoproterenol,

ISO). Under β-adrenergic stimulation with ISO, Ca^{2+} transient amplitude, SR Ca^{2+} load, and latency of pro-arrhythmic spontaneous Ca^{2+} waves (SCWs) were decreased in cardiomyocytes from old rabbits. Additionally, with β-adrenergic stimulation, pretreatment of myocytes from old rabbit hearts with the mitochondrial-specific ROS scavenger (2-(2,2,6,6-tetramethylpiperidin-1-oxyl-4-ylamino)-2-oxoethyl) triphenylphosphonium chloride (mito-TEMPO) ablated most SCWs and increased latency to levels comparable to young. These data suggests that increased rate of ROS production by mitochondria lead to the thiol-oxidation of RyRs, which underlies the hyperactivity of RyRs and thereby shortened refractoriness of Ca^{2+} release in cardiomyocytes from the aging heart. This mechanism likely plays an important role in the increased incidence of arrhythmia and sudden death in the aging population.

Abbreviations:

Ca^{2+}	calcium
DCFDA	chloromethyl-2',7'-dichlorodihydrofluoroscein diacetate
DTDP	2,2′-dithiodipyridine
DTT	dithiothreitol
FCCP	carbonyl cyanide *p*-(trifluoromethoxy) phenylhydrazone
ISO	isoproterenol
LTCC	L-type calcium channel
mBB	monobromobimane

Mito-TEMPO (MT)	(2-(2,2,6,6-tetramethylpiperidin-1-oxyl-4-ylamino)-2-oxoethyl) triphenylphosphonium chloride
NCX	sodium-calcium exchanger
PLB	phospholamban
ROS	reactive oxygen species
RyR	ryanodine receptor
SCW	spontaneous Ca^{2+} wave
SERCA	SR (ER) Ca^{2+}-ATPase
SR	sarcoplasmic reticulum
TMRE	tetramethylrhodamine ethyl ester

4.2 Introduction

Aging is associated with increased incidence of cardiac arrhythmia and sudden cardiac death [1, 2]. Previously, in an aging rabbit model, we have shown that aging alters the structure and the electrical and mechanical activity of the heart causing both systolic and diastolic dysfunction, slowing conduction velocity, and altering conduction anisotropy, which provides a pro-arrhythmic substrate that increases the risk of malignant arrhythmia [3]. Although much is known regarding the substrate that predisposes and sustains arrhythmias in the aging heart, the underlying age-associated molecular trigger remains to be thoroughly examined. At the cellular level, aberrant calcium (Ca^{2+}) handling is recognized as an important contributor to the electrical dysfunction associated with aging [4-7]. However, the specific molecular mechanisms underlying age-associated abnormal Ca^{2+} handling in the heart have yet to be fully elucidated.

Diminished capacity to maintain redox balance has been proposed to be an underlying factor leading to abnormal cardiac function characteristic of aging [8-10]. In aged rat and rabbit ventricles, Morita *et al*. showed that exposure to oxidative stress led to early afterdepolarizations (EAD) in myocytes and EAD-mediated tachyarrhythmias at the tissue level [11]. Recent studies identified SR Ca^{2+} release channel, ryanodine receptor (RyR), as a protein target that is sensitive to oxidation, and post-translational modifications of RyRs by reactive oxygen species (ROS) have been implicated in alterations of Ca^{2+} homeostasis in conditions accompanied by oxidative stress, such as heart failure or myocardial infarct [12-18]. Specifically, accelerated leak of $[Ca^{2+}]_{SR}$ via

oxidized RyRs was shown to result in diminished systolic Ca^{2+} release that determines strength of contraction and in enhanced propensity to generation of pro-arrhythmic diastolic Ca^{2+} waves during *β*-adrenergic stimulation [16-18]. Yet, the role of redox-mediated alterations of Ca^{2+} handling (RyRs in particular) with regard to aging and Ca^{2+}-triggered arrhythmias remains to be investigated. Moreover, it is well established that mitochondria, one of the main sources of ROS in myocytes, if damaged or dysfunctional, could increase ROS production rate up to 10-fold [19]. Dysfunctional mitochondria have been implicated as a mechanism for ventricular arrhythmia by altering ion channels' function, action potential heterogeneity, and cell excitability [20-22], and mitochondria-derived ROS recently has been connected to the oxidation of RyRs [23, 24].

The goal of this study was to test the hypothesis that changes in Ca^{2+} homeostasis associated with aging are caused by post-translational modification of RyRs by mitochondria-derived ROS generated in the old heart. Importantly, we sought to examine the mechanisms and effects of ROS generation and determine whether exposure of cardiomyocytes from old rabbits to a reducing agent and a mitochondria-specific ROS scavenger reverses the age-related pro-arrhythmogenic cellular phenotype. Our results show that an age-associated increase in rate of ROS production by mitochondria leads to the thiol-oxidation of RyRs, which underlies the hyperactivity of RyRs and thereby shortened refractoriness of Ca^{2+} release in cardiomyocytes from the aging heart. We conclude that this mechanism contributes to age-associated reduction in exercise capacity and to increased risk of arrhythmia and sudden death.

4.3 Methods

Animal Ethical Statement

All animal work was performed in accordance with the local guidelines of the institutions and only after approval by the Institutional Animal Care and Use Committee in accordance with the *Guide for the Care and Use of Laboratory Animals* published by the U.S. National Institutes of Health (NIH Publication No. 85-23, revised 1996).

Cardiomyocyte Isolation

Ventricular myocytes were isolated from young (5-9 months) and old (4-6 years) female, New Zealand White rabbits (RSI Farms, Mocksville, NC, USA) as previously described [25, 26]. The rabbits were anaesthetized with ketamine (60 $mg \cdot kg^{-1}$), xylazine (15 $mg \cdot kg^{-1}$ IM) and buprenorphine (0.03 $mg \cdot kg^{-1}$ SQ), and sodium pentobarbital (150 $mg \cdot kg^{-1}$, IV). Hearts were quickly excised after thoracotomy and retrogradely perfused on a Langendorff apparatus with solution containing collgenase I (Roche Applied Science, Indianapolis, IN, USA) at 37°C.

Cellular Electrophysiology

Since the voltage dependence and ion channel kinetics are dependent on temperature, ionic currents and action potentials were recorded at physiological temperature (36 ± 1 °C) using standard whole-cell patch clamp technique with an Axopatch-200B amplifier (Molecular Devices). Intracellular solution contains: (in mM) 120 KCl, 5 $MgCl_2$, 0.36

$CaCl_2$, 5 EGTA, 5 HEPES, 5 glucose, 5 K_2-ATP, 5 Na_2-CrP, 0.25 Tris-GTP (pH 7.2). Pipette resistance was 2-4 MΩ. Capacitance and 70% of the series resistance were routinely compensated for. Action potentials and Ca^{2+} currents were recorded in Tyrode solution containing (in mM): 140 NaCl, 5.4 KCl, 0.33 NaH_2PO_4, 1 $MgCl_2$, 1 $CaCl_2$, 5 HEPES, and 7.5 glucose (pH 7.4). Action potentials were recorded under current clamp using 1.2X threshold current injection at 1 Hz. Ca^{2+} currents were recorded using voltage steps between -40 to 40 mV from a holding potential of -50 mV. E4031-sensitive I_{Kr}, Chromanol 293B-sensitive I_{Ks}, I_{to}, and I_{K1} currents were measured and analyzed under voltage clamp using modified external solutions and voltage protocols as described in Brunner *et al.* [25]. Data were sampled at 2.5-5 kHz and filtered at 1 kHz. Current-voltage relationships are normalized to the cell capacitances and presented as mean ± SEM.

Confocal Microscopy Measurements of Intracellular and Intra-SR Ca^{2+} and Ca^{2+} Sparks

Intracellular Ca^{2+} cycling, intra-SR Ca^{2+} cycling, and Ca^{2+} spark activity in isolated rabbit ventricular myocytes were monitored by Leica SP2 confocal laser scanning system equipped with a 60× oil-immersion objective in linescan and x-y mode using Ca^{2+}-sensitive indicators Fluo-3, Fluo-5N, and Fluo-4 and Rhod-2 (Invitrogen/Molecular Probes, Carlsbad, CA, USA), respectively. All experiments were performed at 23 ± 1 °C due to practical limitations of our inability to warm buffers to physiological temperature with the confocal setup; however, slowing down the kinetics allowed us to gain mechanistic insights with fewer experiments.

For intracellular Ca^{2+} cycling measurements, cells were loaded with Fluo-3 for 12 min., and after 20 min. desertification, and the dye was excited with the 488 nm linescan of an argon laser. Emission was collected at 500 – 600 nm. Cells were studied in Tyrode solution (in mM: 140 NaCl, 5.4 KCl, 1.8 $CaCl_2$, 0.5 $MgCl_2$, 10 HEPES and 5.6 glucose, pH 7.3) at baseline and with 30 nM isoproterenol (ISO) – a β-adrenergic receptor agonist. Myocytes were paced via field stimulation at 1 Hz using extracellular platinum electrodes. To assess the SR Ca^{2+} load and decay kinetics, 20 mM caffeine was applied at the end of the experiments. Sodium-calcium exchanger (NCX) activity was estimated by measuring the rate of decay of caffeine-induced Ca^{2+} transients (k_{caff}), and SR (ER) Ca^{2+}-ATPase (SERCA) activity was estimated via a derived rate of decay (k_{SR}) by subtracting the rate of decay of caffeine-induced Ca^{2+} transients (k_{caff}) from the rate of decay of pacing-induced Ca^{2+} transients [18, 27].

To test the propensity for triggered activity, myocytes were paced at 1 Hz for 1 min., and the latency between the last paced stimulus in the pacing train to the first SCW was calculated. Also to assess the effect of mitochondria-derived ROS on cardiomyocytes from old rabbits, these myocytes were pretreated with the mitochondria-specific ROS scavenger (2-(2,2,6,6-tetramethylpiperidin-1-oxyl-4-ylamino)-2-oxoethyl) triphenylphosphonium chloride (mito-TEMPO, 25 μM, Enzo Life Sciences, Farmingdale, NY, USA) for 10 min. These intracellular Ca^{2+} cycling measurements were performed under β-adrenergic stimulation with 30 nM ISO.

For Ca^{2+} spark recordings, the cardiac myocytes were permeabilized with saponin (0.01% for ~20 s). The intracellular solution contained (mM): 120 potassium aspartate,

20 KCl, 0.81 $MgCl_2$, 1 KH_2PO_4, 0.5 EGTA, 3 MgATP, 10 phosphocreatine, 0.03 Fluo-4 pento potassium salt, 20 HEPES (pH 7.2) and 5 U ml^{-1} creatine phosphokinase, 100 nM free [Ca^{2+}]. To assess the SR Ca^{2+} load, 20 mM caffeine was applied at the end of the experiments. The dye was excited with the 488 nm line of an argon laser. Emission was collected at 500 – 600 nm. For intra-SR [Ca^{2+}] measurements, cells were incubated with Fluo-5N for 2-3 hr. and were permeabilized with saponin (0.01% for ~20 s), and the dye was excited with the 488 nm line of an argon laser in x-y mode. Emission was collected at 500 – 590 nm. SERCA activity was assessed by depleting the SR by the application of 10 mM caffeine, chelating Ca^{2+}, and SR Ca^{2+} uptake was measured by reapplying of 250 nM Ca^{2+} in the presence of the RyR inhibitor ruthenium red [28]. To assess the effect of a reducing agent on $[Ca^{2+}]_{SR}$, intra-SR [Ca^{2+}] measurements were performed in permeabilized myocytes young and old before and after application of 1 mM dithiothreitol (DTT). The Fluo-5N signal was normalized to the minimum (10 mM caffeine) and maximum (20 µM cyclic adenosine monophosphate (cAMP) + 40 µM Ruthenium Red) fluorescence. The Fluo-5N signal was converted to [Ca^{2+}] using the formula: $[Ca^{2+}]_{SR} = K_d \cdot (F - F_{min}) \cdot (F_{max} - F)^{-1}$, where K_d was 400 µM as previously described [18, 29].

Confocal Microscopy Measurements of Intracellular ROS and Mitochondrial Membrane Potential

ROS production was measured in isolated rabbit ventricular myocytes in Tyrode solution at 23 ± 1 °C using the ROS-sensitive dye 5-(and-6) chloromethyl-2',7'-

dichlorodihydrofluoroscein diacetate (DCFDA, 20 μM, incubated for 30 min.) as previously described [16]. The DCFDA dye was excited with the 488 nm line of an argon laser in x-y mode, and emission was collected at 500–530 nm. ROS production was measured at baseline and after application of 30 nM ISO in cardiomyocytes from young and old rabbits and cardiomyocytes pretreated with mito-TEMPO from old rabbits.

Mitochondrial membrane potential was monitored with a voltage-sensitive fluorescent indicator, tetramethylrhodamine ethyl ester (TMRE) as previously described [23]. Isolated rabbit ventricular cardiomyocytes were loaded with 1 nM TMRE (10 min), and TMRE fluorescence was measured in x-y mode. TMRE was excited at 543 nm with a helium–neon laser, and the emission signals were collected at 570–650 nm. TMRE fluorescence was normalized to the minimum fluorescence signal obtained with the mitochondrial uncoupler carbonyl cyanide *p*-(trifluoromethoxy) phenylhydrazone (FCCP, 50 μM). Mitochondrial membrane potential was monitored at baseline and after application of 30 nM ISO.

RyR Oxidation and Western Blotting of Ca^{2+} Handling Proteins

The content of free thiols in RyRs was determined with monobromobimane (mBB, EMD Millipore, Billerica, MA, USA) fluorescence method as previously described [16, 30]. Myocytes were incubated with 20 mM mBB for 1 hr. in the dark at room temperature, and the proteins from cell lysates were acetone precipitated and resolved via SDS-PAGE. To compare relative oxidation between samples, RyR oxidation was normalized

to minimum and maximum RyR thiol oxidation: the samples were incubated with 10 mM DTT (a reducing agent) or 200 µM 2,2'-dithiodipyridine (DTDP, oxidizing agent), respectively.

The levels of calsequestrin (CASQ2, Thermo Fisher, Waltham, MA, USA), phospholamban (PLB, Thermo Fisher), SERCA (Thermo Fisher), NCX (Thermo Fisher), α1c subunit L-type calcium channel (LTCC, EMD Millipore), and RyR (Thermo Fisher) proteins were determined by immunoblotting. Tissue homogenates proteins (20-30 µg) were resolved on a 4–20 % gel via SDS-PAGE, transferred onto nitrocellulose membranes, and probed with mouse monoclonal antibodies specific for these proteins and subsequently probed with a donkey anti-mouse secondary antibody (Thermo Fisher). Blots were developed with SuperSignal West Pico and Femto (Thermo Fisher) and quantified and analyzed by using GeneSnap (Syngene, Cambridge, UK) and ImageJ (US National Institutes of Health, Bethesda, MD, USA) softwares.

Statistical Analysis

Data are presented as mean ± SEM of n measured cells or rabbits. Statistical comparisons between groups were performed with Student's t test (paired and unpaired) and one-way ANOVA where appropriate. Differences were considered statistically significant at $p < 0.05$.

4.4 Results

Preserved Baseline Cellular Eectrophysiology and Ca^{2+} Homeostasis in Myocytes from Aging Hearts

First we examined the effect of aging on basic cellular electrophysiology and Ca^{2+} homeostasis under basal conditions. The intracellular Ca^{2+} cycling in paced (1 Hz) isolated cardiomyocytes from young and old rabbits was monitored in the line scan mode of a confocal microscope using the Ca^{2+} indicator Fluo-3. The effects of aging on cytosolic Ca^{2+} cycling at baseline conditions are illustrated in **Figure 4.1A** and summarized in **Figure 4.1B – E**. Aging did not change Ca^{2+} transient and caffeine transient amplitudes nor did it change transient decay rates indicating that aging does not alter NCX and SERCA activities at basal conditions. Importantly, aging does not alter baseline cellular electrophysiology parameters, including AP duration and Ca^{2+} and potassium currents, in single cardiomyocytes (**S. Figure 4.1**). Moreover, we did not observe any significant changes in expression levels of important Ca^{2+} handling proteins (**S. Figure 4.2**), including LTCC, RyR, NCX, SERCA and PLB.

Aging Alters Spark Activity and SR Load in Cardiomyocytes

To assess the effect of aging in a large animal model on RyR and SERCA activity directly, we employed saponin-permeabilized cells experimental system measuring SR Ca^{2+} content and parameters of spontaneous local Ca^{2+} release events through RyR clusters, Ca^{2+} sparks (**Figure 4.1 F – K).** Aging reduced spark amplitude and spark size

(full width at half maximum**,** FWHM) but had no significant effect of spark frequency. Parallel assessment of SR Ca^{2+} load via the amplitude of the caffeine-induced Ca^{2+} transients in saponin-permeabilized myocytes revealed a small but significant reduction of SR Ca^{2+} content in aging myocytes in comparison with young controls (**Figure 4.2G** and **4.2K**). Preserved spark frequency under conditions of reduced SR Ca^{2+} load suggest that RyRs are more active in cardiomyocytes from old rabbits. Since enhanced RyR-mediated SR Ca^{2+} leak can effectively mask possible changes in SERCA function, the following protocol to assess SERCA activity was employed. First, intact cells were loaded with membrane-permeable low affinity Ca^{2+} indicator Fluo-5N. Then, myocytes were permeabilized to washout indicator from the cytosol, and fluorescence signal from Fluo-5N entrapped in the SR was monitored using confocal microscopy. SR Ca^{2+} was fully depleted with caffeine (10 mM), and SR Ca^{2+} refilling upon caffeine washout was prevented by $[Ca^{2+}]_{cyt}$ removal (0 mM $[Ca^{2+}]$ and 1.5 mM [EGTA] in intracellular solution). Further, RyRs were blocked using RyR-specific inhibitor Ruthenium Red (RuRed, 40 µM, [28]) followed by instant application of 250 nM $[Ca^{2+}]_{cyt}$ to measure SERCA-mediated Ca^{2+} uptake in the absence of RyR-mediated Ca^{2+} leak. **Figure 4.1L** illustrates and **Figure 4.1M** summarizes that aging does not change SERCA activity, which is consistent with the above-mentioned k_{SR} data from intracellular Ca^{2+} measurements in intact cells. Taken together, these results suggest that impairment of the ability of SR to retain Ca^{2+} in aging is caused primarily by abnormally high activity of RyRs which is consistent with findings of previous studies in aging rats [31].

Redox Modification of RyRs with Aging

We directly examined the extent of RyR redox modification in myocytes from young and old myocytes depicted in the results of a mBB fluorescence labelling assay in **Figure 4.2A** and summarized in **Figure 4.2B**. The fraction of RyR free thiols was decreased significantly in cardiomyocytes from old rabbits indicating that aging lead to increased RyR oxidation. Next, to investigate the role of redox status in the age-related increase of RyR activity and reduction of SR Ca^{2+} load, we examined the effect of antioxidant DTT on SR Ca^{2+} content in saponin-permeabilized myocytes with SR entrapped low affinity Ca^{2+} indicator Fluo-5N from young and old rabbits depicted in **Figure 4.2C** and summarized in **Figure 4.2D**. Consistent with the spark data, myocytes from old rabbits exhibited lower SR Ca^{2+} load, and application of 1 mM DTT restored the SR Ca^{2+} content in myocytes from old rabbits to the levels comparable to myocytes from young animals.

Age-related Depolarization of Mitochondria and Increased ROS Production

To further examine the mechanism of RyR oxidation in aging myocytes, we performed mitochondrial membrane potential measurements with TMRE and ROS production rate experiments with ROS-sensitive indicator DCFDA. **Figure 4.3A** shows representative images of mitochondrial membrane potential in young and old myocytes as measured by TMRE fluorescence at 0 s. As depicted in **Figure 4.3B** and summarized in **Figure 4.3C**, myocytes from old rabbits had more depolarized mitochondria membrane at baseline and after β-adrenergic stimulation. Additionally, β-adrenergic stimulation

further depolarized mitochondrial membrane potential in both young and old myocytes by 3.45 % and 6.94 %, respectively (paired analysis). Since ROS via mitochondrial dysfunction has been shown to be a source of protein oxidation in the heart [12, 23], we investigated the effect of aging on myocyte ROS production using DCFDA as shown in **Figure 4.4A** and summarized in **Figures 4.4B** and **4.4C**. We observe that cardiomyocytes from old rabbits show a significantly higher rate of ROS production compared to young myocytes at baseline, which is exacerbated by 87.5 % with *β*-adrenergic stimulation. Importantly, myocytes from old rabbit hearts that were preincubated with the mitochondria-specific ROS scavenger mito-TEMPO exhibited a markedly reduced rate of ROS production when compared to old myocytes at baseline and with β-adrenergic stimulation. Furthermore, under β-adrenergic stimulation, we observe no statistically significant difference in the rate of ROS production between young myocytes and old myocytes pretreated with mito-TEMPO. These data further implicate the important role of age-associated mitochondrial dysfunction on increased ROS production and protein redox status in the heart.

Age-Associated Aberrant Ca^{2+} Handling is Reversed with Mitochondria-Specific ROS Scavenger

To further investigate the role of aging on aberrant Ca^{2+} dynamics and mitochondria ROS, we examined intracellular Ca^{2+} cycling in paced (1 Hz) myocytes from young and old rabbits and old myocytes pretreated with mito-TEMPO and challenged with β-adrenergic agonist ISO (30 nM). The effects of aging on Ca^{2+} cycling under β-

adrenergic stimulation are illustrated in **Figure 4.5A** and summarized in **Figures 4.5C** and **4.5D**. Myocytes from old rabbit hearts had significantly lower Ca^{2+} transient amplitude and caffeine transient amplitude when compared to young myocytes – reduced about 30% for both parameters. Moreover, myocytes from old rabbit hearts in the presence of the mitochondria-specific ROS scavenger mito-TEMPO exhibited significantly higher caffeine transient amplitudes when compared to untreated old myocytes. This increase in caffeine transient amplitude was comparable to young cardiomyocytes indicating that treatment with mito-TEMPO restores SR Ca^{2+} load under these conditions. Additionally as portrayed in **Figure 4.5B**, the arrhythmogenic potential associated with aging was examined by measuring spontaneous Ca^{2+} waves (SCWs) in myocytes in the presence of ISO after cessation of 1 Hz pacing for 1 min. As shown in **Figures 4.5E** and **4.5F,** we observed a ~40% increase in the rate of occurrence of SCWs as well and an almost 4-fold reduction in SCW latency time in old myocytes when compared to young myocytes. Furthermore, pretreatment with mito-TEMPO reversed this age-related effect: not only did mito-TEMPO pretreatment reduce the number of old myocytes that exhibited SCWs (comparable to the young myocytes), but also mito-TEMPO pretreatment significantly increased RyR refractoriness in old myocytes as evidenced by an increase in SCW latency time. Thus, mito-TEMPO reversed the aging cellular phenotype in cardiomyocytes elucidating the major role of mitochondrial ROS in aberrant Ca^{2+} dynamics and arrhythmogenesis in the aging heart.

4.5 Discussion

Here, we present a novel finding demonstrating a mechanism that is involved with normal age progression and its relation to alterations in Ca^{2+} cycling as it pertains to increased arrhythmogenic potential in the aging heart. We showed that aging significantly increased SR Ca^{2+} leak via post-translational thiol oxidation of RyRs caused by differential production of mitochondrial ROS. This led to diminished systolic Ca^{2+} release as well as the development of SCWs in the presence of β-adrenergic agonist ISO. Thus, the major age-related differences in Ca^{2+} homeostasis occurs at the level of the SR and manifests at sarcolemma as reduction in pacing-induced systolic Ca^{2+} release due to decreased SR Ca^{2+} content as well as potentially malignant SCWs under *β*-adrenergic stimulation. This mechanism may be an underlying trigger for age-related, Ca^{2+}-dependent arrhythmias.

Redox Modification of RyR with Age

Although it has been shown that aging is associated with aberrant RyR function [31], the molecular mechanism underlying the increase in RyR activity has yet to be investigated. Thus, an important finding of this study is that aging significantly increases ROS levels in rabbit cardiomyocytes leading to RyRs' oxidation rendering them hyperactive. It is known that the RyR is a highly cysteine rich protein [30], and it has been shown to be highly susceptible to oxidation [13, 16, 23, 24, 32, 33]. Forms of ROS, such as superoxide or hydrogen peroxide have also been shown to increase the open

probability of RyR [13, 16, 34-38]; moreover, these modifications are sensitive to reversal by reducing agent DTT [13, 16, 39-41]. Here, we provide direct evidence of increased age-associated RyR thiol oxidation, and we observe that the exposure of permeablized myocytes to DTT reduced SR Ca^{2+} leak restoring SR Ca^{2+} content in old myocytes (**Figure 4.2**), which, when taken together, indicate that RyR oxidation via increased ROS is the mechanism of exacerbated SR Ca^{2+} leak in cardiomyocytes in aging. Of note, age-related changes in RyR activity do not translate into readily detectable changes in parameters of Ca^{2+} transients under basal conditions. It is consistent with largely preserved baseline contractile function of the aging heart and bears similarity to other conditions associated with RyR hyperactivity including CPVT or early stages of HF [18, 42-44]. Additionally, previous studies imply that function of other important Ca^{2+} handling proteins including SERCA, NCX, and LTCC can be effectively regulated by ROS [45-49]. In our present study, we show a lack of age-associated changes in parameters, such as of I_{Ca}, SERCA-mediated SR Ca^{2+} uptake, and Ca^{2+} removal by NCX, which suggests that the age-associated increase in levels of ROS in our experimental model is not sufficient to modify their activity in old rabbit cardiomyocytes. Additionally, the latter findings are consistent with previously reported lack of changes in I_{Ca} and SERCA function in large animal models of tachypacing-induced cardiomyopathy and myocardial infarct model of sudden cardiac death – both conditions which are accompanied by accelerated rate of ROS production [17, 18]. Therefore, our data elucidate RyR as a primary highly sensitive target for modulation by ROS in the aging heart within cascade of Ca^{2+}-induced Ca^{2+} release (CICR) and is

affected before the changes in activity of other important Ca^{2+} handling proteins [50-53], which can take place at more advanced stages of aging.

The Role of Mitochondrial ROS on Increased Arrhythmic Potential with Age

It has been well established by Harman *et al.* and others that mitochondria are a major source of age-related ROS and that they are the primary source of ROS in cardiomyocytes [8, 54, 55]. Also, previous studies have revealed that the distances between mitochondria and RyRs SR Ca^{2+} release clusters are sufficiently short in cardiomyocytes to establish local Ca^{2+} communication [56-58]. Expectedly, this close proximity would be permissive for retrograde transmission of signals from mitochondria in the form of transitory ROS that can effectively modify RyR function. Indeed Zhou *et al.* show that changes in mitochondrial membrane potential ($\Delta\Psi_m$) can directly affect the redox environment and alter Ca^{2+} handling in pig cardiomyocytes [58]. Although severe uncoupling of $\Delta\Psi_m$ leads to the cessation of oxidative phosphorylation and ROS production, it has been demonstrated that mild uncoupling of the mitochondria membranes leads to increased respiration and increased levels of ROS, such as superoxide and hydrogen peroxide [59-61]. Here, we show that $\Delta\Psi_m$ is reduced by ~25% in myocytes from old rabbit hearts (**Figure 4.3**) and represents a mild uncoupling, which we posit as the likely mechanism leading to increased ROS production, oxidation of RyR, and the subsequent pro-arrhythmic dysfunction described below in old cardiomyocytes.

Under β-adrenergic stimulation, when both LTTC-mediated Ca^{2+} influx and SERCA-mediated Ca^{2+} uptake are enhanced, hyperactivity of RyRs is directly linked to increased frequency of SCWs that, via an electrogenic NCX, translates into arrhythmogenic deflections of membrane potential in the form of delayed or early depolarizations [62, 63]. We show in myocytes from old rabbits that mitochondrial ROS increases oxidation of RyR and enhances RyR functional activity, which results in increased arrhythmic potential as evidenced by reduced RyR refractoriness manifested in increased frequency of SCWs in the presence of ISO (**Figure 4.5B**). These data are in line with previous works that show redox modification of RyRs by mitochondrial ROS enhances RyR functional activity that results in increased frequency of SCWs [23, 24]. Additionally, scavenging mitochondrial ROS during β-adrenergic stimulation resulted in a 3-fold reduction of rate of ROS generation (**Figure 4.4**), and in these myocytes, the Ca^{2+} transient amplitude was increased, the frequency of SCWs were reduced, and the SR Ca^{2+} content assessed by rapid application of caffeine was normalized to that comparable to young myocytes (**Figure 4.5 B – F**). Positive inotropic response to β-adrenergic stimulation characteristic of normal hearts is largely ascribed to the PKA-mediated increase in phosphorylation of LTCCs resulting in increased I_{Ca}, phosphorylation of PLB that accelerates SERCA-mediated Ca^{2+} uptake, and phosphorylation of RyR at its PKA and CaMKII sites that is thought to increase RyR activity and synchronize Ca^{2+} release [64-68]. However, these same processes likely contribute to the age-related changes in Ca^{2+} dynamics under β-adrenergic stimulation. The cumulative effects of ISO-induced RyR phosphorylation by PKA and CaMKII as well as increased RyR oxidation would lead to increased SR Ca^{2+} leak and lower Ca^{2+}

transient amplitude as we observe in old myocytes. Similarly, according to Terentyev *et al*., ROS modification results in increased sensitivity of RyR to luminal Ca^{2+} [16]; therefore, increased SR Ca^{2+} load in comparison to baseline in ISO-treated cells will further enhance SR Ca^{2+} leak via oxidized RyRs resulting in lowered SR Ca^{2+} content and Ca^{2+} transient amplitude. Also consistent with the recent report of Bovo *et al.,* in the presence of ISO, we detect further acceleration of ROS production by mitochondria (**Figure 4.4**), which further exacerbates oxidative damage to RyR in old myocytes (**S. Figure 4.3**) and is a possible mechanism to explain the differential response by *β*-adrenergic stimulation with regard to age.

Conclusion

These data reveal a novel mechanism underlying the development of age-associated pro-arrhythmic Ca^{2+} waves and decreased RyR refractoriness during *β*-adrenergic stimulation. Differential rate of mitochondrial ROS production with age along with sympathetic stimulation is critical in altering RyR redox status, leading to SR Ca^{2+} leak, and causing the development of pro-arrhythmic spontaneous Ca^{2+} waves. Since an age-related increase of mitochondrial ROS shifts the normal ROS balance into a deleterious range, maintenance of normal ROS production and mitochondrial integrity are important research and therapeutic targets that are paramount in preventing redox imbalance that leads to age-related cardiac dysfunction and Ca^{2+}-dependent arrhythmias.

4.6 Figures

Figure 4.1: Aging reduces ability to maintain SR Ca^{2+} content by increasing RyR-mediated Ca^{2+} leak at preserved SERCA-mediated uptake.

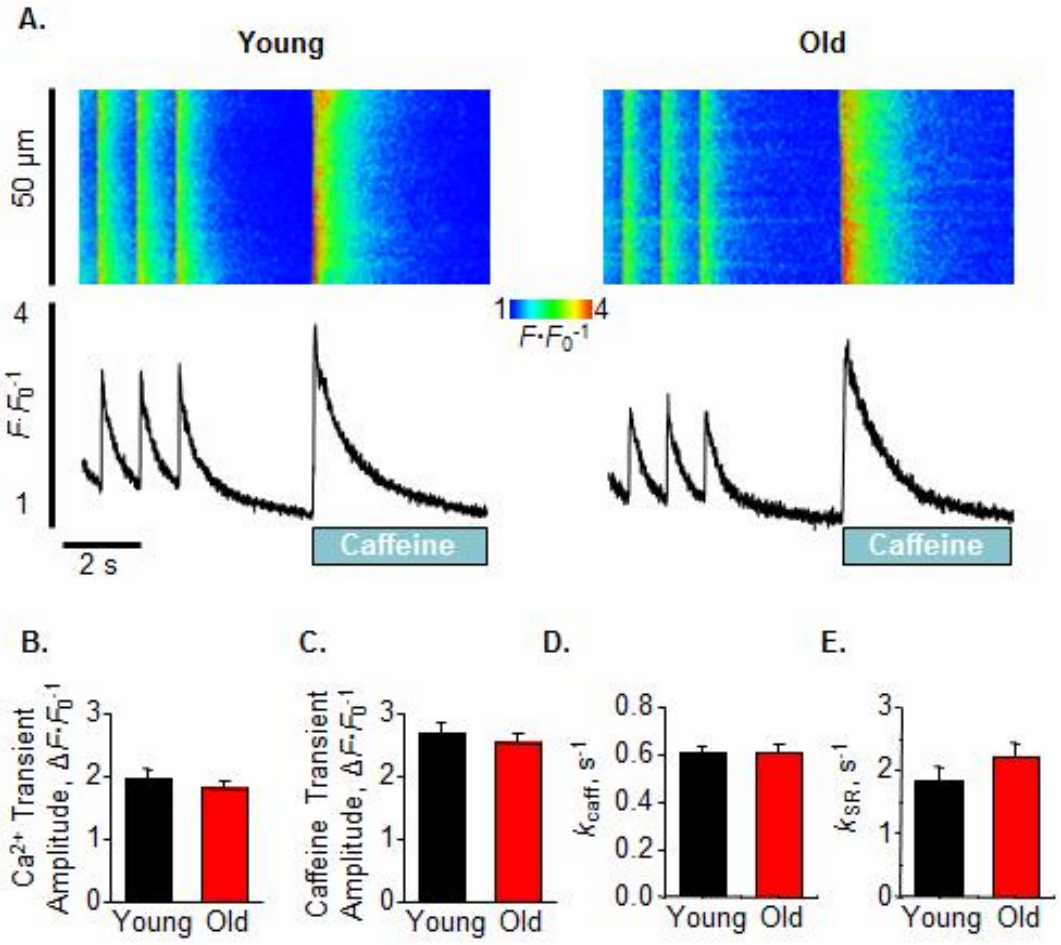

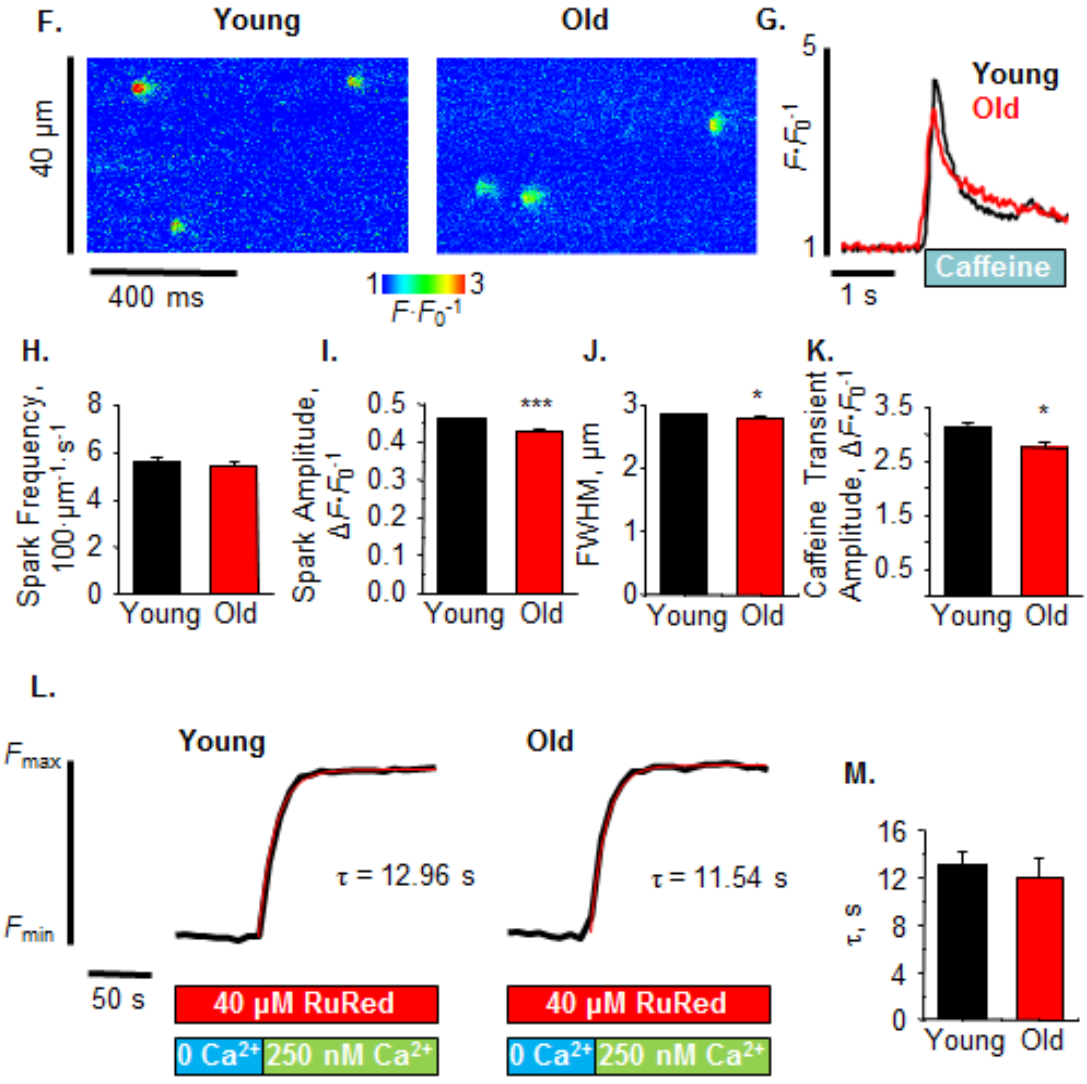

A. Representative confocal line scan images and Fluo-3 $F{\cdot}F_0^{-1}$ profiles at 1Hz. **Graphs B. – E.** depict average date form Ca^{2+} transient amplitude (young, 1.94 ± 0.17 vs. old, 1.80 ± 0.13 $\Delta F{\cdot}F_0^{-1}$), caffeine transient amplitude (2.69 ± 0.16 vs. 2.52 ± 0.16 $\Delta F{\cdot}F_0^{-1}$), and decay rate constants (from exponential fit): k_{caff}: 0.61 ± 0.03 vs. 0.61 ± 0.04 s^{-1} and k_{SR}: 1.83 ± 0.23 vs. 2.21 0.23 s^{-1}. For Ca^{2+} dynamics, *n* = 12 – 23 cells from 3 – 4 heart preparations; all values are *NS* and ± SEM. **F.** Representative confocal line scan images with Fluo-4 of spark activity in saponin-permeabilized cardiomyocytes from

young and old rabbits. **G.** Representative Fluo-4 $\Delta F \cdot F_0^{-1}$ profiles of caffeine-induced Ca^{2+} transients in permeabilized cardiomyocytes from young and old rabbits. **Bar graphs H – K** show average data for spark frequency (young, 5.62 ± 0.18 vs. old, 5.47 ± 0.17 $100 \cdot \mu m^{-1} \cdot s^{-1}$, *P* = NS) spark amplitude (0.46 ± 0.004 vs. 0.43 ± 0.004 $\Delta F \cdot F_0^{-1}$, ***$P < 0.001$), FWHM (2.85 ± 0.01 vs. 2.81 ± 0.01 µm, *$P < 0.05$), and caffeine transient amplitude (2.13 ± 0.10 vs. 1.76 ± 0.09 $\Delta F \cdot F_0^{-1}$, *$P < 0.05$), respectively. For caffeine application, *n* = 20 – 35 cells, and for spark analysis *n* = 205 – 247 cells; *n*= 3,431 – 4,395 sparks from 3 – 4 heart preparations. All values are ± SEM. **L.** Representative tracing of time-dependent changes in luminal Fluo-5N signal in permeabilized cardiomyocytes from young and old rabbits after depletion of SR Ca^{2+}, and chelating $[Ca^{2+}]_{cyt}$, blocking of RyRs, and reapplication of 250 nM of Ca^{2+}. **M.** Average time constants (τ) from exponential fit of SR Ca^{2+} uptake for permeabilized cardiomyocytes from young and old rabbits (13.08 ± 1.11 vs. 12.01 ± 1.58 s, *P* = NS). *n* = 19 – 52 cells from 3 – 4 heart preparations; all values are ± SEM.

Figure 4.2: Increased thiol oxidation underlies increased RyR-mediated SR Ca^{2+} leak in cardiomyocytes from old rabbits.

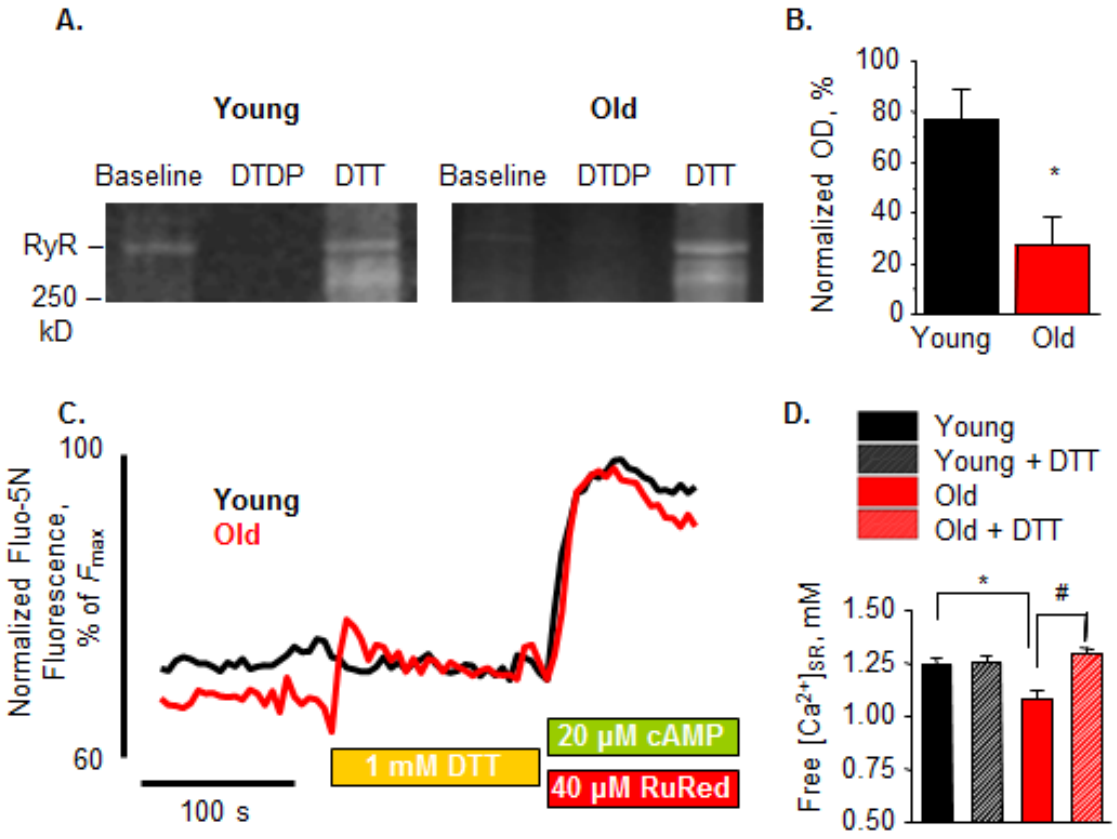

A. and **B.** Representative mBB fluorescence intensity signals of RyR from cardiomyocytes from young and old rabbits and pooled data for free thiol contents normalized by DTT and DTDP: young, 77.89 ± 12.02 vs. old, 27.39 ± 11.09 %. *P < 0.05. Cells were from 4-6 heart preparations. **C.** Representative tracing of time-dependent changes in luminal Fluo-5N signal in permeabilized cardiomyocytes from young and old rabbits after the addition of 1 mM DTT. Data are normalized to the minimum (10 mM caffeine) and maximum (20 µM cAMP + 40 µM RuRed) fluorescence. **D.** Average data for $[Ca^{2+}]_{SR}$ before and after DTT application in cardiomyocytes from young and old rabbits. Fluo-5N signal was converted to $[Ca^{2+}]$ using the formula:

$[Ca^{2+}]_{SR}=K_d\cdot(F–F_{min})\cdot(F_{max}–F)^{-1}$, where K_d was 400 μM. $[Ca^{2+}]_{SR}$ were as follows: young, 1.25 ± 0.04; young + DTT, 1.27 ± 0.04; old, 1.10 ± 0.03; and old + DTT 1.25 ± 0.04 mM. **P* < 0.05 for young vs. old (unpaired analysis), $^{\#}P$< 0.05 for old vs. old + DTT (paired analysis), and **P* = NS for young + DTT and old + DTT (unpaired analysis). *n*= 7– 13 cells from 2 – 3 heart preparations. All values are ± SEM. *The experiment in Panels A and B was not performed by the author.*

Figure 4.3: Old cardiomyocytes have mild mitochondrial uncoupling, which is exacerbated in the presence of ISO.

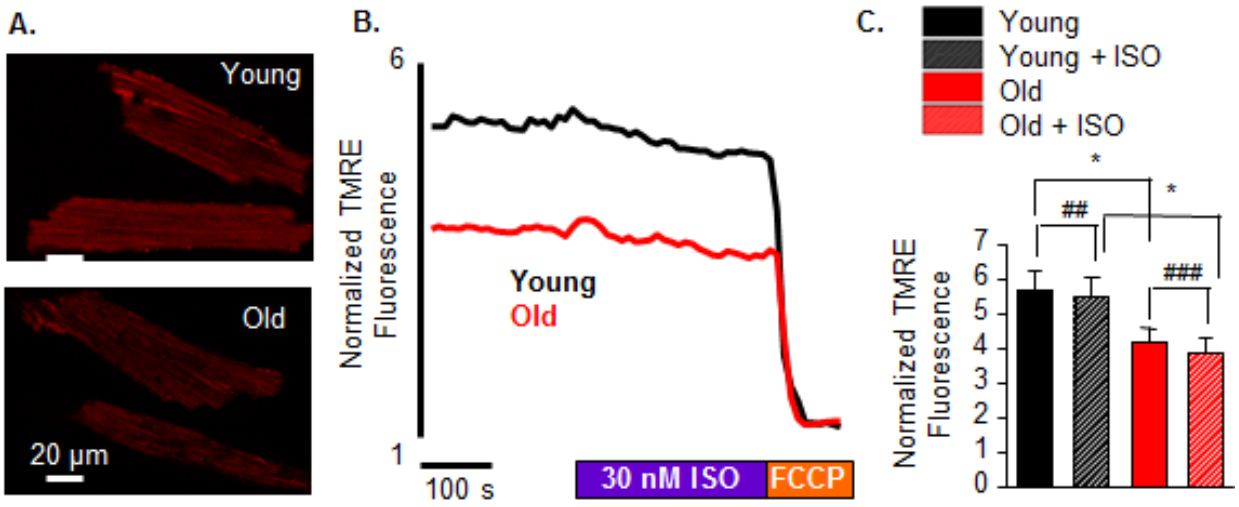

A. Representative images of mitochondrial membrane potential at 0 s measured by using TMRE. **B.** and **C.** Traces and average data of normalized TMRE fluorescence at baseline and ISO (30 nM). Data are normalized to the minimum TMRE fluorescence in the presence of electron transport chain uncoupler FCCP (50 μM): young, 5.71 ± 0.55; young + ISO, 5.51 ± 0.53; old, 4.16 ± 0.42; and old + ISO, 3.87 ± 0.41. *P < 0.05 for young vs. old and for young + ISO vs. old + ISO (unpaired analysis), $^{\#\#}P$ < 0.01 young vs. young + ISO (paired analysis), and $^{\#\#\#}P$ < 0.001 old vs. old + ISO (paired analysis). n= 20 – 21 cells from 2 – 4 heart preparations; all values are ± SEM.

Figure 4.4: Rate of ROS production is higher in old cardiomyocytes and is attenuated with a mitochondrial ROS scavenger.

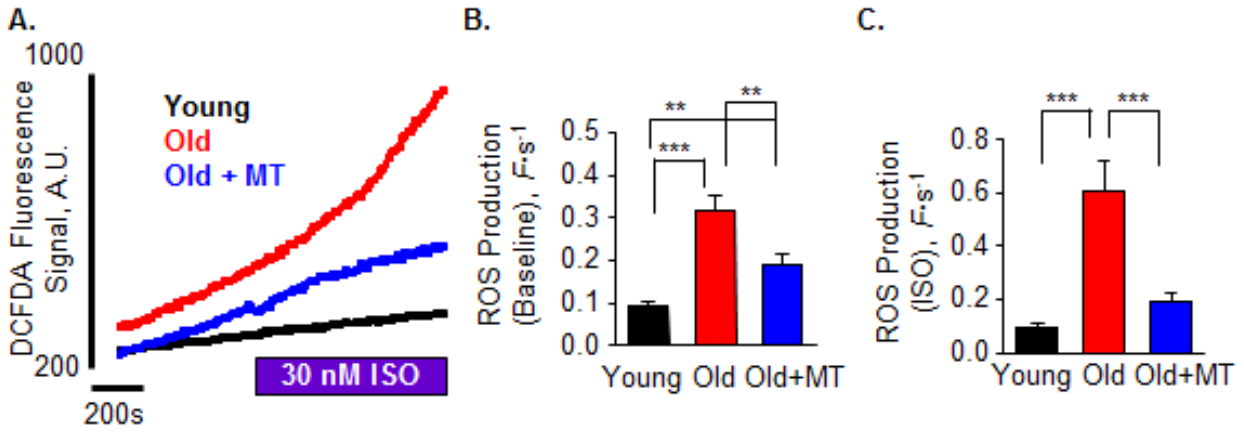

A. Changes in DCFDA fluorescence signal at baseline and with ISO (30 nM) with cardiomyocytes from young and old rabbits and from cardiomyocytes pretreated with mito-TEMPO (MT, 25 μM) for 10 min. from old rabbits. **B.** The average data for rate of ROS production at baseline: young, 0.09 ±0.01; old, 0.32 ±0.04; and old + MT, 0.19 ± 0.03 $F{\cdot}s^{-1}$. ***P < 0.001 for young vs. old and **P < 0.01 for young vs. old + MT and for old vs. old + MT. **C.** The average data for rate of ROS production with 30 nM ISO: young, 0.09 ± 0.01; old, 0.60 ± 0.12; and old + MT, 0.19 ± 0.04 $F{\cdot}s^{-1}$. ***P < 0.001 for young vs. old and for old vs. old + MT, and P = NS for young vs. old + MT. n= 8 – 20 cells from 2 – 4 heart preparations; all values are ± SEM.

Figure 4.5: Mitochondrial ROS scavenger mito-TEMPO reverses the effects of aging with regard to SR Ca^{2+} load and refractoriness of RyR-mediated Ca^{2+} release under β-adrenergic stimulation.

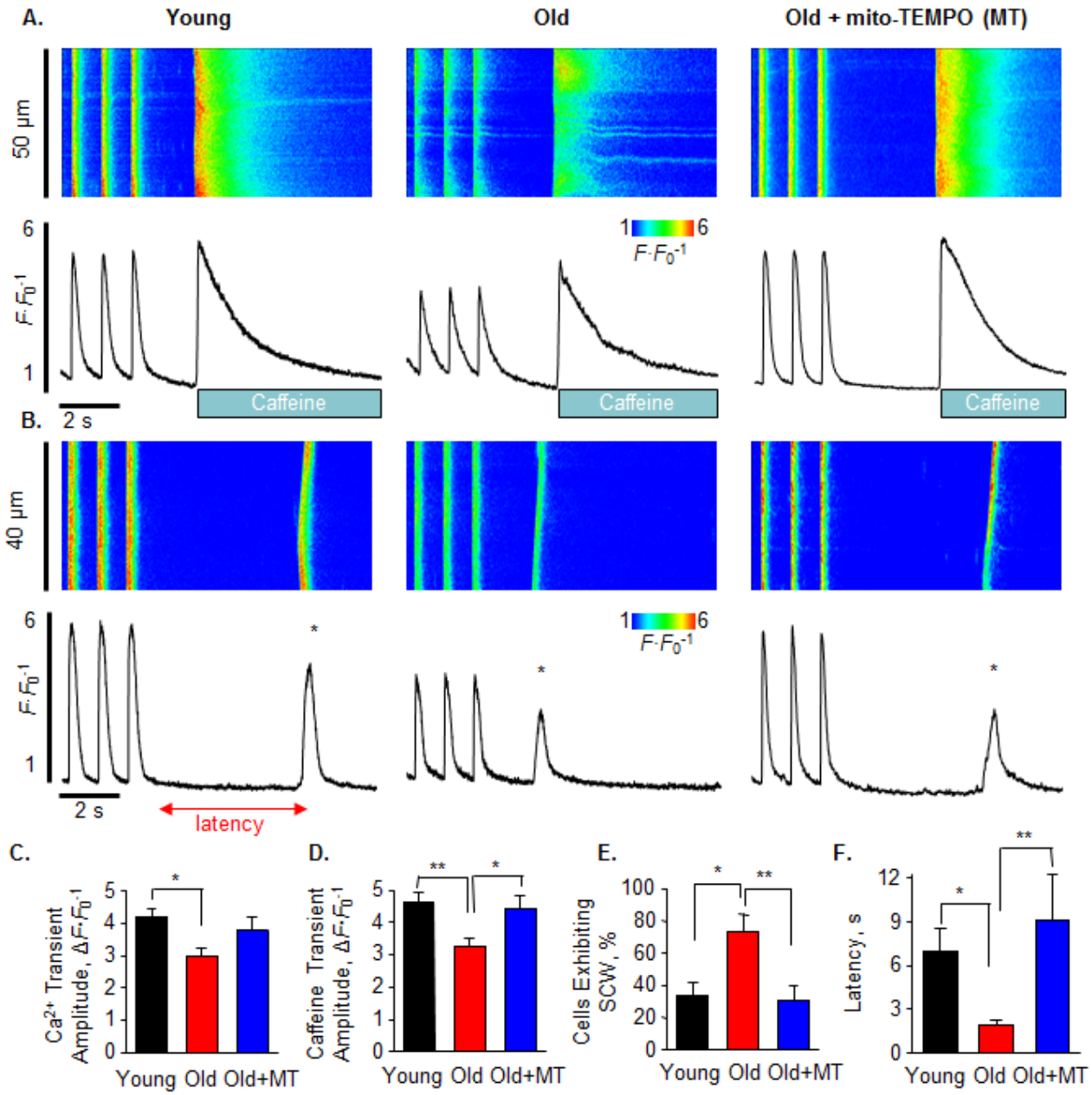

A. Confocal line scan images and corresponding temporal Fluo-3 $F \cdot F_0^{-1}$ profiles at 1 Hz from cardiomyocytes from young and old rabbits and from cardiomyocytes pretreated with mito-TEMPO (25 μM) for 10 min. from old rabbits with 30 nM ISO. **B.** Confocal line scan images and Fluo-3 $F \cdot F_0^{-1}$ profiles at the end of 1 min. 1 Hz pacing train with cardiomyocytes from young and old rabbits and from cardiomyocytes pretreated with mito-TEMPO (25 μM) for 10 min. from old rabbits rabbits with 30 nM ISO. Spontaneous calcium waves (SCW) are indicated by an asterisk. **C.** Average data for Ca^{2+} transient amplitude: young, 4.22 ± 0.24; old, 2.98 ± 0.26; and old + MT, 3.80 ± 0.42 $\Delta F \cdot F_0^{-1}$. *P < 0.05 for young vs. old, and P = NS for old vs. old + MT and for young vs. old + MT. **D.** Average data for caffeine transient amplitude: young, 4.65 ± 0.27; old, 3.25 ± 0.27; and old + MT, 4.44 ± 0.41 $\Delta F \cdot F_0^{-1}$. **P < 0.01 for young vs. old, *P < 0.05 for old vs. old + MT, and P = NS for young vs. old + MT. **E.** Average data for percentage of cells exhibiting SCWs: young, 33.33 ± 8.75; old, 73.68 ± 10.38; and old + MT, 26.93 ± 8.87 %. *P < 0.05 for young vs. old, **P < 0.01 for old vs. old + MT, and P = NS for young vs. old + MT. **F.** Average data for and SCW latency: young, 6.94 ± 1.58; old, 1.88 ± 0.34; and old + MT, 9.11 ± 3.15 s. *P < 0.05 for young vs. old, **P < 0.01 for old vs. old + MT, and P = NS for young vs. old + MT. n= 8 – 30 cells from 3 – 4 heart preparations; all values are ± SEM.

Supplemental Figure 4.1: Aging does not alter baseline cellular electrophysiology parameters in rabbit cardiomyocytes.

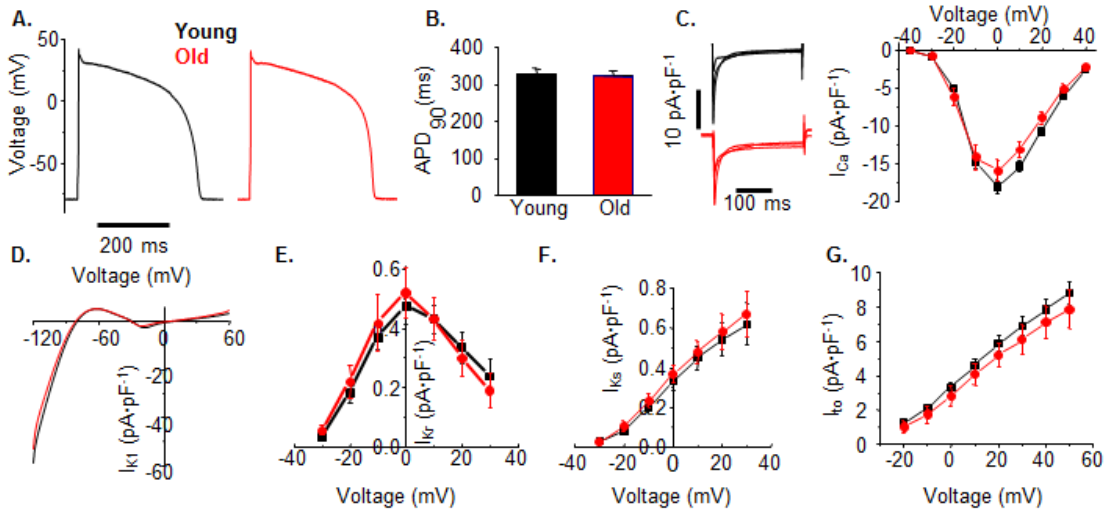

A. and **B.** Representative AP waveforms and average APD_{90}. **C.** Representative current traces at -20, 0, and 20 mV and average IV curves for peak I_{Ca}. **D.** Quasi-IV curve for I_{K1} measured with a voltage ramp from -120 to 60 mV. **Panels E** and **F.** Average steady-state IV curves measured at the end of voltage steps for I_{Kr} and I_{Ks}. **G.** Average IV curves for peak I_{to}. *n*= 5 to 22 cells from 3 – 6 hearts; all values are *NS* and ± SEM. *This experiment was not performed by the author.*

Supplemental Figure 4.2: Aging does not change protein expression levels of important Ca^{2+} handling proteins.

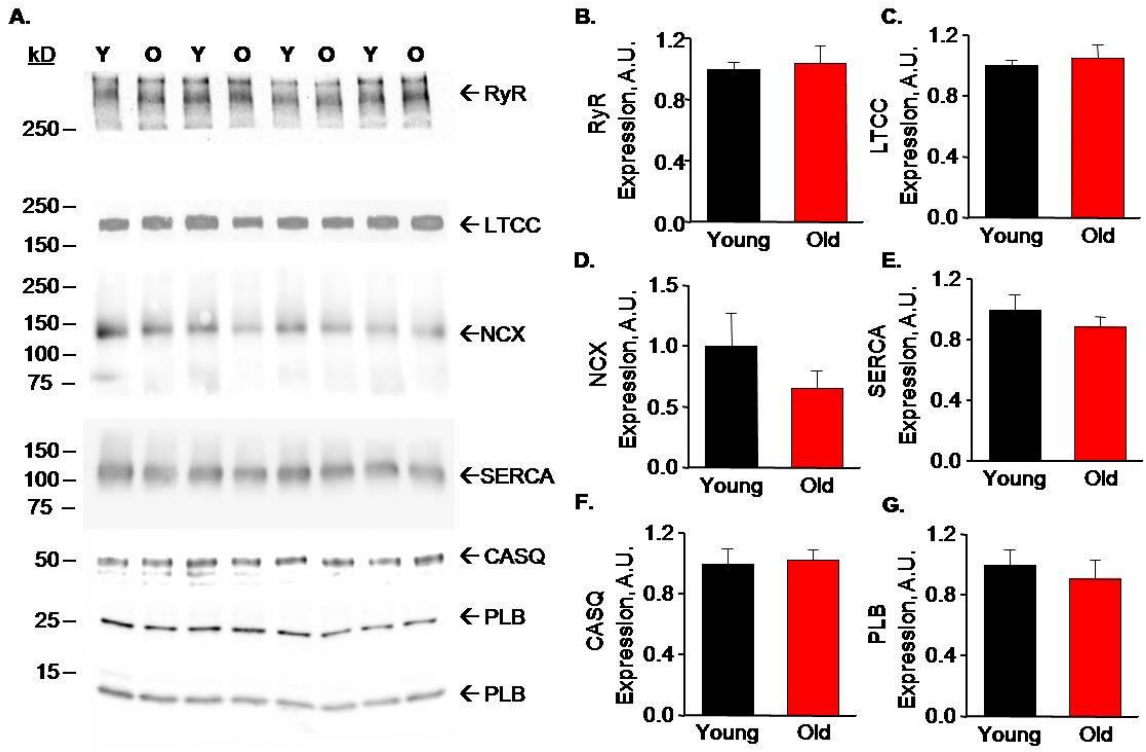

A. Representative Western blot images of proteins involved in Ca^{2+} handing. **Graphs B. – G.** depict average normalized OD data for the relative protein expression of RyR, LTCC (Cav1.2), NCX, SERCA, CASQ, and PLB, respectively. 10 – 30 µg of protein was used. Protein expression was normalized to GAPDH, α-tubulin, or CASQ. *n*= 4 heart preparations. For all values *P* = NS; all values are ± SEM.

Supplemental Figure 4.3: Increased age-related RyR thiol oxidation in the presence of ISO.

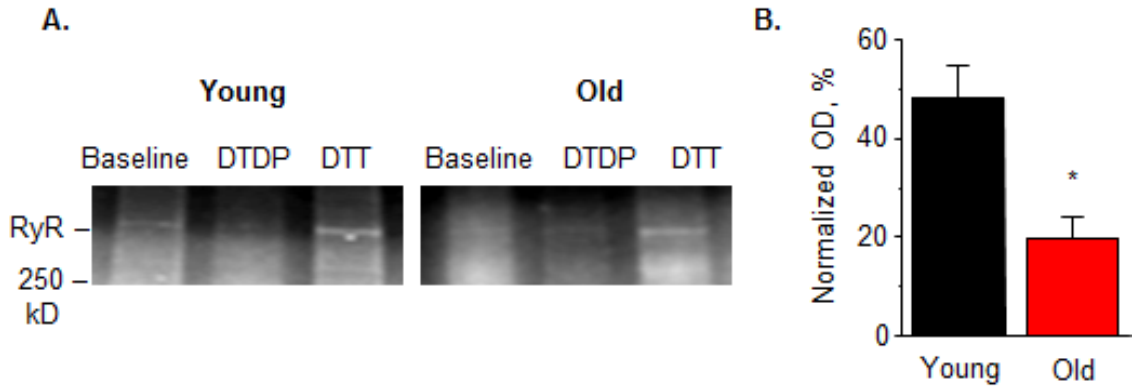

A. and **B.** Representative mBB fluorescence intensity signals of RyR from cardiomyocytes from young and old rabbits incubated with 30 nM ISO for 10 min. and pooled data for free thiol contents normalized by DTT and DTDP: young, 48.08 ± 6.86 vs. old, 19.54 ± 4.68%. *P < 0.05. Cells were from 4-5 heart preparations. *This experiment was not performed by the author.*

4.7 References

1. Kannel WB, Cupples LA, Dagostino RB: **Sudden-Death Risk in Overt Coronary Heart-Disease - the Framingham-Study**. *Am Heart J* 1987, **113**(3):799 -- 804.
2. Lakatta EG: **Cardiovascular Regulatory Mechanisms in Advanced Age**. *Physiol Rev* 1993, **73**(2):413-467.
3. Cooper LL, Odening KE, Hwang MS, Chaves L, Schofield L, Taylor CA, Gemignani AS, Mitchell GF, Forder JR, Choi BR *et al*: **Electromechanical and Structural Alterations in the Aging Rabbit Heart and Aorta**. *Am J Physiol - Heart C* 2012, **302**(8):H1625 -- H1635.
4. Bers DM, Eisner DA, Valdivia HH: **Sarcoplasmic Reticulum Ca^{2+} and Heart Failure - Roles of Diastolic Leak and Ca^{2+} Transport**. *Circ Res* 2003, **93**(6):487 -- 490.
5. Janczewski AM, Lakatta EG: **Modulation of Sarcoplasmic Reticulum Ca^{2+} Cycling In Systolic And Diastolic Heart Failure Associated With Aging**. *Heart Fail Rev* 2010, **15**(5):431 -- 445.
6. Clusin WT: **Calcium and Cardiac Arrhythmias: DADs, EADs, and Alternans**. *Crit Rev Cl Lab Sci* 2003, **40**(3):337 -- 375.
7. Eisner DA, Trafford AW: **No Role for the Ryanodine Receptor in Regulating Cardiac Contraction?** *News Physiol Sci* 2000, **15**:275 -- 279.
8. Chaudhary KR, El-Sikhry H, Seubert JM: **Mitochondria and the Aging Heart**. *J Geriatr Cardiol* 2011, **8**(3):159-167.

9. Liu T, O'Rourke B: **Regulation of Mitochondrial Ca^{2+} and Its Effects on Energetics and Redox Balance in Normal and Failing Heart**. *J Bioenerg Biomembr* 2009, **41**(2):127 -- 132.

10. Aon MA, Cortassa S, O'Rourke B: **Redox-Optimized ROS Balance: A Unifying Hypothesis**. *Biocim Biophys Acta* 2010, **1797**(6-7):865 -- 877.

11. Morita N, Sovari AA, Xie Y, Fishbein MC, Mandel WJ, Garfinkel A, Lin SF, Chen PS, Xie LH, Chen F *et al*: **Increased Susceptibility of Aged Hearts to Ventricular Fibrillation During Oxidative Stress**. *Am J Physiol - Heart C* 2009, **297**(5):H1594 -- 1605.

12. Giordano FJ: **Oxygen, Oxidative Stress, Hypoxia, and Heart Failure**. *J Clin Invest* 2005, **115**(3):500 -- 508.

13. Zima AV, Blatter LA: **Redox Regulation of Cardiac Calcium Channels and Transporters**. *Cardiovasc Res* 2006, **71**(2):310-321.

14. Belevych AE, Terentyev D, Viatchenko-Karpinski S, Terentyeva R, Sridhar A, del Rio C, Nishijima Y, Carnes C, Billman G, Gyorke S: **Redox-Modification of Ryanodine Receptor Underlies Sarcoplasmic Reticulum Luminal Calcium-Dependent Cardiac Alternans in a Canine Model of Sudden Cardiac Death**. *Circulation* 2008, **118**(18):S347 -- S347.

15. Gyorke S, Carnes C: **Dysregulated Sarcoplasmic Reticulum Calcium Release: Potential Pharmacological Target in Cardiac Disease**. *Pharmacol Therapeut* 2008, **119**(3):340 -- 354.

16. Terentyev D, Gyorke I, Belevych AE, Terentyeva R, Sridhar A, Nishijima Y, de Blanco EC, Khanna S, Sen CK, Cardounel AJ *et al*: **Redox Modification of**

Ryanodine Receptors Contributes to Sarcoplasmic Reticulum Ca^{2+} Leak in Chronic Heart Failure. *Circ Res* 2008, **103**(12):1466 -- 1472.

17. Belevych AE, Terentyev D, Terentyeva R, Ho HT, Gyorke I, Bonilla IM, Carnes CA, Billman GE, Gyorke S: **Shortened Ca^{2+} Signaling Refractoriness Underlies Cellular Arrhythmogenesis in a Postinfarction Model of Sudden Cardiac Death**. *Circ Res* 2012, **110**(4):569 -- 577.

18. Belevych AE, Terentyev D, Terentyeva R, Nishijima Y, Sridhar A, Hamlin RL, Carnes CA, Gyorke S: **The Relationship between Arrhythmogenesis and Impaired Contractility in Heart Failure: Role of Altered Ryanodine Receptor Function**. *Cardiovasc Res* 2011, **90**(3):493 -- 502.

19. Grivennikova VG, Kareyeva AV, Vinogradov AD: **What Are the Sources of Hydrogen Peroxide Production by Heart Mitochondria?** *Biochim Biophys Acta* 2010, **1797**(6-7):939-944.

20. Brown DA, Aon MA, Frasier CR, Sloan RC, Maloney AH, Anderson EJ, O'Rourke B: **Cardiac Arrhythmias Induced by Glutathione Oxidation Can Be Inhibited by Preventing Mitochondrial Depolarization**. *J Mol Cell Cardiol* 2010, **48**(4):673 -- 679.

21. Brown DA, O'Rourke B: **Cardiac Mitochondria and Arrhythmias**. *Cardiovasc Res* 2010, **88**(2):241 -- 249.

22. O'Rourke B, Ramza BM, Marban E: **Oscillations of Membrane Current and Excitability Driven by Metabolic Oscillations in Heart-Cells**. *Science* 1994, **265**(5174):962 -- 966.

23. Ho HT, Stevens SCW, Terentyeva R, Carnes CA, Terentyev D, Gyorke S: **Arrhythmogenic Adverse Effects of Cardiac Glycosides Are Mediated by Redox Modification o Ryanodine Receptors**. *J Physio* 2011, **589**(19):4697 -- 4708.

24. Bovo E, Lipsius SL, Zima AV: **Reactive Oxygen Species Contribute to the Development of Arrhythmogenic Ca^{2+} Waves During β-Adrenergic Receptor Stimulation in Rabbit Cardiomyocytes**. *J Physiol* 2012, **590**(14):3291 -- 3304.

25. Brunner M, Peng XW, Liu GX, Ren XQ, Ziv O, Choi BR, Mathur R, Hajjiri M, Odening KE, Steinberg E *et al*: **Mechanisms Of Cardiac Arrhythmias And Sudden Death In Transgenic Rabbits With Long QT Syndrome**. *J Clin Invest* 2008, **118**(6):2246 -- 2259.

26. Liu GX, Choi BR, Ziv O, Li WY, de Lange E, Qu ZL, Koren G: **Differential Conditions for Early After-Depolarizations and Triggered Activity in Cardiomyocytes Derived from Transgenic LQT1 and LQT2 Rabbits**. *J Physiol* 2012, **590**(5):1171 -- 1180.

27. Walden AP, Dibb KM, Trafford AW: **Differences in Intracellular Calcium Homeostasis Between Atrial and Ventricular Myocytes**. *J Mol Cell Cardiol* 2009, **46**(4):463 -- 473.

28. Belevych A, Kubalova Z, Terentyev D, Hamlin RL, Carnes CA, Gyorke S: **Enhanced Ryanodine Receptor-Mediated Calcium Leak Determines Reduced Sarcoplasmic Reticulum Calcium Content in Chronic Canine Heart Failure**. *Biophys J* 2007, **93**(11):4083 -- 4092.

29. Shannon TR, Guo T, Bers DM: **Ca^{2+} Scraps - Local Depletions of Free [Ca^{2+}] in Cardiac Sarcoplasmic Reticulum During Contractions Leave Substantial Ca^{2+} Reserve**. *Circ Res* 2003, **93**(1):40 -- 45.

30. Xu L, Eu JP, Meissner G, Stamler JS: **Activation of the Cardiac Calcium Release Channel (Ryanodine Receptor) by Poly-S-Nitrosylation**. *Science* 1998, **279**(5348):234 -- 237.

31. Zhu XS, Altschafl BA, Hajjar RJ, Valdivia HH, Schmidt U: **Altered Ca^{2+} Sparks and Gating Properties of Ryanodine Receptors in Aging Cardiomyocytes**. *Cell Calcium* 2005, **37**(6):583 -- 591.

32. Liu G, Abramson JJ, Zable AC, Pessah IN: **Direct Evidence for the Existence and Functional Role of Hyperreactive Sulfhydryls on the Ryanodine Receptor-Triadin Complex Selectively Labeled by the Coumarin Maleimide 7-diethylamino-3-(4'-maleimidylphenyl)-4-methylcoumarin**. *Mol Pharmacol* 1994, **45**(2):189 -- 200.

33. Donoso P, Sanchez G, Bull R, Hidalgo C: **Modulation of Cardiac Ryanodine Receptor Activity by ROS and RNS**. *Front Biosci* 2011, **16**:553 -- 567.

34. Kawakami M, Okabe E: **Superoxide Anion Radical-Triggered Ca^{2+} Release from Cardiac Sarcoplasmic Reticulum Through Ryanodine Receptor Ca^{2+} Channel**. *Mol Pharmacol* 1998, **53**(3):497-503.

35. Zima AV, Copello JA, Blatter LA: **Effects of Cytosolic Nadh/Nad^{+} Levels on Sarcoplasmic Reticulum Ca^{2+} Release in Permeabilized Rat Ventricular Myocytes**. *J Physiol* 2004, **555**(Pt 3):727 -- 741.

36. Boraso A, Williams AJ: **Modification of the Gating of the Cardiac Sarcoplasmic Reticulum Ca^{2+}-Release Channel by H_2O_2 and Dithiothreitol**. *Am J Physiol* 1994, **267**(3 Pt 2):H1010 -- 1016.

37. Oba T, Koshita M, Yamaguchi M: **H_2O_2 Modulates Twitch Tension and Increases P_o Of Ca^{2+} Release Channel in Frog Skeletal Muscle**. *Am J Physiol* 1996, **271**(3 Pt 1):C810 -- 818.

38. Anzai K, Ogawa K, Kuniyasu A, Ozawa T, Yamamoto H, Nakayama H: **Effects of Hydroxyl Radical and Sulfhydryl Reagents on the Open Probability of the Purified Cardiac Ryanodine Receptor Channel Incorporated into Planar Lipid Bilayers**. *Biochem Biophys Res Commun* 1998, **249**(3):938 -- 942.

39. Eager KR, Roden LD, Dulhunty AF: **Actions of Sulfhydryl Reagents on Single Ryanodine Receptor Ca^{2+}-Release Channels from Sheep Myocardium**. *Am J Physiol* 1997, **272**(6 Pt 1):C1908 --1918.

40. Zable AC, Favero TG, Abramson JJ: **Glutathione Modulates Ryanodine Receptor from Skeletal Muscle Sarcoplasmic Reticulum. Evidence for Redox Regulation of the Ca^{2+} Release Mechanism**. *J Biol Chem* 1997, **272**(11):7069 -- 7077.

41. Haarmann CS, Fink RH, Dulhunty AF: **Oxidation and Reduction of Pig Skeletal Muscle Ryanodine Receptors**. *Biophys J* 1999, **77**(6):3010 -- 3022.

42. Belevych AE, Terentyev D, Viatchenko-Karpinski S, Terentyeva R, Sridhar A, Nishijima Y, Wilson LD, Cardounel AJ, Laurita KR, Carnes CA *et al*: **Redox Modification of Ryanodine Receptors Underlies Calcium Alternans in a**

Canine Model of Sudden Cardiac Death. *Cardiovasc Res* 2009, **84**(3):387 -- 395.

43. Lehnart SE, Wehrens XHT, Marks AR: **Defective Ryanodine Receptor Interdomain Interactions May Contribute to Intracellular Ca^{2+} Leak - A Novel Therapeutic Target In Heart Failure**. *Circulation* 2005, **111**(25):3342 -- 3346.

44. Yano M, Ikeda Y, Matsuzaki MU: **Altered Intracellular Ca^{2+} Handling in Heart Failure**. *J Clin Invest* 2005, **115**(3):556 -- 564.

45. Squier TC: **Oxidative Stress and Protein Aggregation During Biological Aging**. *Exp Gerontol* 2001, **36**(9):1539 -- 1550.

46. Barnes K, Samson S, Grover A: **Sarco/Endoplasmic Reticulum Ca^{2+}-Pump Isoform Serca3a Is More Resistant to Superoxide Damage Than SERCA2b**. *Mol Cell Biochem* 2000, **203**(1-2):17 -- 21.

47. Eigel BN, Gursahani H, Hadley RW: **ROS Are Required for Rapid Reactivation of Na^{+}/Ca^{2+} Exchanger in Hypoxic Reoxygenated Guinea Pig Ventricular Myocytes**. *Am J Physiol - Heart C* 2004, **286**(3):H955 - H963.

48. Tsai CT, Wang DL, Chen WP, Hwang JJ, Hsieh CS, Hsu KL, Tseng CD, Lai LP, Tseng YZ, Chiang FT *et al*: **Angiotensin II Increases Expression of Alpha 1C Subunit of L-Type Calcium Channel through a Reactive Oxygen Species and Camp Response Element-Binding Protein-Dependent Pathway in HL-1 Myocytes**. *Circ Res* 2007, **100**(10):1476 -- 1485.

49. Zeng Q, Zhou Q, Yao F, O'Rourke ST, Sun C: **Endothelin-1 Regulates Cardiac L-Type Calcium Channels via NAD(P)H Oxidase-Derived Superoxide**. *J Pharmacol Exp Ther* 2008, **326**(3):732 -- 738.

50. Xu A, Narayanan N: **Effects of Aging on Sarcoplasmic Reticulum Ca^{2+}-Cycling Proteins and Their Phosphorylation in Rat Myocardium**. *Am J Physiol* 1998, **275**(6 Pt 2):H2087 -- 2094.

51. Lim CC, Apstein CS, Colucci WS, Liao R: **Impaired Cell Shortening and Relengthening with Increased Pacing Frequency Are Intrinsic to the Senescent Mouse Cardiomyocyte**. *J Mol Cell Cardiol* 2000, **32**(11):2075 -- 2082.

52. Isenberg G, Borschke B, Rueckschloss U: **Ca^{2+} Transients of Cardiomyocytes from Senescent Mice Peak Late and Decay Slowly**. *Cell Calcium* 2003, **34**(3):271 -- 280.

53. Howlett SE, Grandy SA, Ferrier GR: **Calcium Spark Properties in Ventricular Myocytes Are Altered in Aged Mice**. *Am J Physiol - Heart C* 2006, **290**(4):H1566 -- H1574.

54. Harman D: **The Biologic Clock: The Mitochondria?** *J Am Geriatr Soc* 1972, **20**(4):145 -- 147.

55. Miquel J, Economos AC, Fleming J, Johnson JE: **Mitochondrial Role in Cell Aging**. *Exp Gerontol* 1980, **15**(6):575 -- 591.

56. Ramesh V, Sharma VK, Sheu SS, Franzini-Armstrong C: **Structural Proximity of Mitochondria to Calcium Release Units in Rat Ventricular Myocardium May Suggest a Role in Ca^{2+} Sequestration**. *Ann NY Acad Sci* 1998, **853**:341 -- 344.

57. Szalai G, Csordas G, Hantash BM, Thomas AP, Hajnoczky G: **Calcium Signal Transmission between Ryanodine Receptors and Mitochondria**. *J Biol Chem* 2000, **275**(20):15305 -- 15313.

58. Zhou L, Aon MA, Liu T, O'Rourke B: **Dynamic Modulation of Ca^{2+} Sparks by Mitochondrial Oscillations in Isolated Guinea Pig Cardiomyocytes under Oxidative Stress**. *J Mol Cell Cardiol* 2011, **51**(5):632 -- 639.

59. Johnson-Cadwell LI, Jekabsons MB, Wang A, Polster BM, Nicholls DG: **'Mild Uncoupling' Does Not Decrease Mitochondrial Superoxide Levels in Cultured Cerebellar Granule Neurons but Decreases Spare Respiratory Capacity and Increases Toxicity to Glutamate and Oxidative Stress**. *J Neurochem* 2007, **101**(6):1619 -- 1631.

60. Tretter L, Adam-Vizi V: **Uncoupling Is without an Effect on the Production of Reactive Oxygen Species by *In Situ* Synaptic Mitochondria**. *J Neurochem* 2007, **103**(5):1864 --1871.

61. Shabalina IG, Nedergaard J: **Mitochondrial ('Mild') Uncoupling and ROS Production: Physiologically Relevant or Not?** *Biochem Soc T* 2011, **39**:1305 -- 1309.

62. Pogwizd SM, Bers DM: **Na/Ca Exchange in Heart Failure - Contractile Dysfunction and Arrhythmogenesis**. *Ann NY Acad Sci* 2002, **976**:454 -- 465.

63. Bers DM, Pogwizd SM, Schlotthauer K: **Upregulated Na/Ca Exchange Is Involved in Both Contractile Dysfunction and Arrhythmogenesis In Heart Failure**. *Basic Res Cardiol* 2002, **97 Suppl 1**:I36 -- 42.

64. Marx SO, Reiken S, Hisamatsu Y, Jayaraman T, Burkhoff D, Rosemblit N, Marks AR: **PKA Phosphorylation Dissociates Fkbp12.6 from the Calcium Release Channel (Ryanodine Receptor): Defective Regulation in Failing Hearts**. *Cell* 2000, **101**(4):365 -- 376.

65. Wehrens XHT, Lehnart SE, Reiken SR, Marks AR: **Ca^{2+}/Calmodulin-Dependent Protein Kinase II Phosphorylation Regulates the Cardiac Ryanodine Receptor**. *Circ Res* 2004, **94**(6):E61 -- E70.

66. Wang W, Wehrens XHT: **Stress Synchronizes Calcium Release and Promotes SR Calcium Leak**. *J Physiol* 2010, **588**(3):391 -- 392.

67. Curran J, Brown KH, Santiago DJ, Pogwizd S, Bers DM, Shannon TR: **Spontaneous Ca Waves in Ventricular Myocytes from Failing Hearts Depend on Ca^{2+}-Calmodulin-Dependent Protein Kinase II**. *J Mol Cell Cardiol* 2010, **49**(1):25 -- 32.

68. Huke S, Bers DM: **Ryanodine Receptor Phosphorylation at Serine 2030, 2808 and 2814 in Intact Rat Cardiomyocytes**. *Biophys J* 2007:132a.

Chapter 5: Conclusion and Future Directions

As people age, the risk of arrhythmia and sudden cardiac death significantly increases. Indeed, arrhythmia leading to SCD kills more people than “colorectal cancer, breast cancer, prostate cancer, auto accidents, AIDS, firearms, and house fires combined” [1, 2]. The focus of this dissertation was to advance our understanding of how and why cardiac function changes in such a way as to render the elderly more susceptible to sudden death. To that end, we used the rabbit heart, which is a physiologically relevant model in which to study electrical, mechanical, and structural aspects of cardiac and vascular function to address the following specific aims:

> **Specific Aim 1:** To characterize the age-associated changes in left ventricular function, excitation, and contractility via a series of *in vivo* hemodynamic and electrophysiological studies in young and old rabbits.
>
> **Specific Aim 2:** To identify, quantify, and compare cellular senescence and hypertrophy in heart tissue and cells from young and old rabbits using known biomarkers of cellular senescence and pathological hypertrophy.
>
> **Specific Aim 3: (a)** To characterize the age-related changes in calcium (Ca^{2+}) dynamics, action potential durations (APDs), and depolarizing and repolarizing currents in myocytes derived from young and old rabbits and **(b)** to describe an underlying mechanism for these changes.

In order to realize this charge, we established and characterized a rabbit model of cardiac aging, thoroughly examined the pro-arrhythmic substrates, and identified a novel mechanism that indicts calcium as a source of pro-arrhythmic trigger.

5.1 Electromechanical and Structural Alterations in the Aging Rabbit Heart and Aorta Reveal Age-Associated Substrates for Arrhythmia

The heart remodels with age: aging results in increased fibrosis and reduced cellular coupling in the cardiac muscle [3, 4] and the specialized conduction system [5], which slows activation and conduction velocity throughout both the ventricle [6] and the His-Purkinje system [5, 7-9]. In ***Chapter 2*** of the dissertation, we performed a series of studies, including *in vivo* hemodynamic, aortic stiffness, electrophysiologic, and echocardiographic studies as well as *ex vivo* optical mapping, high-field magnetic resonance imaging (MRI), and histochemical experiments – in order to thoroughly characterize effects of aging on the electromechanical structure and function of the rabbit heart and aorta, which can be manifested as arrhythmogenic substrates. We found that aging increased aortic stiffness and reduced diastolic and systolic myocardial compliance in old rabbits. Although beyond the scope of this work, increased hemodynamic stress could cause coronary damage and lead to ischemia, which significantly increases incidence of arrhythmia and risk of SCD. Electrophysiological studies – *in vivo* and *ex vivo* (optical mapping) – revealed age-related slowing of ventricular and His-Purkinje, altered conduction anisotropy (particularly slowed conduction in the transverse direction), and a greater inducibility in old rabbits. Increased conduction anisotropy was associated with a higher VF-inducibility rate and a changed spatial organization of wave propagations during VF in old rabbits suggesting that increased conduction velocity anisotropy provided a pro-arrhythmogenic substrate.

Since transverse conduction is hampered in aging hearts, we believe that conduction blocks across the transverse direction may provide a substrate for VF maintenance. In addition, Sirius Red staining depicted vast amounts of interstitial fibrosis in the ventricles of old rabbits, and MRI showed a deterioration of the free-running Purkinje fiber network in ventricular and septal walls in old hearts as well as aging-related alterations of the myofibrillar orientation and myocardial sheet structure. These age-related changes in fibrosis and myocardial sheet and fiber orientation likely account for this slowed conduction velocity and provide a structural substrate for reentrant arrhythmias, thereby increasing susceptibility to ventricular fibrillation.

5.2 The Rabbit Model of Cardiac Aging is Absent of Cellular Senescence and Markers Pathological Hypertrophy

The processes that underlie the age-related, pro-arrhythmic changes in the mammalian heart at the cellular and molecular level remain relatively unknown. To follow-up our characterization of the substrate in the aging rabbit heart, we identified two processes – cellular senescence and pathological hypertrophy – that could possibly underlie age-related, pro-arrhythmic triggers at the cellular and molecular level. Pathological hypertrophy has a well-established link to increased arrhythmic SCD risk [10-14]. However, cellular senescence's putative link between arrhythmia and SCD continues to be controversial despite *in vivo* data connecting it to advancing cardiac and organismal age [15, 16] and studies focused on atherogenesis [17] and heart failure [16, 18]. In ***Chapter 3***, we hypothesized that these two processes alter cellular function and provide

sufficient trigger for arrhythmias in the aging heart contributing to the increased risk of sudden cardiac death. Contrary to this, however, a series of molecular biological and biochemical assays did not reveal any evidence of cellular senescence or significant differences between tissues from young and old rabbits in molecular markers of pathological hypertrophy. Thus, we conclude that cellular senescence and pathological hypertrophy do not play a role in the cellular pro-arrhythmic phenotype associated with normal aging in the absence of pathology in the aging rabbit heart. However, aging was associated with increased lysosomal *β*-galactosidase staining indicating an accumulation of phagosomes in aging cardiac tissue, which suggests that decreased autophagy may be an underlying process that could lead to cardiac remodeling associated with aging that in some way alters a substrate and/or trigger.

5.3 Redox Status of Ryanodine Receptors (RyR) by Mitochondria-Derived Reactive Oxygen Species (ROS) Disrupts Calcium (Ca^{2+}) Homeostasis and Likely Underlies Enhancement of Arrhythmia Triggers in the Aging Heart under Adrenergic Stress

Aberrant calcium (Ca^{2+}) handling is an important contributor to the electrical and contractile dysfunction associated with aging and arrhythmia [19, 20], but specific mechanisms that cause abnormal Ca^{2+} homeostasis that could lead to pro-arrhythmic triggers in aging heart are not clear. In ***Chapter 4***, we hypothesized that changes in normal Ca^{2+} cycling are caused by post-translational modification of RyR by mitochondrial ROS. We found that cardiomyocytes from old rabbit hearts were

characterized by increased RyR activity (leading to RyR-mediated SR Ca^{2+} leak), increased rate of ROS production, and mildly depolarized mitochondria membrane potentials. All of these were exacerbated after β-adrenergic stimulation (30 nM isoproterenol, ISO). Also β-adrenergic stimulation unmasked changes in Ca^{2+} homeostasis at the sarcolemma: Ca^{2+} transient amplitude, SR Ca^{2+} load, and latency of pro-arrhythmic spontaneous Ca^{2+} waves (SCWs) were decreased in cardiomyocytes from old rabbits. Most importantly, with β-adrenergic stimulation, pretreatment of cardiomyocytes from old rabbit hearts with a mitochondrial-specific ROS scavenger reversed the aging cellular phenotype. Thus, the data presented in ***Chapter 4*** revealed a novel mechanism underlying the development of age-associated pro-arrhythmic Ca^{2+} waves and decreased RyR refractoriness during *β*-adrenergic stimulation. We showed that differential rates of mitochondrial ROS production with age along with sympathetic stimulation is critical in altering RyR redox status, leading to SR Ca^{2+} leak, and causing the development of pro-arrhythmic spontaneous Ca^{2+} waves as potential triggers of malignant arrhythmia.

5.4 Study Challenges and Limitations

This dissertation research presented us with various challenges and study limitations. Acquiring sufficient numbers of old rabbits from breeders was a serious challenge since many facilities sacrifice rabbits after they are no longer reproducing, which generally occurs before *old* age (e.g., 3.5 years in this study). Nonetheless, we were able to locate a facility that allowed us to obtain a steady flow of 6 – 8 old rabbits per quarter in

order to perform these studies. For these studies, *old* rabbits were retired female breeders. A logistical limitation was that we were unable to control for time between retirement of breeding and the inclusion into the study. Also, each old rabbit had an unknown number of litters, and the reproduction effort has been shown to affect lifespan [21, 22]. However, we are certain that all of these old breeding rabbits produced multiple litters since they were survived to 3.5 years or more. Thus, the differences in reproduction effort likely have minimal impact on this group.

Moreover, the *old* group was overall more heterogeneous as evidenced by larger reported standard deviations and standard error means for most experimental parameters. In our *in vivo* hemodynamic studies, we saw an age-associated increase in the variances (as a measure of group variability) of PWV (0.08 vs. 0.13 m^2/s^2), ESPVR (17.64 vs. 69.79 $mmHg^2/ml^2$), and EDPVR (0.25 vs. 2.23 $mmHg^2/ml^2$). Additionally, the aging electrical phenotype was less homogenous, and we observed an age-related increase in the variances other electrical measures, such as PQ interval (2.50 vs. 75.13 ms^2), AH interval (3.30 vs. 15.98 ms^2), QRS duration (0.30 vs. 83.77 ms^2), and the QT index (10.90 vs. 36.28 $\%^2$). Thus, for the purposes of the electrical characterization via optical mapping, we established a screening method using echocardiography to assess the thickness of the posterior and septum walls in old rabbits. Yet, we found that the variances of both parameters also increased with age: PW, 0.19 vs. 0.33 mm^2 and IVS, 0.15 vs. 0.44 mm^2. As a major contributor to the pro-arrhythmic substrate, the level of fibrosis also varied in the old rabbits as evidenced by an increase in the variance for total fibrosis with age: 1.06×10^{-6} vs. 1.6×10^{-4} $\%^2$. This phenomenon was also mirrored at the cellular and molecular levels. For example, with regard to the rate of ROS

production, cells from aging rabbit hearts had more varied rates at baseline (0.002 vs. 0.010 F^2/s^2) and in the presence of isoproterenol (0.004 vs. 0.101 F^2/s^2) as assessed by the variances. Clearly, aging process as reflected in the various physiological parameters studies varied between individual rabbits reflecting a well know phenomena in humans [23-25].

In the earlier studies (i.e., ***Chapters 2*** and ***3***), *old* rabbits were defined as those aged 3.5 – 6 years which is a much broader age range than the *young* group (aged 5 – 9 months). An additional potential contributor to this could be differences in genetic background; due to limited numbers of rabbits, we also used multiple rabbit venders. Potentially different interacting genes could have an influence on experimental genes and specific aging phenotypes of interest. Despite less homogeneity within the *old* group, as well as our use of multiple rabbit sources between and within age groups, we were nevertheless able to the resolve most age-related differences at the *in vivo,* organ, and cellular levels. However, while the differences in genetic background of these rabbits did not impact of the findings in these studies, it likely underlies the increase in the variance discussed above.

In ***Chapter 2***, we used several complementary techniques to gain a thorough assessment of the age-related differences in electromechanical function and structure. Both the *in vivo* hemodynamic and electrophysiology studies were minimally invasive and allowed for the rabbits to be survived for future studies. After heart harvest, most heart tissues were used for multiple biochemical and structural assays in ***Chapters 2 – 4***; however, optical mapping and MRI studies were terminal studies but provided more

insight into age-related changes in the substrate compared to *in vivo* electrophysiology. Moreover, we have shown an age-related decrease in cardiac and aortic compliance (***Chapter 2*** and ***Appendix A***); yet, further studies are warranted to investigate the effects of increased hemodynamic stress on the aging heart with regard to substrates and triggers of arrhythmia at the molecular level. Although beyond the scope of this dissertation, this may involve new aging animal models with induction of ventricular and aortic stiffness.

A major challenge for this work was confirmation of results of ***Chapter 3***, which were contrary to observations in aging rodent models with regard to cellular senescence [15, 16, 26] and pathological hypertrophy [27]. We used a series of assays to assess the senescent cellular phenotype, and the results were reproducibly negative. Yet, ***Chapter 4*** shows that myocytes from *old* rabbits exhibit a different cellular phenotype than cells from *young* rabbits with regard to calcium cycling, ROS production, and response to *β*-adrenergic stimulation. Additionally, we show age-related depolarization of global mitochondrial membrane potential; however, we were limited in directly assessing the membrane potentials of mitochondria. Performing this, along with doing electron microscopy to assess age-associated changes in mitochondrial size and morphology, merits further study in our aging model. Discussed below, we believe further studies to determine the underlying process leading to the age-related alterations calcium dynamics warrant additional investigation. Moreover, although beyond the scope of these studies, the role of cardiofibroblasts and their interactions with cardiomyocytes in age-related arrhythmogenesis remains unknown. Using this rabbit model, we could gain further functional and mechanistic insight into the cellular aging cardiac phenotype from

cultured cardiofibroblasts and co-cultured systems with cardiomyocytes. Therefore, although we were unable to find classic markers of cellular senescence in cardiac cells in our rabbit model, perhaps a broader interpretation of cardiac senescence at the cellular level may be justified.

5.5 Future Directions

Aging is associated with increased risk of several other cardiovascular diseases; however, many of the studies are performed in younger animal models, and the data derived from these studies are not likely directly transferable to the older population. We have characterized a physiological relevant rabbit model of aging that may be an ideal model in which to perform these studies of age-related, cardiac diseases and the associated mechanisms of arrhythmia. One *in vivo* model of interest is myocardial infarction (MI).

5.5A Myocardial Infarction (MI) Model

MI is a leading cause of death, and the incidence and prevalence of myocardial infarction increase with age [28]. In animal models, MI is achieved by occluding the left anterior descending (LAD) coronary artery resulting in infarct [29]. This infarct and its associated border region constitute both anatomical and physiologic substrate and triggers for arrhythmia. Most of the MI studies are performed using young dogs or pigs [30-33]; however, we have produced the MI model in old rabbits using a coil to occlude the LAD with a closed-chest, minimally invasive procedure. Our preliminary

observations reveal that this model is very arrhythmomogenic and presents an opportunity to use a more relevant model to study MI. Additionally, acute MI is associated with the activation of cardiofibroblasts to cardiomyofibroblasts and differentiation of mesenchymal stem cells (mainly into myofibroblasts) that contribute to healing and scar formation [34-36]. Once the infarct wound is healed, many of the associated myofibroblasts are eliminated via apoptosis, but the scar and some of the associated myofibroblasts persist [37-39]. Yet, the mechanism underlying myofibroblast survival in MI scars is unknown, and with characteristics similar to senescence, we hypothesis that cellular senescence may contribute to myofibroblast persistence. These myofibroblasts have enhanced deposition of extracellular matrix and fibrosis [40], and along with the permanent scar tissue, may have the potential to alter both electrical and mechanical properties of the heart making it more susceptible to arrhythmia [41].

5.5B Autophagy and the Aging Heart

As discussed in ***Chapter 1***, the process of autophagy is responsible for shuttling and degrading damaged organelles, proteins, and macromolecules by using lysosomal and autophagosomes for quality control of the cell (reviewed in [42] and [43]). Mitophagy is the specific autophagic elimination of mitochondria (as reviewed in [44]). Mitochondrial uncouplers (that reduce the mitochondria membrane electrochemical gradient) have been shown to induce stress causing translocation of Parkin, an E3 ubiquitin ligase, from the cytoplasm specifically to damaged mitochondria [45]. Recruited to damaged mitochondria by PTEN-induced putative kinase 1 (PINK1) [46-48], Parkin has been shown to mediate selective elimination of damaged mitochondria through poly-

ubiquitination and maintain organelle fidelity through mitophagy, and thus, are specific makers for this process [45]. Finally p62 links mitophagy-ubiquitin system and the autophagic machinery [49] and is essential to mitochondrial clearance [50].

In ***Chapter 2***, we showed that the aging is associated with decreased compliance of the aorta and ventricle, which likely makes the aging rabbit heart more susceptible to the effects of increased hemodynamic load via increased velocity and ill-timing of the reflected wave and increased stiffness of the ventricle. The role of autophagy in response to hemodynamic stress remains unclear [51, 52]. Zhu *et al.* have shown that autophagy in the heart is a maladaptive response to hemodynamic stress, increases fibrosis, and leads to failure [53]. However, induction of autophagy has been shown to be an adaptive response and protective against hemodynamic stress in cardiomyocytes from failing hearts [54]. Future studies could focus on how aging affects autophagy in the presence of hemodynamic stress.

It is well established that mitochondria are a major source of age-related ROS in cardiomyocytes [55-57], and since mitochondria ROS was implicated in RyR oxidation in ***Chapter 4***, perhaps downregulation of autophagy (or mitophagy) is an underlying process associated with aging that may alter physiologic substrate and trigger contributing to arrhythmogenesis. Autophagy declines with age [58] and particularly in our model, as evidenced by lysosomal *β*-galactosidase activity (**Figure 3.3 A – C**) and Western blotting (**Figure 5.1**): the LC3II to LC3I ratio decreases with age indicating that autophagy is reduced in the aging rabbit heart. Also in ***Chapter 3***, we observed an age-related upregulation of total p53 in the aging heart (**Figure 3.5**). However, the

interpretation of this preliminary result remains unclear: nuclear p53 has been shown to promote autophagy [59, 60]; whereas, cytosolic p53 has been shown inhibit autophagy [61, 62]. Thus, going forward, we will continue to investigate the hypothesis that decreased autophagy in cardiomyocytes is the process that underlies age-associated phenotypic changes calcium dynamics.

5.6 Conclusion

The scope of the work presented in this dissertation revealed both aspects of substrate and trigger from *in vivo* to the molecular level. At the *in vivo* and *ex vivo* levels, it is clear that extensive fibrosis, along with alteration to myofibrillar orientation and myocardial sheet structure, create anatomical substrates important to maintain ventricular fibrillation. Likewise, by producing electrical heterogeneity within the cardiac tissue, changes to the conduction network and conduction anisotropy provide physiologic substrates that sustain arrhythmia. Moreover, in isolated cells, we show that major age-related changes in Ca^{2+} homeostasis manifests at sarcolemma potentially malignant spontaneous calcium waves under *β*-adrenergic stimulation, which likely trigger extrasystolic activity that could lead to initiation of arrhythmias. Taken together, aging enhances the development of both substrates and triggers in the heart promoting a higher incidence of age-associated ventricular arrhythmias and SCD. Going forward, we will utilize the aging rabbit model to more appropriately and thoroughly address mechanisms of arrhythmia in the presence of age-associated, co-morbidities.

5.7 Figure

Figure 5.1: LC3II/LC3I protein expression decreases with age in the rabbit heart.

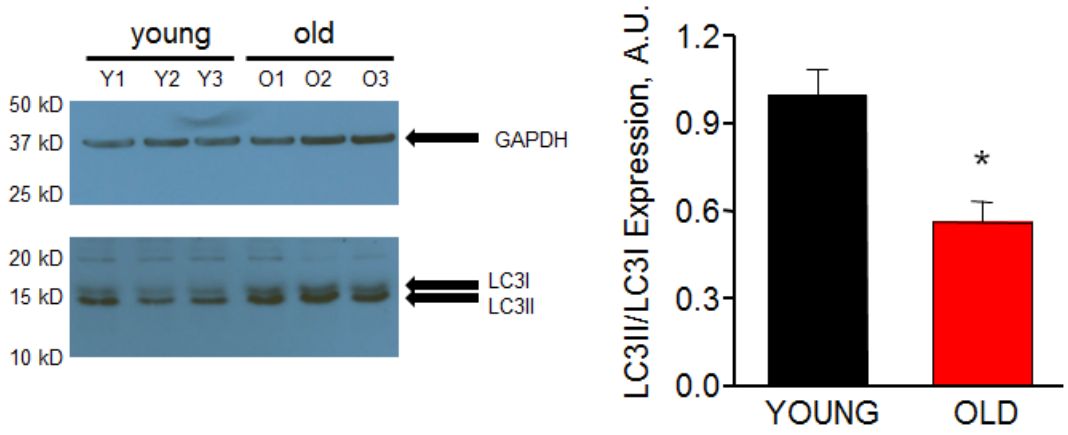

Average normalized OD data for the relative protein expression of LC3II to LC3I ratio. 30 µg of protein was used. Protein expression was normalized to GAPDH. *P <0.05. n = 3 rabbits; all values are ± SEM.

5.8 References

1. Lloyd-Jones D, Adams R, Carnethon M, De Simone G, Ferguson TB, Flegal K, Ford E, Furie K, Go A, Greenlund K *et al*: **Heart Disease and Stroke Statistics--2009 Update: a Report from the American Heart Association Statistics Committee and Stroke Statistics Subcommittee**. *Circulation* 2009, **119**(3):e21 -- 181.
2. **Sudden Cardiac Arrest: a Health Care Crisis** [http://www.sca-aware.org/about-sca]
3. Eghbali M, Robinson TF, Seifter S, Blumenfeld OO: **Collagen Accumulation in Heart Ventricles as a Function of Growth and Aging**. *Cardiovasc Res* 1989, **23**(8):723 -- 729.
4. Rossi S, Baruffi S, Bertuzzi A, Miragoli M, Corradi D, Maestri R, Alinovi R, Mutti A, Musso E, Sgoifo A *et al*: **Ventricular aActivation is Impaired in Aged Rat Hearts**. *Am J Physiol - Heart C* 2008, **295**(6):H2336 -- 2347.
5. Gottwald M, Gottwald E, Dhein S: **Age-Related Electrophysiological and Histological Changes in Rabbit Hearts: Age-Related Changes in Electrophysiology**. *Int J Cardiol* 1997, **62**(2):97 -- 106.
6. Dhein S, Hammerath SB: **Aspects of the Intercellular Communication in Aged Hearts: Effects of the Gap Junction Uncoupler Palmitoleic Acid**. *Naunyn-Schmiedebergs Arch Pharmacol* 2001, **364**(5):397 -- 408.

7. Taneja T, Mahnert BW, Passman R, Goldberger J, Kadish A: **Effects of Sex and Age on Electrocardiographic and Cardiac Electrophysiological Properties in Adults**. *Pacing Clin Electrophysiol* 2001, **24**(1):16 -- 21.

8. Fleg JL, Das DN, Wright J, Lakatta EG: **Age-Associated Changes in the Components of Atrioventricular Conduction in Apparently Healthy Volunteers**. *J Gerontol* 1990, **45**(3):M95 --100.

9. Schmidlin O, Bharati S, Lev M, Schwartz JB: **Effects of Physiological Aging on Cardiac Electrophysiology in Perfused Fischer 344 Rat Hearts**. *Am J Physiol* 1992, **262**(1 Pt 2):H97 -- 105.

10. Spirito P, Maron BJ: **Relation Between Extent of Left Ventricular Hypertrophy and Occurrence of Sudden Cardiac Death in Hypertrophic Cardiomyopathy**. *J Am Coll Cardiol* 1990, **15**(7):1521 --1526.

11. Benjamin EJ, Levy D: **Why Is Left Ventricular Hypertrophy So Predictive of Morbidity and Mortality?** *Am J Med Sci* 1999, **317**(3):168 -- 175.

12. Sugden PH, Clerk A: **Cellular Mechanisms of Cardiac Hypertrophy**. *J Mol Med* 1998, **76**(11):725 -- 746.

13. Chien KR: **Stress Pathways and Heart Failure**. *Cell* 1999, **98**(5):555 -- 558.

14. Dhalla NS, Temsah RM, Netticadan T: **Role of Oxidative Stress in Cardiovascular Diseases**. *J Hypertens* 2000, **18**(6):655 -- 673.

15. Chimenti C, Kajstura J, Torella D, Urbanek K, Heleniak H, Colussi C, Di Meglio F, Nadal-Ginard B, Frustaci A, Leri A *et al*: **Senescence and Death of Primitive Cells and Myocytes Lead to Premature Cardiac Aging and Heart Failure**. *Circ Res* 2003, **93**(7):604 -- 613.

16. Torella D, Rota M, Nurzynska D, Musso E, Monsen A, Shiraishi I, Zias E, Walsh K, Rosenzweig A, Sussman MA *et al*: **Cardiac Stem Cell and Myocyte Aging, Heart Failure, and Insulin-Like Growth Factor-1 Overexpression**. *Circ Res* 2004, **94**(4):514 -- 524.

17. Minamino T, Miyauchi H, Yoshida T, Ishida Y, Yoshida H, Komuro I: **Endothelial Cell Senescence in Human Atherosclerosis: Role of Telomere in Endothelial Dysfunction**. *Circulation* 2002, **105**(13):1541 -- 1544.

18. Morimoto M: **General Physiology of Rabbits**. In: *Rabbit Biotechnology. Volume 3*, edn. Edited by Houdebine L, Fan J. Dordrecht; Heidelberg; London; New York: Springer; 2009 27 -- 35.

19. Bers DM: **Cardiac Excitation-Contraction coupling**. *Nature* 2002, **415**(6868):198 -- 205.

20. Bers DM: **Excitation-Contraction Coupling and Cardiac Contractile Force**, Second edn. Dordrecht, The Netherlands: Kluwer Academic Publishers; 2001.

21. Murray WS: **Biological Significance of Factors Influencing the Incidence of Mammary Cancer in Mice**. *J Natl Cancer Inst* 1965, **34**:21 -- 41.

22. Muehlbock O: **Factors Influencing the Life-Span of Inbred Mice**. *Gerontologia* 1959, **3**:177-183.

23. Cevenini E, Invidia L, Lescai F, Salvioli S, Tieri P, Castellani G, Franceschi C: **Human Models of Aging and Longevity**. *Expert Opin Biol Ther* 2008, **8**(9):1393 -- 1405.

24. Weinert BT, Timiras PS: **Invited Review: Theories of Aging**. *J Appl Physiol* 2003, **95**(4):1706 -- 1716.

25. Rowe JW, Kahn RL: **Human Aging: Usual and Successful**. *Science* 1987, **237**(4811):143 -- 149.

26. Inuzuka Y, Okuda J, Kawashima T, Kato T, Niizuma S, Tamaki Y, Iwanaga Y, Yoshida Y, Kosugi R, Watanabe-Maeda K *et al*: **Suppression of Phosphoinositide 3-Kinase Prevents Cardiac Aging in Mice**. *Circulation* 2009, **120**(17):1695-1703.

27. Lieber SC, Qiu HY, Chen L, Shen YT, Hong C, Hunter WC, Aubry N, Vatner SF, Vatner DE: **Cardiac Dysfunction in Aging Conscious Rats: Altered Cardiac Cytoskeletal Proteins as a Potential Mechanism**. *Am J Physiol - Heart C* 2008, **295**(2):H860 -- H866.

28. Boengler K, Schulz R, Heusch G: **Loss of Cardioprotection with Ageing**. *Cardiovasc Res* 2009, **83**(2):247 -- 261.

29. Zhou XH, Li LD, Wu LM, Wang W, Han L, Yang J, Qiao HX, Zhou XF: **A Minimally Invasive Model of Myocardial Infarction Made by Video-Assisted Thoracoscopic Surgery**. *Method Find Exp Clin* 2007, **29**(4):283 -- 290.

30. Amado LC, Gerber BL, Gupta SN, Szarf G, Schock R, Nasir K, Kraitchman DL, Lima JAC: **Accurate and Objective Infarct Sizing by Contrast-Enhanced Magnetic Resonance Imaging in a Canine Myocardial Infarction Model**. *J Am Coll Cardiol* 2004, **44**(12):2383 -- 2389.

31. Storey P, Chen Q, Li W, Seoane PR, Harnish PP, Fogelson L, Harris KR, Prasad PV: **Magnetic Resonance Imaging of Myocardial Infarction Using a Manganese-Based Contrast Agent (EVP 1001-1): Preliminary Results in a Dog Model**. *J Magn Reson Imaging* 2006, **23**(2):228 -- 234.

32. Reffelmann T, Sensebat O, Birnbaum Y, Stroemer E, Hanrath P, Uretsky BF, Schwarz ER: **A Novel Minimal-Invasive Model Of Chronic Myocardial Infarction in Swine**. *Coron Artery Dis* 2004, **15**(1):7-12.

33. Belevych AE, Terentyev D, Viatchenko-Karpinski S, Terentyeva R, Sridhar A, Nishijima Y, Wilson LD, Cardounel AJ, Laurita KR, Carnes CA *et al*: **Redox Modification of Ryanodine Receptors Underlies Calcium Alternans in a Canine Model of Sudden Cardiac Death**. *Cardiovasc Res* 2009, **84**(3):387 -- 395.

34. Dewald O, Ren GF, Duerr GD, Zoerlein M, Klemm C, Gersch C, Tincey S, Michael LH, Entman ML, Frangogiannis NG: **Of Mice and Dogs: Species-Specific Differences in the Inflammatory Response Following Myocardial Infarction**. *Am J Pathol* 2004, **164**(2):665 -- 677.

35. Dobaczewski M, Gonzalez-Quesada C, Frangogiannis NG: **The Extracellular Matrix as a Modulator of the Inflammatory and Reparative Response Following Myocardial Infarction**. *J Mol Cell Cardiol* 2010, **48**(3):504 -- 511.

36. Carlson S, Trial J, Soeller C, Entman ML: **Cardiac Mesenchymal Stem Cells Contribute to Scar Formation after Myocardial Infarction**. *Cardiovasc Res* 2011, **91**(1):99 -- 107.

37. Willems IEMG, Havenith MG, Demey JGR, Daemen MJAP: **The Alpha-Smooth Muscle Actin-Positive Cells in Healing Human Myocardial Scars**. *Am J Pathol* 1994, **145**(4):868 -- 875.

38. Desmouliere A, Redard M, Darby I, Gabbiani G: **Apoptosis Mediates the Decrease in Cellularity During the Transition between Granulation-Tissue and Scar**. *Am J Pathol* 1995, **146**(1):56 -- 66.

39. Sun Y, Kiani MF, Postlethwaite AE, Weber KT: **Infarct Scar as Living Tissue**. *Basic Res Cardiol* 2002, **97**(5):343 -- 347.

40. Gabbiani G: **The Myofibroblast in Wound Healing and Fibrocontractive Diseases**. *J Pathol* 2003, **200**(4):500 -- 503.

41. Miragoli M, Salvarani N, Rohr S: **Myofibroblasts Induce Ectopic Activity in Cardiac Tissue**. *Circ Res* 2007, **101**(8):755 -- 758.

42. De Meyer GR, De Keulenaer GW, Martinet W: **Role of Autophagy in Heart Failure Associated with Aging**. *Heart Fail Rev* 2010, **15**(5):423 -- 430.

43. Gurusamy N, Das DK: **Is Autophagy a Double-Edged Sword for the Heart?** *Acta Physiol Hung* 2009, **96**(3):267 -- 276.

44. Youle RJ, Narendra DP: **Mechanisms of Mitophagy**. *Nat Rev Mol Cell Bio* 2011, **12**(1):9 -- 14.

45. Narendra D, Tanaka A, Suen DF, Youle RJ: **Parkin Is Recruited Selectively to Impaired Mitochondria and Promotes Their Autophagy**. *J Cell Biol* 2008, **183**(5):795 -- 803.

46. Narendra DP, Jin SM, Tanaka A, Suen DF, Gautier CA, Shen J, Cookson MR, Youle RJ: **PINK1 Is Selectively Stabilized on Impaired Mitochondria to Activate Parkin**. *PLOS Biol* 2010, **8**(1).

47. Vives-Bauza C, Zhou C, Huang Y, Cui M, de Vries RLA, Kim J, May J, Tocilescu MA, Liu WC, Ko HS *et al*: **PINK1-Dependent Recruitment of Parkin to Mitochondria in Mitophagy**. *Proc Natl Acad Sci USA* 2010, **107**(1):378 -- 383.

48. Matsuda N, Sato S, Shiba K, Okatsu K, Saisho K, Gautier CA, Sou Y, Saiki S, Kawajiri S, Sato F *et al*: **PINK1 Stabilized by Mitochondrial Depolarization Recruits Parkin to Damaged Mitochondria and Activates Latent Parkin for Mitophagy**. *J Cell Biol* 2010, **189**(2):211 -- 221.

49. Pankiv S, Clausen TH, Lamark T, Brech A, Bruun JA, Outzen H, Overvatn A, Bjorkoy G, Johansen T: **p62/SQSTM1 Binds Directly to ATG8/LC3 to Facilitate Degradation of Ubiquitinated Protein Aggregates by Autophagy**. *J Biol Chem* 2007, **282**(33):24131 -- 24145.

50. Geisler S, Holmstrom KM, Skujat D, Fiesel FC, Rothfuss OC, Kahle PJ, Springer W: **PINK1/Parkin-Mediated Mitophagy Is Dependent on VDAC1 and p62/SQSTM1**. *Nat Cell Biol* 2010, **12**(2):119 -- 131.

51. Nishida K, Kyoi S, Yamaguchi O, Sadoshima J, Otsu K: **The Role of Autophagy in the Heart**. *Cell Death Differ* 2009, **16**(1):31 -- 38.

52. Levine B, Kroemer G: **Autophagy in Aging, Disease and Death: The True Identity of a Cell Death Impostor**. *Cell Death Differ* 2009, **16**(1):1-2.

53. Zhu HX, Tannous P, Johnstone JL, Kong YL, Shelton JM, Richardson JA, Lei V, Levine B, Rothermel BA, Hill JA: **Cardiac Autophagy is a Maladaptive Response to Hemodynamic Stress**. *J Clin Invest* 2007, **117**(7):1782 -- 1793.

54. Nakai A, Yamaguchi O, Takeda T, Higuchi Y, Hikoso S, Taniike M, Omiya S, Mizote I, Matsumura Y, Asahi M *et al*: **The Role of Autophagy in**

Cardiomyocytes in the Basal State and in Response to Hemodynamic Stress. *Nat Med* 2007, **13**(5):619 -- 624.

55. Chaudhary KR, El-Sikhry H, Seubert JM: **Mitochondria and the Aging Heart**. *J Geriatr Cardiol* 2011, **8**(3):159 -- 167.

56. Harman D: **The Biologic Clock: The Mitochondria?** *J Am Geriatr Soc* 1972, **20**(4):145-147.

57. Miquel J, Economos AC, Fleming J, Johnson JE: **Mitochondrial Role in Cell Aging**. *Exp Gerontol* 1980, **15**(6):575 -- 591.

58. Brunk UT, Jones CB, Sohal RS: **A Novel Hypothesis of Lipofuscinogenesis and Cellular Aging Based on Interactions between Oxidative Stress and Autophagocytosis**. *Mutat Res* 1992, **275**(3-6):395 -- 403.

59. Feng Z, Zhang H, Levine AJ, Jin S: **The Coordinate Regulation of the p53 and mTOR Pathways In Cells**. *Proc Natl Acad Sci USA* 2005, **102**(23):8204 -- 8209.

60. Crighton D, Wilkinson S, O'Prey J, Syed N, Smith P, Harrison PR, Gasco M, Garrone O, Crook T, Ryan KM: **DRAM, a p53-Induced Modulator of Autophagy, Is Critical for Apoptosis**. *Cell* 2006, **126**(1):121 -- 134.

61. Tasdemir E, Maiuri MC, Galluzzi L, Vitale I, Djavaheri-Mergny M, D'Amelio M, Criollo A, Morselli E, Zhu C, Harper F *et al*: **Regulation of Autophagy by Cytoplasmic p53**. *Nat Cell Biol* 2008, **10**(6):676 -- 687.

62. Morselli E, Tasdemir E, Maiuri MC, Galluzzi L, Kepp O, Criollo A, Vicencio JM, Soussi T, Kroemer G: **Mutant p53 Protein Localized in the Cytoplasm Inhibits Autophagy**. *Cell Cycle* 2008, **7**(19):3056 -- 3061.